POLITECNICO DI TORINO

Corso di Laurea Magistrale
in Ingegneria Energetica e Nucleare

Tesi di Laurea Magistrale

Preparation and characterisation of joints with preceramic polymers with the aim of energy efficiency and savings

Relatore

prof. Monica Ferraris

Candidato

Virginia Pastorelli

Marzo 2023

Alla mia famiglia

Ad Andrea, la mia luce

Abstract

The energy sector is responsible for a significant amount of pollutant emissions associated with the entire production-to-consumption chain, so the need for efficiency measures to reduce production costs, energy use and consumption, and pollutant emissions is of primary interest. Obviously, this would not be possible without continuous developments and improvements in the materials field. The strong synergy between these two sectors, focused on innovation, is the key to this thesis.

This thesis work develops a preliminary technical feasibility project for the joining of ceramic materials by means of polymer-derived ceramics (PDCs). In particular, ceramics are of great interest because of their exceptional properties of mechanical, thermal and chemical stability, corrosion resistance and environmental inertness, but high production costs and energy expenditure, combined with the complexity of obtaining large assemblies of complex shapes, limit the field and effective applications. Joints and preceramic polymers fit into this picture as solutions to these problems.

The starting point is the current state-of-the-art: once the parameters useful for the realisation of the processes had been identified, it was possible to proceed with the experimental tests. The parallel realisation of a coating and a joint made it possible to understand the real behaviour of the precursor. Analyses such as scanning electron microscopy (SEM), energy dispersive spectroscopy (EDS), X-ray diffraction (XRD) and thermogravimetric analysis (TGA) were used to characterise the components obtained. Then, tensile mechanical tests were realised to measure the strength of the joints.

Three different preceramic polymers were used, including two silica precursors, one organic and one inorganic, and a silicon carbide precursor, and three different substrates, including a metallic one with a ceramic coating (alumina-coated aluminium substrate), a composite one (CMC of alumina-zirconia matrix reinforced with alumina fibers), and a ceramic one (monolithic SiC). Most of the work has focused on the organic silica precursor, with an initial study carried out on Al-Al_2O_3 substrates, firstly with the polymer alone and then with the polymer filled with silica nanoparticles. As this type of substrate could not be heated to high temperatures, the curing behaviour of the polymer was investigated. The addition of fillers improved the results already obtained for the polymer in all respects. Therefore, it was possible to extend the study to CMC substrates after they had undergone a surface modification with plasma to improve the adhesion between the filled polymer and the substrates. This treatment made it possible to obtain a joint and to study the pyrolysis step in which the conversion from polymer-to-ceramic takes place. The joint plane was then analysed by CT-scan. On the other hand, the inorganic silica precursor was used to carry out a single preliminary test, leaving the possibility to evaluate its behaviour in the future. Similarly, the work involving silicon carbide was an early stage investigation of the precursor behaviour and the adhesion on the specific substrate, with the aim of being able to realise nuclear grade 'total-SiC' joints.

Summary

Figures index

Tables index

Acronyms

Al: Aluminium

Al_2O_3: Aluminium Oxide (Alumina)

C: Carbon

CMC: Ceramic matrix composite

CVD: Chemical Vapour Deposition

CVI: Chemical Vapour Infiltration

CT: Computed Thermography

CTE: Coefficient of Thermal Expansion

EDS: Energy Dispersive Spectroscopy

FESEM: Field Emission Scanning Electron Microscope

GHGs: Greenhouse Gases

HTS: High-temperature Superconductor

ICC: International Congress on Ceramics

IPCC: Intergovernmental Panel on Climate Change

MTS: Methyltrichlorosilane

O: Oxygen

PCM: Phase Change Material

PDC: Polymer-derived Ceramic

PHPS: Perhydropolysilazane

PWR: Pressurized Water Reactor

SEM: Scanning Electron Microscope

Si: Silicon

SiC: Silicon Carbide

SOFC: Solid Oxide Fuel Cell

SPS: Spark Plasma Sintering

TGA: Thermal Gravimetric Analysis

TE: Thermoelectric

USW: Ultrasonic Welding

UTS: Ultimate Tensile Stress

XRD: X-Ray Diffraction

ZrO_2: Zirconium Dioxide (Zirconia)

ἔλπηθαι ἀνέλπιστον

[ERACLITO, Frammento 18]

1 Introduction

Engineering materials always play a significant role in the current and upcoming future world. Materials characterize everyday aspect of life, directly contribute to the advancement of technologies and to the development of new applications in each sector. This is the reason why a growing awareness of them is necessary to have a continuous improvement not only on the technological point of view but also on the energetic and environmental ones.

In particular, it is universally recognised that the climate change poses a real threat to the planet and the living beings that inhabit it, so several appropriate strategies have been designed to counter it. The European Green Deal has established 2050 net-zero emissions target to threat climate change: manufacturing and energy sectors are responsible for at least 40% of European emissions, so are central in the transition to low-carbon economy [1], all the more so since energy demand and consumption are on the rise. In the same scenario, the review of the Intergovernmental Panel on Climate Change (IPCC) has presented a road map to achieve the mitigation in which the three pillars refer to energy efficiency, alternate energy technologies able to reduce or eliminate greenhouse gases (GHGs), and strategies to sequester them [2]. Energy technologies are part of a crucial infrastructure: important selection criteria are investment and operation costs, efficiency, robustness toward dynamic operation and tolerance to pollutants, and long-term reliability due to the fact infrastructures should be resilient and operational for at least 20 years [3].

The energy objectives cannot be reached without the consolidation of the bridge between material science and energy engineering application: the main requirement is the knowledge of the relationships between the structures and properties of the materials and the appropriate scope of applications, without neglecting energy costs. Existing technologies have to be optimized to obtain fuel consumption reduction and new ones have to be developed in order to produce green energy without the use of fossil fuels, main responsible for GHGs emissions [4]. Moreover, it is possible to refer towards the need to improve material processing and refinement methods to reduce the energetic costs and the ecological impact due to the processes themselves and the disposal [5] and to develop new materials, known as advanced materials, to make use more economically and exploit more the renewables sources.

Obviously, this scenario involves challenges in the development of materials for nuclear energy applications, fissions as well as fusion, in order to have structures for fuels and to facilitate the disposal of radioactive waste; for hydrogen which is an important energy vector but at the same time a dangerous gas due to its explosive property and its small dimensions, responsible for the accumulation near dislocation sites or micro-voids, and so of the embrittlement phenomenon in case of certain metals (e.g., iron, titanium and nickel); for new high strength, low density structural materials as well as material with higher temperature capabilities to engine components [5]. Ceramics already play and will play an important role in all the mitigation strategies and the cited applications. The main drawback is related to the huge amount of energy required for the consolidation and densification at high temperature. In particular the attention is also on polymer-derived ceramics (PDCs): this emerging technology is an attractive approach to increase the quality of life for all human beings making a wide range of ceramic forms and components and, at the same time, to ensure the reduction of energy consumption [2] thanks to the possibility of using lower process temperatures than those required for manufacturing the ceramic materials themselves.

1.1 Ceramics for Sustainable Applications

Ceramics are of interest for a wide spectrum of industries and in particular in energy applications like energy conversion and storage technologies, transfer and distribution of energy, and energy savings, due to their high hardness, high temperature strength, high chemically stability, refractory nature, and environmental inertness. For definition, they are inorganic materials consisting of both metallic and non-metallic elements bonded together chemically [5], obtained mainly by sintering process. They can be crystalline, non-crystalline or a mixture of both. The main drawback is about the tendency to be brittle.

A subcategory is represented by advanced ceramic materials with tailored properties, identified as the core of established and emerging energy technologies. At the International Congress on Ceramics (ICC), in 2006, the need for a ceramic roadmap was established in order to address future challenges and needs [6]. The decision was taken by researchers and engineers aware of the need to improve the competitiveness and the sustainability of manufacturing to meet targets. In particular the roadmap, obtained for the time frame from 2010 to 2025 in the specific area of application of energy and environment, shows the tasks to improve the energy sector and have low emissions and, at the same time, threat the pollution of soil, water and air. In Figure 1.1, the main tasks refer to the usage of high temperatures and so the implementation of thermal barrier coatings and composites for e.g. gas turbines, burner nozzles, heat exchangers and sensors for structural integrity; high-temperature fuel cells in high-power regime (>100 kW) and low-temperature ones in the long term; high-temperature superconductors (HTS); nanoscale ceramics for batteries of higher storage capacity, storage capacitors and for hydrogen storage; ceramic filter membranes and catalytically active materials for water treatment; ceramic separation membranes for combustion processes.

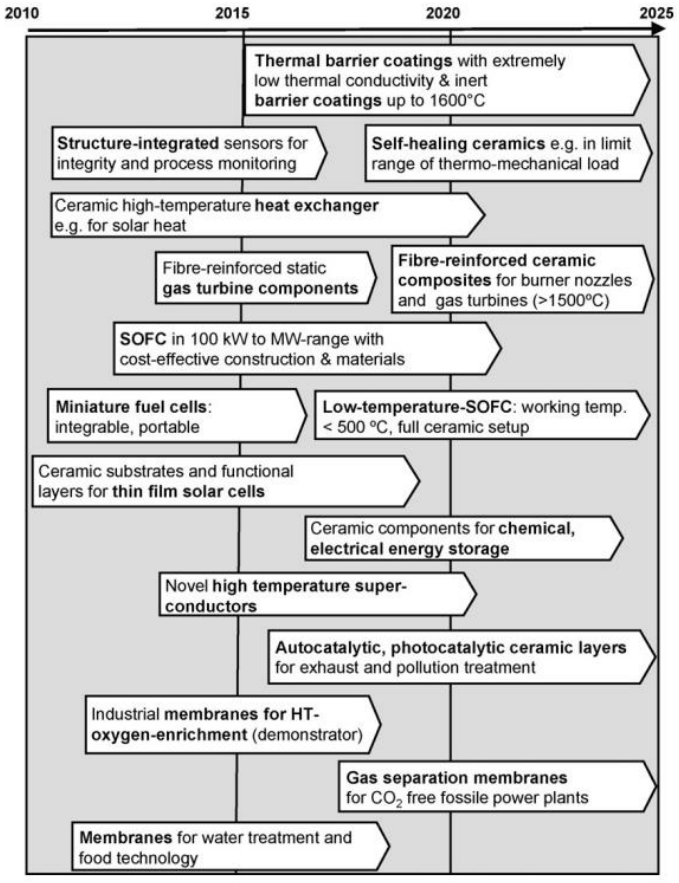

Figure 1.1: Roadmap for energy and environment [6]

The research areas identified did not remain as such but were developed. The study of Konegger et al. [2], published in 2014, is a detailed overview on ceramic materials for energy applications and their sustainability. Therefore, the following is a brief discussion of crucial examples in order to show the further improvement and the sustainability of the energy sector. In the Figure 1.2, the applications examples for ceramics in a broad range of energy, environmental and sustainable technologies are reported.

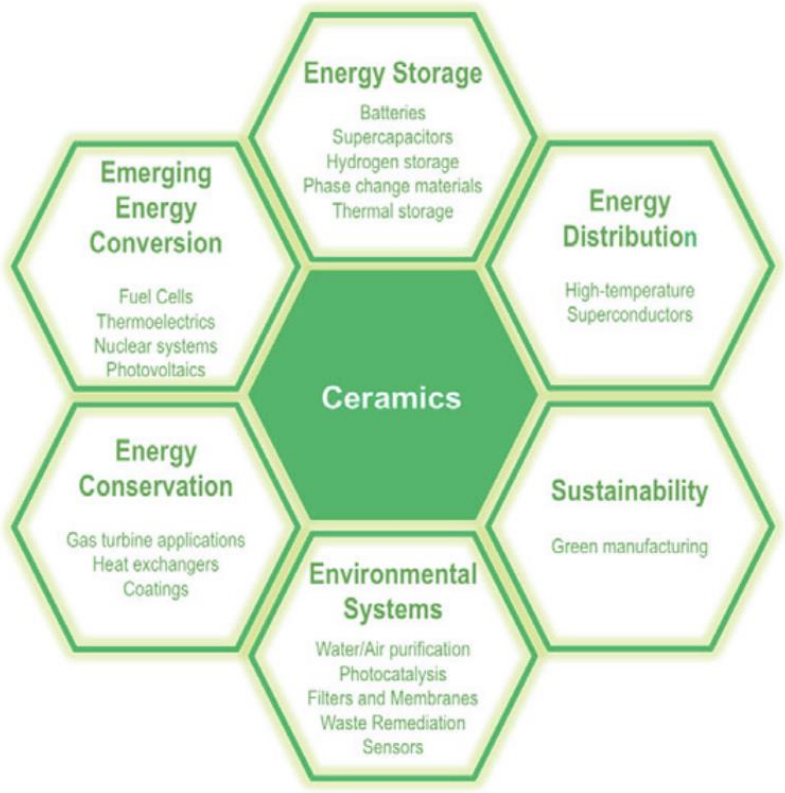

Figure 1.2: Examples for applications of ceramics in energy, environmental and sustainable technologies [2]

In particular, ceramic materials are crucial in all high-temperature applications, above 1000 °C, such as gas turbines, concentrated solar power and thermoelectric (TE), where there is no competition with other types of materials [2], [3]. In gas turbines, also, ceramic matrix composites (CMCs) reinforced with fibres serve as revolutionary, lightweight structural materials for static and even mobile parts [3]. Barrier coatings, environmental and thermal, made of ceramic layers are essential for the protection of the underlying metallic or ceramic substrates from corrosion and extreme temperature, respectively. In concentrated solar power, receivers require materials able to absorb sunlight, have a low emission and withstand high temperatures. Furthermore, in TE electrical power is generated from heat by employing the Seebeck effect [2]: an electromotive force is generated using a temperature gradient. The heat involved could be waste industrial heat or heat generated by alternative renewable energy sources such as solar thermal and geothermal. So, the materials employed, n-type and p-type ones, have not only to withstand high temperatures but also to be stable under harsh environmental conditions. There are studies on both types of materials: calcium cobaltite, $Ca_3Co_4O_9$, and $Sr(Ba)Nb_2O_6$ for p-type and n-type materials, respectively.

Fuel cells, in particular Solid Oxide Fuel Cells (SOFC), have gained interest due to their flexibility in terms of fuels used (methane, natural gas, biogas), to the high energy conversion efficiency and the wide range of applications [2]. According to the stack dimension, SOFC could be suitable to power plants as well as to household energy supplies. Ceramic materials are used in anodes and cathodes, as

interconnects, as sealants in the form of glass ceramics but mainly as electrolyte material. For the latter, Oxygen ion-conducting ceramic compounds are used as solid electrolyte while partially cation-substituted zirconia (ZrO_2), ceria (CeO_2), $LaGaO_3$ materials are the main currently used.

Considering heat exchangers, their use allows to recover the thermal energy released during a process and to exploit more sources such as solar thermal and geothermal energy and to achieve an energy efficiency. A broad number of ceramics materials (Al_2O_3, ZrO_2, Al_2TiO_5, AlN, Si_3N_4) and ceramic matrix composites (C/C-SiC, SiC/Al_2O_3) have been used commonly even if SiC is considered the most promising material for this kind of applications [2].

About nuclear power plants, ceramic materials are used for classic use such as nuclear fuel (UO_2, PuO_2, ThO_2, mixed oxides) and nuclear radiation absorbents (B_4C). For example, in control rods are required materials with specific profiles in terms of mechanical, thermal and radiation stability. A material of interest is the Silicon carbide (SiC), including its composites, due to the ability to resist high temperatures and its tolerance to neutron radiation, for both advanced fission and fusion applications. Also, SiC/SiC composites made from chemically vapor-infiltrated (CVI) and high purity crystalline SiC fibres have shown superior performance compared to conventional systems [2]. Finally, ceramics are found as moderators, barriers and host materials to immobilize radioactive waste materials for extremely long time [3].

Concerning the energy storage field, high-efficiency and capacity systems are needed in order to suitable exploit the intermittent renewable energy sources such as solar or wind energy [2]. Li-ion batteries occupy a prominent place due to the wide range of applications from mobile communications devices to electric vehicles. Ceramics are used like solid electrolytes, such as perovskite (La,Li)TiO_3, or composites separators in liquid electrolyte, such as nanoscaled Al_2O_3, SiO_2, ZrO_2 or respective mixtures, in order to increase the safety of the battery cell providing high-dimensional stability at high temperatures. Large-scale storage represents a big challenge mainly due to high costs, so chemical storage has been identified as a valid alternative. Examples refers to hydrogen storage in which zeolites are involved, and thermal one, such as phase change materials (PCMs) stored in porous ceramic containers. This kind of thermal storage uses the excess thermal energy to warm up or melt the PCM, thus storing it in the form of sensible or latent heat until the point of necessity; when the demand rises, the storage energy is released by cooling of the storage material.

In the energy distribution sector [2], high-temperature superconductors (HTS) yttrium barium copper oxide (YBCO) cuprates and Hg-containing cuprates are currently under small-scale field tests in order to increase the efficiency of the energy grids with the substitution of metallic conductors responsible of resistive losses.

The sustainability in the production process refers to the green manufacturing, so in the use of higher efficiency and cost-effective materials with lower GHG emissions and energy required for the manufacture: refractories characterised by higher thermal insulation capacity and commodity building ceramics such as cement, bricks and glass, due to the low amount of energy required and the reduced emissions, are the main interests [2].

Environmental systems include technologies for the reduction and/or purification of solid, liquid, and gaseous emissions, the remediation of waste, as well as the monitoring of potentially harmful or undesired compounds in natural and industrial environments [2]. Ceramics are suitable for filtration and purification stem due to high temperature, corrosion stability and high mechanical strength: they are used for filtration of particulates from diesel engine exhaust gases or in presence of hot corrosive gases in industrial processes. The porous structures required for this kind of application are also of interest in case of catalysis applications. On the other hand, ceramic membranes are being considered for gas

separation applications. Few examples are given from the separation of energy carriers like H_2 and CH_4 from product gas streams in coal gasification, steam reforming or biogas production, and the removal of H_2O and H_2S impurities from hydrocarbon streams. The separation is possible thanks to selective ion conduction which uses mixed ion-conducting ceramics such as perovskite-type compounds for oxygen or hydrogen separation, or microporous structures for size exclusion phenomena, using silica or zeolites. The latter materials are of great importance in the development of Carbon Capture and Storage (CCS), allowing for the sequestration of CO_2 from flue gas of combustion processes and offering an alternative to the classic chemical absorption techniques. Also, chemical inertness and anti-fouling properties are the mainly advantage in the use of porous ceramics for water purification: filters are prepared from Al_2O_3, SiC and TiO_2 in order to ensure micro- and ultra-filtration. Also, the modification with metals or organic encapsulating compounds permit the removal of pollutants such as heavy metals, radioactive compounds, complex organic compounds. Another application is hazardous waste remediation in which a glass matrix is used to immobilize conventional and radioactive wastes and prevent further release. Indeed, crystalline ceramic or glass ceramic immobilization materials are needed for refractory and volatile wastes while compounds in the alumina-silicate system are an economic and sustainable alternative for toxic and nuclear wastes. Finally, advanced ceramic-based sensor systems allow to monitor pollutants: the aim is to develop low-cost sensors with quick response in time, high sensitivity and reliability, even in harsh environments, permitting the detection of a wide variety of gases and hydrocarbons. Nowadays the sensors used include semiconducting CO sensors made of SnO_2, electrochemical CO_2 sensors containing Li_3PO_4 as electrolyte or electrochemical NO_x sensors based on YSZ.

In order to have an overall view of the situation, the circular economy should be considered and so the repair of components, reuse, and recycling of materials instead of throwing everything away [3].

The wide range of domains illustrated, underline how ceramics play an ever-increasing role in the energetic and sustainable development without forgetting the manufacturing problems. The polymer-derived ceramic process is a central element in the satisfaction of the challenge. This kind of process is able to make ceramic fibers, coating and porous ceramics, to control the composition and the purity of the ceramics desired, to make a wide range of desirable forms and unusual micro- and nano-structures [2]. At the same time, PDCs are characterized by low production costs with respect to the ones of ceramics themselves, a liquid phase which allows to easily shape the precursor and a semi-conductive behaviour after pyrolyzation above certain temperatures or in certain atmospheric conditions.

1.2 Joining

The key of the innovative and sustainable manufacturing is identified in the joining technology [7], [8]. In particular it is possible to recognise a synergy between joining technology and engineering and technological applications: there is a continuous development of novel processes as well as improvements of existing ones.

In order to better understand what joining is, some definitions may be considered [7]. Messler considers joining as “the process used to bring separate parts of components together to produce a unified whole assembly or structural entity” underling the act of form a unit which can be considered continuous. The same concept is expressed from Campbell, who defines joining as “a large number of processes used to assemble individual parts into a larger, more complex components or assembly”. The Sub-Platform on Joining [8] of the EU Manufacture Technology platform defines joining as “Creating a bond of some

description between materials or components to achieve a specific physical performance". The bond can be obtained through different processes like mechanical, chemical or thermal mechanism.

From the definitions, it becomes clear how crucial the joining process is fundamental as it is not possible to manufacture a product composed by only one piece with all kind of materials. A metal as well as a metallic alloy allow to obtain easily large-scale components and also of particular geometries, but it is not the same for ceramic and composite materials due to their brittleness and poor toughness. For this kind of materials is difficult, if not impossible, to create large objects and even complex geometries.

Joining allows the use of a wide range of approaches, materials and techniques. The purpose is to obtain complex structures made of the same or different materials with a joint which can be permanent or temporary. Furthermore, to join different material means to have an interface, so a discontinuity which is considered a source of troubles. The discontinuity configures itself as the weakest part of the obtained stability [14], so interface discontinuities should be minimized, which means that the difference in the thermal expansion coefficients (CTEs) must be minimized. This is not the only problem of dissimilar materials because they should be difficult to join due to their different chemical composition and physical properties. An ideal joint is difficult to obtain due to the fact several requirements have to be satisfied: it has to effectively transmit forces among the joint members and through the assembly, meet the structural design requirement, and be produced at minimal cost possible [13].

The final aim to join components of different materials is to obtain a structure with the desired physical-chemical-mechanical performance.

1.3 Project context

The thesis work arose in the research context of the GLANCE (Glasses, ceramics and composites) group of the Department of Applied Science and Technology (DISAT) of the Politecnico di Torino, headed by the Professor Monica Ferraris, in collaboration with the inter-departmental centre J-TECH@PoliTO (Advanced Joining Technologies).

The research is focused on the development of joining of different kind of substrates through polymer-derived ceramics. In particular, three different materials are used: an aluminium (Al) substrate with an alumina (Al_2O_3) coating, a composite material composed of a ceramic matrix reinforced with ceramic fibres (CMC) in which the matrix is composed of alumina and zirconia (ZrO_2) and the fibres are made of alumina, and a ceramic material, silicon carbide (SiC). Each substrate is used for a particular type of application. Moreover, two silica (SiO_2) precursor polymers, Durazane 1800 and Durazane 2250 known as PHPS, from the German global company Merck are used for the studies on the first two substrates while a SiC precursor from the American company Tethon 3D, manufacturer of polymer resins used mainly for ceramic 3D printing, is used for the last one.

Specifically, with regard to the alumina-coated aluminium substrates, the intention is to find a way to bond them on the alumina side that did not involve the use of classic adhesives. Experimentation with silica pre-ceramic polymers then followed. Therefore, the expected results suggest that the use of precursors can be extended to CMC substrates, although a polymer adhesion problem and surface modification techniques are expected in order to proceed.

Ceramic Matrix Composites are currently used only in sectors such as aerospace due the high production costs. Since they are materials able to withstand high temperatures and corrosive environment and, at the same time, guarantee energy efficiency and high-performances, CMCs are perfect to the exploitation

of renewable energy sources characterized by a fluctuation nature and capable to generate extreme conditions. The European project "CEM-WAVE" [9][10] has the aim to produce CMCs with an innovative process based on Microwave-assisted Chemical Vapour Infiltration (MW-CVI) technologies, in order to reduce processing costs and make CMCs suitable for process industries in energy-intensive sectors such as steelmaking.

On the other hand, the European projects "Il Trovatore" [11] and "Scorpion" [12] have the scope to individuate the best candidate ATF cladding materials for use in Gen-II and Gen-III/III+ LWR reactors and to validate them in an industrially-relevant environment. So, the possibility to bond SiC with its precursor is a technique of interest for LWR reactor containment tubes. In particular, the pipes containing the pellets must be hermetically sealed at both ends in order to protect the fuel from external contamination and avoid retention of gaseous products. The sealing process should take place by means of plugs to be coupled with the pipe once it has been filled with pellets: therefore, joining methods requiring high pressure and/or temperature cannot be used, and a pressureless joint is even preferable. It is clear that the difficulties lie in first obtaining adhesion between the polymer and the substrates and, after the treatment, to maintain the required nuclear grade standards. The starting point is represented by the process patented by General Atomics (San Diego, California, USA), a company that deals with innovative technologies in the energy and defence sectors.

As ceramic materials and ceramic matrix composites are difficult to machine to achieve structures of the desired dimensions and geometries, finding an effective joining method with the ceramic material of interest could represent a breakthrough for their manufacturer and in the applications in which they could be involved.

1.4 Thesis objectives and structure

The thesis work aims to evaluate the technical feasibility of joining different types of substrates, according to the engineering application, with preceramic polymers. Once the joint has been obtained, it must be analysed using an optical and electronic microscope and then tested to assess its strength and thus its goodness.

In order to reach the targets, the work starts with a careful literature search on polymer-derived ceramics in order to gain a thorough understanding of the reactions that govern the conversion process and the more suitable methods to process them. Subsequently, thermogravimetric analysis has been conducted in order to determine the thermal stability as a function of the change in mass of the sample during heating at constant temperature or at a gradient. Once the preliminary analysis has been completed, the experimental study is conducted following the instructions in the data sheets or provided directly by the precursors' companies. In the end, some analysis and mechanical tests have been performed in order to have a complete overview.

The work presents the development of some preliminary cases and improvements concerning only the filler addition; the technical parameters like temperature and time of the process and all the procedure followed have been maintained the same.

The thesis is divided into four main parts: a theoretical overview, a collection of the materials and instruments used including the methods of analysis, the description of the experimental part and the results obtained, and a concluding part. Therefore, the chapters are organised as follows.

The chapter 2 is dedicated to an overview on the different types of joining and the processes used, including the state-of-the-art.

The chapter 3 has the aim to introduce and clarify what pre-ceramic polymers are, what are their properties and their uses, for which types of processes they can be used, what the conversion to ceramic materials consists of and what are the possible improvements in the use of the precursors.

The chapter 4 is a presentation of the specific polymer-derived ceramics under research in which all the reaction involved are stated. At the same time, the specifications of each substrate are presented. Subsequently, the instruments and the procedures used for each part of the work are reported, starting from the preparation through the realization of the main processes until the analysis and the mechanical tests conducted to prove the joints obtained.

The chapter 5 is the main chapter of the work because it represents the core of the experimental analysis. All the results obtained are then discussed in detail in order to present the work carried out in a clear and comprehensive manner. Naturally, the work carried out on CMCs, following the initial results obtained on alumina-coated aluminium substrates, is presented with a certain consistency.

The chapter 6 is designed as a concluding chapter in which all the results obtained are briefly summarised in order to have a global understanding and to be able to focus attention on further improvements and developments.

2 Joining

The first rule is to avoid joining if possible, otherwise the appropriate type and material of joining must be carefully chosen, also depending on the applicability in an industrial context. Joining includes a large number of processes used to obtain a larger and more complex component by assembling individual parts. The selection of the more appropriate joint type has to be done according to the type of substrates to be bonded, the application, and the type of service loading the assembly will be exposed during its service life [13]. At the same time, the joint can be between components of the same material, of different materials and either permanent or temporary.

In order to obtain a good joint and assure the stability of the assembly obtained, the interface discontinuities should be minimized. So, the design process is fundamental to avoid stress concentration, cracks, corrosion, which can be concentrated into the discontinuities. The properties, which vary within the interfaces, are:

- Crystallographic properties, so the crystalline lattices are different;
- Electronic properties, materials have different electronic or bonding configurations;
- Mechanical properties, like the elastic modulus;
- Thermomechanical properties, so if the thermal expansion coefficients are very different, thermal stresses are capable to undermine the stability of the joint;
- Thermodynamic properties, the materials may not be in thermodynamic equilibrium and tend to react with each other to form a reaction product. Also, the thermodynamic equilibrium achieved must be stable under operating conditions.

In the end, a joint is only industrially usable if its reliability can be increased as much as possible.

2.1 Types of joining

At the heart of the joining process, one or a combination of several mechanisms can be identified [2], [14]. The fundamental mechanisms utilize three different kind of forces:

1. With purely mechanical origin, so the joint is formed through a mechanical mechanism (physical interface between the articles to be joined);
2. With physical origin (electromagnetic);
3. With chemical reaction origin, so the bond is formed through chemical reaction between the articles to be joined.

These mechanisms are reflected into mechanical, direct (welding and solid-state diffusion), and non-direct (adhesive bonds) joinings, respectively. The subcategory of brazing, classified as non-direct joining, is attributable at a force of physical origin.

It is clear that joining processes are constantly evolving, also thanks to the introduction of new techniques and advanced materials for which a joining solution must be found. Traditional and emerging joining options are summarised in Table 1 below.

Traditional options	Emerging options
Mechanical joining – a distinct shift from fastners to integral attachments	
Fastening	**Fastening**
Bolt	Integral fasteners (SEMs, PEMs)
Screw	Snap-fit fasteners
Rivet	Self clinching fasteners
Pin	Blind rivets
Key	Punch rivets
Couple	
Attaching	**Attaching**
Tongues-and-grooves	Integral snap fits (polymers,
Dovetails	metals, composites)
Wedges	Integral micro-mechanical
Integral threads	interlocks (IMMIs)
Flanges	Deformed-in interlocks
Integral snap fits (polymers)	
Welding – a growth in sophistication and quality through automation	
Fusion processes	**Fusion processes**
Electric arc	High-energy beam
Oxy-fuel gas	Resistance
Reistance	Electric arc
High-energy beam	Oxy-fuel gas
Nonfusion processes	**Nonfusion processes**
Pressure	Friction
Friction	Diffusion
Diffusion	Pressure
	Solid-state deposition
Brazing – new niches in joining dissimilar materials	
Brazing of metals	Brazing metals-to-ceramics
Brazing metals-to-ceramics	Brazing ceramics
Brazing ceramics	Brazing metals
Soldering – at risk environmentally and mechanistically	
Eutectic Sn-Pb workhouse	Pb-free workhorse
Fluxing required	Reactive solders
	Fluxless soldering
Adhesive bonding – new capabilities and new levels of performance	
Natural adhesives	Synthetic adhesives
Synthetic adhesives	Morphological adhesive alloys
Blended adhesive alloys	Improved durability
Limited durability	
Hybrid processes – re-emerging	
Rivet-bonding	Hybrids within, rather than
Weld-bonding	between processes
Weld-brazing	
Note: For some processes, the order or priority of usage changes between traditional and emerging options	

Table 1: Options for joining [14]

2.1.1 Mechanical joining

The mechanical joining can be both permanent or temporary but generally it is designed to be disassembled. It is achieved by interlocking parts of the material and/or by the use of screws, hooks and bolts. The advantages of this type of joint are related to the possibility of disassembling components without damaging them, allow relative motion of the components involved, low costs, no need for preparation of the materials surfaces to be joined, and no need for heat for processing. The joined component obtained is able to withstand high mechanical stresses and allows maintenance easily. Moreover, if the screws and bolts are realised of ceramic material, they have a good reliability to

corrosion. On the other hand, there are some drawbacks related to the fact that this kind of joint adds weight at the structure obtained, the holes required for inserting screws and bolts are responsible for stress concentration and, due to the fact that the surfaces of the components involved are not completely parallel, something can penetrate and cause corrosion. This condition is particularly dangerous in the case of the embrittlement of a structure as a result of hydrogen penetration into the grain boundaries and subsequent accumulation, resulting in cracks and propagation of the same until fracture. A disadvantage related only to non-ductile materials, such as ceramics, concerns the reduced temperature range in which the joint can be used due to the possible different CTEs. The result is a concentration of local stresses leading to fracture. Therefore, from a design point of view, it is also necessary to choose materials carefully, so that in operation they are fully tightened.

Regarding applications of ceramic materials, the mechanical joining technique is used to join ceramic matrix composites with metal. In case of CMC combustor and turbine components [15], special attention has to be given to the attachment metal system. The not-easy-to-achieve purpose is to find the right balance between flexibility (decreasing the thermally induced stresses) and rigidity (considering permissible displacements and frequency requirements). Interesting mechanical joints are C/SiC to C/SiC or Ti alloy and SiC/SiC to SiC/SiC or Ti alloy for aerospace applications.

2.1.2 Direct joining

Direct joining, as the name suggests, is the joining of two materials without the interposition of a third. It is therefore permanent and requires cutting to remove. It is usually used for small surfaces and for materials that can be melted. Two basic techniques can be identified: welding and solid-state diffusion.

The welding consists of a local melting of the materials to be joined with the formation of a liquid phase which solidifies creating a continuous interface from the physical and the chemical point of view. It is used for most of metals and for huge temperature ranges. The main drawback refers to the obtainment of a welded area with microstructure and properties different with respect to the starting workpieces [8]. A joint of this type can be obtained by electron beam, laser, friction or microwave. In particular, lasers allow heat to be concentrated in a reduced volume, making it a very precise technique, and complex geometric shapes can be welded using laser beam deflection techniques. Also, pulsed laser welding and ultrasonic welding (USW) are suitable techniques for ceramic bonding.

The solid-state diffusion, or diffusion bonding, is a solid-state welding process consisting in the pressure application on the surfaces of interest which are heated. Then, the joint is obtained through atomic diffusion between the two materials at a temperature which is lower than the melting one. Also, the technique requires an extremely smooth surface finish to provide intimate surface contact. The need to apply pressure while maintaining part alignment imposes severe limitations on joint design. It is an expensive process which needs inert atmosphere, vacuum or pressure, suitable for flat joints even if it can be adapted to cylindrical geometry. In this case, the technique of interest for ceramics is spark plasma sintering (SPS).

2.1.3 Non-direct joining

The non-direct joining is the most common method and is permanent. It uses a material as glue between the two substrates to be joined which can be organic (e.g., polymers) or inorganic (e.g., glasses, metals and alloys). The most important property of the liquid joining material is the wettability, so the ability

to wet the solid on which it is places. Wetting is determined by the surface free energy of the substrate, the surface tension of the liquid coating material, and the interfacial tension between them [16]. In order to satisfy the requirement, the angle between the liquid and the solid, has to be the lowest possible. If it is equal to 0°, it means that a thin layer of liquid is spread on the surface, but the angle must not exceed 90°. Although a good wetting in the liquid state is essential to obtain a good adhesion to the substrates, it does not guarantee it. In case of wettability and adhesion issues, surface modification of the substrate can be operated in order to change its chemical composition. Also, if substrates are characterized by surface roughness and the wettability is good, an increase of the adhesion strength can be observed, since both interfacial area and mechanical interlocking increase [16]. The result of this kind of joint is like a compression force between the two surfaces. Two examples of technology could be identified in adhesive joining and brazing with brazing alloys or glass/glass ceramics.

In case of adhesive joining, a polymer or a glass is used: the liquid or semi-solid-state material is placed between the faying surfaces of the workpiece to be joined and either heat, pressure, or both are applied to get bonding. The adhesive force generated is the one that holds the adhesive and the substrates together, so the stronger the adhesion and the stronger the bonds between the adhesive and the substrates, even if it is not enough to have strong bonds overall. The other force to consider is the cohesion force: this is the force of the adhesive itself. In particular, the design process is important because each type of adhesive offers a unique set of performance and processing capabilities, which are also related to the nature of the adherents. Overall, it is a quick and low-cost process, even conducted at low temperature, but surface preparation (e.g., surface cleaning, pre-treatment) is necessary to achieve a good quality joint. Typical causes of joint failures are poor design, unprepared surface, improper adhesive selection for the substrate or difficult operating environment [7]. Many advantages have been identified, such as the creation of a continuous bond, the formation of a sealed joint capable of preventing corrosion, minimisation of mass and components in an assembly, stress distribution over the joint area and vibration reduction. On the other hand, drawbacks include adequate design of the joint, additional time required for polymerisation, limited thermal resistance and weakening of the bond by atmospheric agents, degradation and chemical agents. The end result is complex geometries and large joints that can withstand medium to low mechanical strength.

Conversely, the brazing process uses a material with a melting temperature lower than that of the substrates to be joined. Once the brazing material has solidified, a compositionally discontinuous but physically continuous joint is obtained. The process is low cost, carried out at low temperatures, even lower than those of the solid diffusion methods, and allows to obtain low residual stresses with respect to the welding. It is a versatile process, suitable for different materials such as metals, ceramics and composites. In some cases where ceramics are involved, preventive metallisation, i.e. the deposition of a metallic layer, can make the ceramic more akin to the brazing alloy. Typical brazing alloys are Cu-X or Ag-Cu-X, where X can be Ti, Zr or Hr, and Ti-Zr(-Be). There are some brazing alloys that are known as ‘active’ because they are able to react with the materials to be joined to increase their wettability. Also, the brazing alloy is used as compensation layer to decrease the mismatch between the low CTE of the ceramic material and the high CTE of the metallic material. If the CTEs are very different, several different layer can be placed between the materials to be joined to compensate for the stresses. The result is a discontinuous structure. The technique is also suitable for CMCs.

Overall, about the composite joints, preceramic polymers can be used as joining materials for high temperature applications for which brazing is not suitable. The problem related to the use of this kind of materials is the organic fraction contained which is removed at high temperatures but the polymer obtained is porous. This is the reason why methods have to be improved in order to have a better joint.

Furthermore, all the technologies mentioned, which are applicable to ceramic materials, will be briefly discussed in the next section.

2.2 State-of-the-art for ceramics and CMC joinings

It has been established that a joint represents a discontinuity and weakness point in a structure but, dealing with ceramic or ceramic matrix composite materials, it is unavoidable. In this way complex geometries and large-scale components could be realised. Due to the fact ceramic materials are used in severe environments (e.g., high temperature, corrosive), where high mechanical, thermal and chemical stability is required, the most appropriate method to join materials, especially in permanent way, should be found. On the other hand, the same high-temperature resistance represents an obstacle in the joining process [17].

From the data of the last 15 years, it has been possible to obtain an overview of the techniques according to the substrates to be joined, as shown in Figure 2.1, and to conclude that joining is preferably carried out in oxide furnaces using non-oxide ceramics [18].

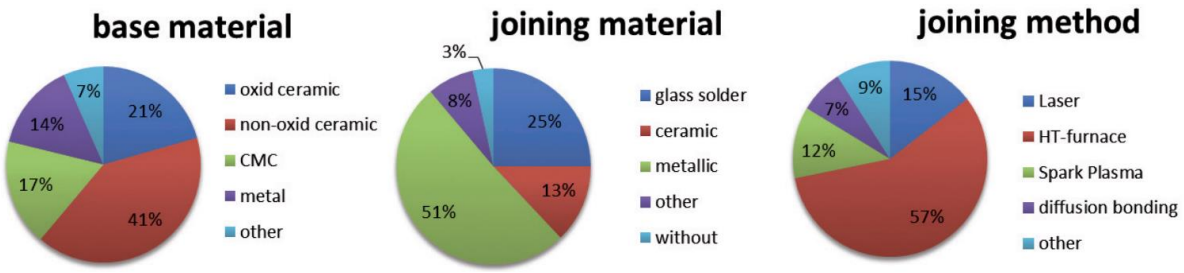

Figure 2.1: Base materials, joining materials and joining methods overview[18]

High temperature stable adhesives such as solders based on glasses, glass-ceramics and metals are most appropriate.

At the same time, the joining technology can be applied in different branches, as it is possible to notice from Figure 2.2. It is evident how this type of joint is used in industry and especially in the energy sector. Focusing on CMCs, joints may be found in thermonuclear fusion reactors, heat exchanger tube end fittings, and gas turbine components [19]. One of the most important advantages is the production of lightweight structures; the others are related to higher performances and increased functionality.

Area of Application	Requirements for Basic Materials	Example	Materials Combination
Electrical industry	Electrically conducting/isolating	Circuit boards	Ceramic-ceramic Ceramic-metal
Power generation	High-temperature stable, good thermal properties, long-term stable, chemically stable, gas tight	Heat exchangers for heat recovery, compound-pipe	Ceramic-ceramic Ceramic-metal CMC-metal
Gas turbine and aviation	Resistant to thermal shock, good mechanical properties, low fatigue, gas tight	Flame tubes, guide and rotating vanes	CMC-CMC CMC-metal
Thermal engineering	Long-term stable, high- temperature stable, resistant to thermal shock, insulating, distortion-free	Carrier structures, insulating elements, ducts, hot gas valves	Ceramic-ceramic CMC-ceramic CMC-CMC CMC-metal
Metal industry	Long-term stable, high- temperature stable, resistant to thermal shock	Continuous process devices, Furnace fans	CMC-CMC, CMC-metal
Medical engineering	Bioinert, long term stable	Dental prostheses	Ceramic-metal

Figure 2.2: Applications of the joining technology [18]

Depending on the specific application, a distinction is made between ceramic-metal and ceramic-ceramic joints. Particular attention is reserved to the last ones as their realisation would increase the portfolio of ceramic applications. The joining options in order of preference are: adhesive, mechanical, brazing, non-fusion welding and fusion welding [7]. The principal problem to overcome is the difference in the CTEs between the ceramic material and the adjacent one.

2.2.1 Pulsed laser welding

Pulsed laser welding is one of the direct joining techniques. The particularity is relative to the locally controllable energy deposition. In this way, the temperature in the most of the assembly remains unchanged and the result is a localized melting rather than an ablation. The process is possible due to the light focus on the interface in order to ensure the optical interaction volume and stimulate nonlinear absorption processes: so, the results are based on the interplay between linear and nonlinear optical properties and laser energy-material coupling [17]. The technology is versatile due to its application on both transparent ceramics with varying absorption properties and conventionally sintered ceramics characterized by limited light transparency (scatter or diffuse light).

This joining approach is used on engineering ceramics such as polycrystalline alumina and yttria-stabilized zirconia (YSZ). In particular, the optical transparency of YSZ can be tuned due to simple thermal treatments. Mild average laser powers (<50W) are necessary to weld ceramic parts and hold high vacuum with leak rates, satisfying hermetic-quality seal standards for military, space, bio-implantable electronics. Two different approaches, so concepts, could be possible: the first one is related to transparent ceramics for hermetic encapsulation, while the second one refers to simple geometries' joint of diffuse ceramics.

In more detail, concept 1 illustrates how to weld a cylindrical cap and a tube: the key is the ceramic's transparency which allows to focus the laser at the interface between the two components while the assembly is rotated. On the other hand, concept 2 mirrors traditional welding of simple geometries: even in this case, the laser is focused on the interface but of two ceramic cylinders from the outside. A small gap is introduced between the components to be joined in order to ensure an adequate optical access to the interface. This technique is used to overcome the problem of high scattering of laser light caused by the residual porosity of sintered ceramics, which is responsible for low penetration into the material, resulting in uneven radiation distribution and possible surface evaporation or ablation.

In order to obtain a weld, a continuous melting along the joint interface is necessary: the key is the dynamic rotation of the ceramics through the beam focus at a specific angular velocity and hold the pulse energy and the repetition rate constant. In this way, an ideal number of incident pulses impinges on an area as guided by the static laser-affected zone (LAZ) diameters, obtained at a specific energy and pulse width, resulting in a continuous weld pool at the mating surfaces. Various tests have shown that an intermediate angular velocity (e.g., $50° s^{-1}$) results in an optimal weld bead reminiscent of some metal welds. A lower angular velocity implies ablation of the components and therefore the weld is not successful, while a higher angular velocity implies a non-uniform melted volume. Moreover, a similar dependency can be found in the distance between the two parts to be joined in the case of concept 2.

In Figure 2.3, the diagram of the process and the corresponding welding result are reported for concept 1 and concept 2, respectively.

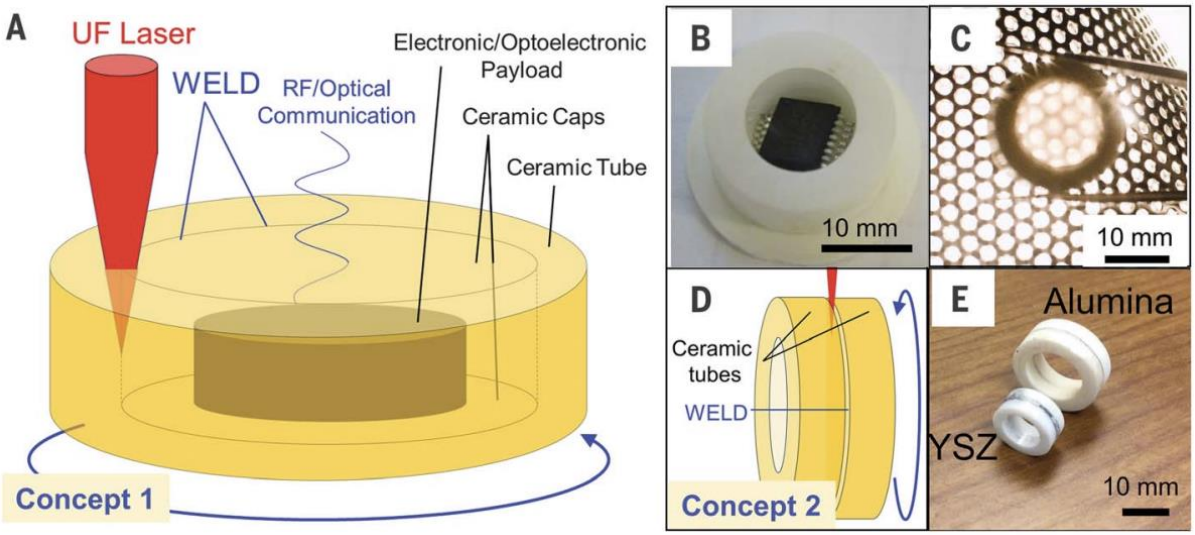

Figure 2.3: Ultrafast laser welding concepts. (A to C) Concept 1, ceramic encapsulation. Scheme of the process (A), sample electronic payload in a ceramic tube (B), welded assembly (C). (D to E) Concept 2, welding of simple ceramic geometries. Scheme of the process (D), welded assembly (E) [17]

The primary importance of this technology lies in being able to use it without heat damage of the electronic components attached to the material being joined; also, the laser can be focused on small areas, so it is a high-precision technology. Another advantage is related to the energy efficiency, considering the energy consumption, with respect to traditional diffusion bonding. On the other hand, a drawback is related to the use of this technique to join very small components. If a controlled laser beam deflection technique is combined, even complex geometric shapes can be welded.

In the end, laser welding is more versatile on transparent ceramics due to the fact that one can focus through the material, allowing the joining of more complex geometries and over multiple interaction zones, increasing the ultimate weld volumes. There is a large scope for optimisation when considering the possibility of intervening in the gap distance, focal length, surface treatments, modification of the non-linear absorption with impurities or thermal treatments.

2.2.2 Ultrasonic welding (USW)

Ultrasonic welding is a direct joining technique, used to bond a ceramic-to-metal. The process involves two workpieces which are placed in compression with each other in order to be welded, and oscillated by ultrasound, at 10-75 kHz, producing shear stresses at the interfaces; also, inserts can be used. When binder is used, firstly the metal is put on the ceramic surface and pressure is applied, then ultrasonic vibration is employed. One variation is to use a metal with a low melting point as the insert material. The process is characterised by localised heating.

This technology is particularly interesting as it allows to weld various ceramics, such as Al_2O_3, SiC, Si_3N_4, AlN, to metals at room temperature, quickly and easily compared to other welding methods [20]. Also, for each ceramic/metal combination optimum welding conditions could be identified and the process is performed in all environments, either in the atmosphere or in vacuum.

In Figure 2.4, the equipment needed and an outline of a joint are showed. The complete system consists of active components, which generate, transmit and apply the ultrasonic waves to the components to be

welded, and passive components, which absorb the resulting forces, hold the workpieces in position and, above all, support the formation of the weld. Active components include an ultrasound generator, a converter, an amplitude transformer (amplifier or booster), a sonotrode (welding tool); in particular, the last three components form the so-called vibrating unit. In contrast, passive components include a workpiece housing and an anvil.

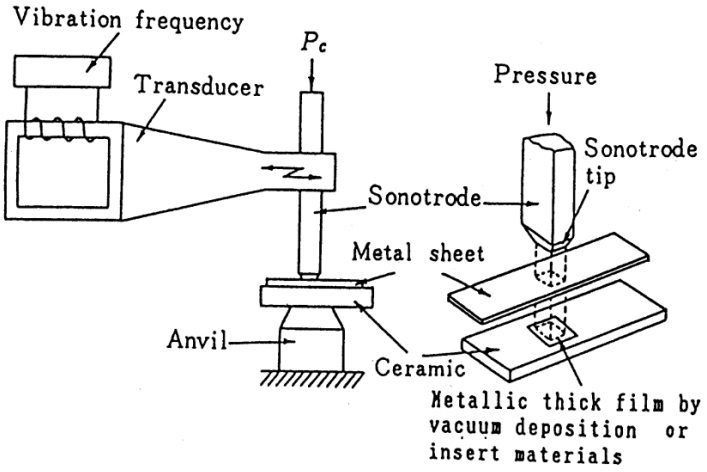

Figure 2.4: Ultrasonic welding scheme process [20]

Obviously, pressure is a fundamental parameter which particularly affects the process: when a low welding pressure is applied, the time duration must be increased (by few minutes), otherwise when it is increased overall, the required duration is reduced. Below certain levels of pressure and duration, it is possible that ultrasonic vibration stops or cannot be used effectively, so a good joint is impossible to obtain.

The technique is suitable to bond dissimilar materials and in particular good results are been obtained using activated metal or low-melting-point metal as insert material, or by metallizing (vacuum-deposition) the contact surface. This is attributable to their promoting the bonding reaction: in addition to the mechanical bond, there is a connection reaction between the atoms attributable to the vibrations of ultrasonic condition. Elastic and plastic deformations bring in contact the two surfaces to bond, so atoms are attracted to each other, then the boundary temperature-rise at the contact surface due to vibration is responsible for the linkage between them. The heat produced by atoms rubbing against each other is called frictional heating.

The advantages are related to: high speed, due to the fact that the bonding time is less than 1 second; low power consumption, so it is an economic process; the joint is formed from a low temperature solid state weld; no flux, braze or solder needed; no pre-cleaning, high temperatures or special environments needed. On the other hand, the drawback is that if the materials to be joined have low mechanical strength, they are not suitable to ultrasonic welding.

2.2.3 Spark plasma sintering (SPS)

Spark Plasma Sintering is a direct joining technique, belonging to solid-state diffusion. Even if the exact nature of the mechanism is still under debate, and in particular the effect of pulsed high current on the generation of spark plasma [21], [22], the process is considered an effective method to obtain a rapid sintering by self-heating of different materials and high-quality joint. The technology is suitable for intermetallic compounds, metal and ceramic matrix composites, amorphous materials, nanostructured

materials, highly refractory metals and ceramics [7]. High quality joint can be obtained in metal-to-metal, ceramic-to-ceramic, ceramic-to-metal joints. The joining by SPS is a novelty in composites field. The advantages are related to safety, reliability, high sintering speed (so short sintering time), low power consumption (due to both the rapid processing and the localized heating), uniform heating for sintered bodies, limited deformation of the joined parts, and reasonable performance [7] [23], [24].

The system is composed basically from a sintering press machine with a vertical single-axis pressurization mechanism, punch electrodes incorporating a water cooler, a water-cooled chamber, a vacuum chamber, a DC-pulsed power generator, a cooling-water control unit, Z-axis position measuring and control unit, temperature measuring and control units, applied pressure display unit, data analysing unit, and various safety interlock devices [22]. A diagram of the plant is showed in Figure 2.5. The DC pulse energizing method generates spark plasma (1), spark impact pressure (2), Joule heating (3), and an electrical diffusion effect (4). Also, the pulsed energy generates an electro-magnetic field effect responsible for electro-migration and preferential orientation of crystalline. If the powder to be synthesised or the substrates to be joined are not a current-conducting, the mould is heated to transfer heat through it.

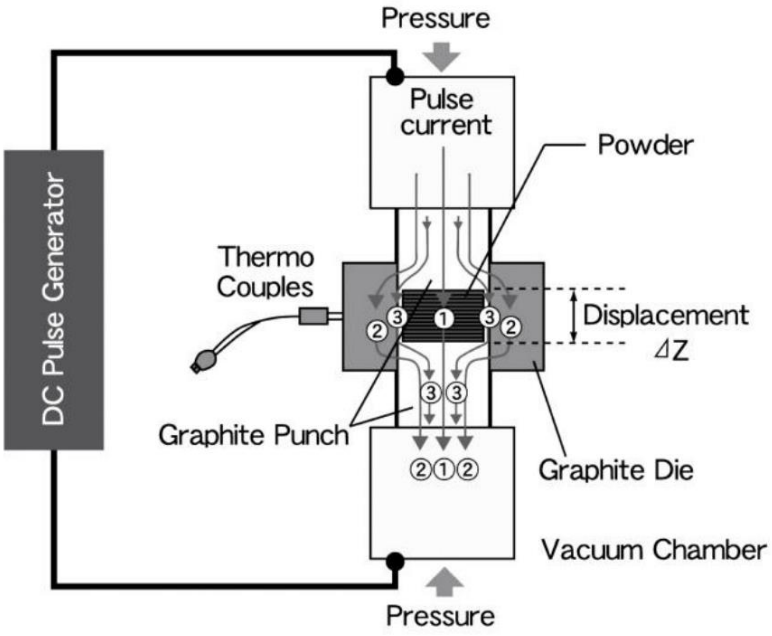

Figure 2.5: Spark Plasma Sintering plant diagram [22]

The materials involved in the joint are heated to high temperatures in a very short time, even at a heating rate of 600 °C/min, and high pressures of up to 1 GPa can be applied at the same time. The process allows to limit the deformation of the joined parts and to highly control the reaction. Also, it is particularly useful in order to increase wettability and to promote bonding. The heat generation depends on pulsed direct electrical current (DC) and the sintering is obtained, also, utilizing uniaxial force under low atmospheric pressure. Therefore, the application of pressure is fundamental; the only case in which a minimal pressure can be applied is just when a viscous joining material, such as glass-ceramic, is used [24]. One limitation of the process is its applicability to small components, at least of 10-20 cm of diameter, and basic geometries.

Considering the ceramics, SPS is employed to join α-SiAlON, β-SiC, ZrB_2-SiC, C/SiC composites and SiC-graphite [21]. It is possible that the flexural strength is higher in the case of the joint because further sintering (post-sintering) has taken place, so the porosity is further reduced.

However, the SPS technique, especially for CMC, promises interesting results particularly for all those extreme applications where it would be avoid having any joints at all, and additionally thermo-mechanical properties of the substrates are not affected by the presence of a joining material in between.

2.2.4 Brazing

Brazing is a well-known non-direct joining technology, characterized by great flexibility and universality, used to join permanently dissimilar materials, especially ceramics to metals. Also, it is used to join dissimilar metals for which welding processes are not suitable due to complicated geometries or incompatibility of metals. Although, the obtained joints are not free of defects caused by thermal stresses induced in the joint field and material deterioration due to the heating [25].

In particular, braze fillers have a melting temperature above 450 °C and the joint obtained is close to a natural connection between the substrates that have to be joined. Some processes are included such as laser brazing, furnace brazing, arc and vacuum brazing [7][25].

On the other hand, there are a number of problems that need to be overcome in order to produce vacuum-tight, thermally stable, high-strength compounds. The main one is wettability [26], [27]: due to the high surface tension caused by the polar bond structure, ceramics cannot be wetted by conventional metallic melts. More specifically, the incompatibility between metal and ceramic is due to the different atomic structures. The problem can therefore be solved in two ways: by metallizing the ceramic component or by using an active brazing agent. In the first case, a metal layer is applied to the ceramic surface before the brazing process: industrially, it is made of Mo/Mn or W/Mn. However, only oxide ceramics can be metallized in this way although there has been recent research into processes suitable for non-oxide ceramics. These include thermal spraying and physical vapour deposition. Instead, in the second case, the wetting between the ceramic and the brazing filler metal takes place directly during the brazing process and even non-oxide ceramics can be involved. The most important active metal is Ti, although other active elements like Nb, V, Ta, Zr, La, Hf, Ni are used [27]. The main active-brazing filler metals are based on the Ag or Ag-Cu system (with approximately 28 wt.% Cu), although copper, gold and palladium are also known to be used as such. The special feature of these fillers is that they contain surface-active elements that allow direct wetting of the ceramic component through chemical reactions; in this way the reaction layer formed helps to achieve a permanent chemical bond between the metal and the ceramic. The specific active metal content in filler depends on the ceramic base materials and should be under reasonable limit in order to avoid joint brittleness. A compromise between good wetting and acceptable ductility must also be found in the choice of active brazing filler: a sufficient amount of metal must be identified to ensure both a uniform reaction zone for good adhesion and wetting of the ceramic. In fact, a reaction zone that is too wide is responsible for the embrittlement of the joint. In addition, strong internal stresses are induced during the process due to differences in thermophysical properties such as Young's modulus and CTE [26]. These can significantly affect the quality of the joint and lead to premature failure of it.

In the process, the surface finish of the ceramic compound has a decisive influence on the compound strength and the metallic base material, and the brazing filler metal should be clean and free of grease. The brazing is performed in furnaces, even if induction heating is possible, in high vacuum ($<10^{-4}$ mbar); an inert atmosphere, usually argon (purity >99.998) but also helium, neon, argon-neon, is required in order to avoid contamination of oxygen or other gases which can affects joint formation oxidising the active metal. Then, the compound is firstly heated at a temperature below the solidus one of the brazing filler metal (about 50-150 °C), until a uniform heating of the joining parts is reached, and subsequently

up to brazing temperature. The holding time at this last temperature is between 5 and 10 minutes: it has to be chosen in order to achieve uniform temperature distribution in the joining area and to avoid the formation of brittle reaction products (if too long). In the end, the compound should be cooled down slowly to allow the relaxation of the thermal induced residual stresses; typically, it is equal to 5 °C/min [26]. All the stages which characterized the process are summarized in Figure 2.6.

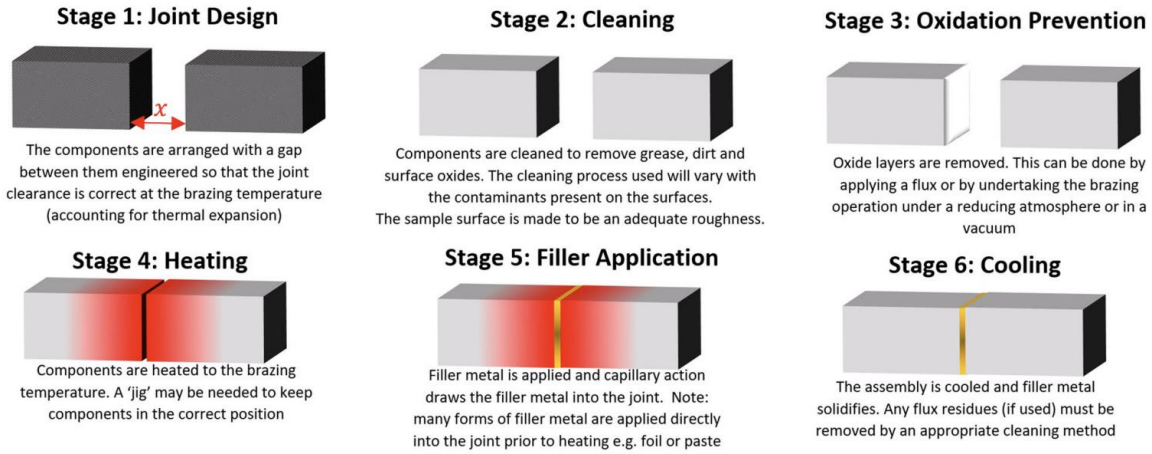

Figure 2.6: Brazing stages diagram [28]

As an alternative to the active filler, a glass solder can be used for brazing directly metal-ceramic compounds. Glass solders have a good wettability on ceramics but are characterized by high brittleness and sensitivity to differences in expansion of the joint partners.

Furthermore, to maximise the success of the process and minimise the thermal stresses induced, it is possible to use slow heating and cooling rates, or metals with a matched thermal expansion to reduce differences in CTEs, and broad the ductile brazing seam or insert soft layers. More specifically, stresses occur because, below the filler solidus temperature, metal shrinks more than ceramic due to its higher CTE. To get an idea of the stresses in the joint, a diagram is shown in Figure 2.7.

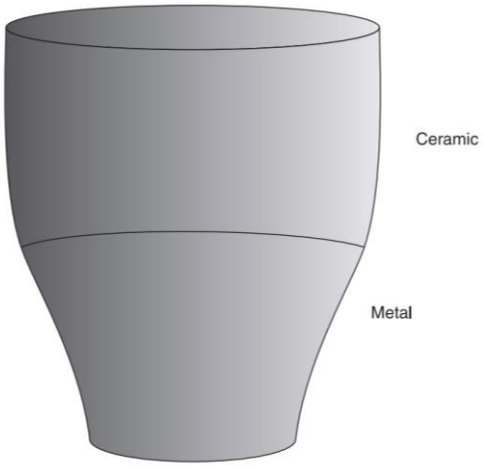

Figure 2.7: Schematic representation of stresses in a metal-ceramic compound [26]

The intensity of the residual stresses depends not only on the thermal expansion coefficient but also on the elastic constants and the geometry of the compound. In particular, high tensile stresses are seen at the edge of the ceramic and are configured as critical due to the fact that ceramic materials have a limited

structural tolerance for them. A good structural design, therefore, can be a good starting point. Then, the broad of the ductile brazing steam (e.g., Ag or AgCu base) allows to reduce the stresses through plastic deformation increasing the strength of the compound, although the risk of brittle phases formation is possible. Thus, soft layers (e.g., Ni, Cu) or layers with a matched CTE (e.g., W, Mo, Ta) are inserted in the brazing seam: they do not melt during the brazing process but interact with the filler metal, plastically deform and absorb the stresses preserving the ceramic layer. Furthermore, a combination of the two methods can be used in order to obtain a graded transition between the parts to be joined.

Furthermore, this technique is suitable to join CMCs with metals: in detail ceramic/filler interfaces are used. A good shear strength of the joint is achieved where the orientation of fibres is perpendicular to the interface: in this case, both ceramic matrix and fibres are welded to metal. However, when fibres are parallel, only the ceramic matrix part is welded to metals, resulting in reduced joining strength. Interlayers are also used to eliminate porosity [27].

The main advantage is related to the ability to achieve precise joint formation, complex shapes and heterogeneous materials [27].

2.3 "Total-SiC" joint

In order to obtain a "total-SiC" joint, the US company General Atomics (San Diego, CA) proposed a process involving an intermediate material with the same composition as the bodies to be joined [29]. The intermediate material is represented by a polymer precursor which can be specifically processed with a heat treatment in order to obtain the desired result. Substantially, the joint should have the same mechanical strength, thermal expansion coefficient and other characteristics of the articles to be joined. At the same time, it may have enhanced durability in harsh environments. So, the development responds to the need in the art to provide joints suitable for nuclear reactors, where materials used are subjected to radiations.

The joint material is composed by three main elements: a matrix corresponding to a polycarbosilane PDC, a plurality of inclusions, preferably in the form of powder distributed throughout the matrix, and a sealing layer. In particular, the inclusions may have a variety of shapes and sizes and include spheres, flakes, whiskers, fibers, irregular shapes, having diameters and/or lengths in the range from nanometers to millimetres. So, an inclusion could be shorter or longer than the critical length to enhance the mechanical performance of the joint: the first one resists pull-out from the matrix as the matrix is subjected to fracture, while the latter improves performance by bridging matrix cracks, sliding within the matrix and then fracturing. Inclusions have the aim to densify the matrix, reinforcing it and preventing the development of cracks and voids due to the shrinkage of the polymer during the conversion process, improving the strength and the durability of the joint. On the other hand, the sealing layer may penetrate partially or fully into the matrix and it is disposed to fill voids, reduce or eliminate surface flaws, increase overall density and improve the mechanical strength. It is important that the region where the sealing layer penetrates into the matrix may have the highest density to fill any residual cracks or voids.

In order to start the joining process, two flat silicon carbide bodies, the articles, are suitably cut to the required dimensions and cleaned. Then, the process consists of six stages, summarized in Figure 2.8:

a) The slurry is prepared with a preceramic polymer and a plurality of inclusions;
b) The obtained mixture is applied between the first and the second articles;
c) A curing treatment is performed on the slurry in order to form a green body;

d) The green body is pyrolyzed to form a solid ceramic containing the plurality of inclusions;
e) The solid ceramic is converted to a matrix comprising a crystallized ceramic polymorph and having the plurality of inclusions therein;
f) The joint is reinforced applying a sealant layer.

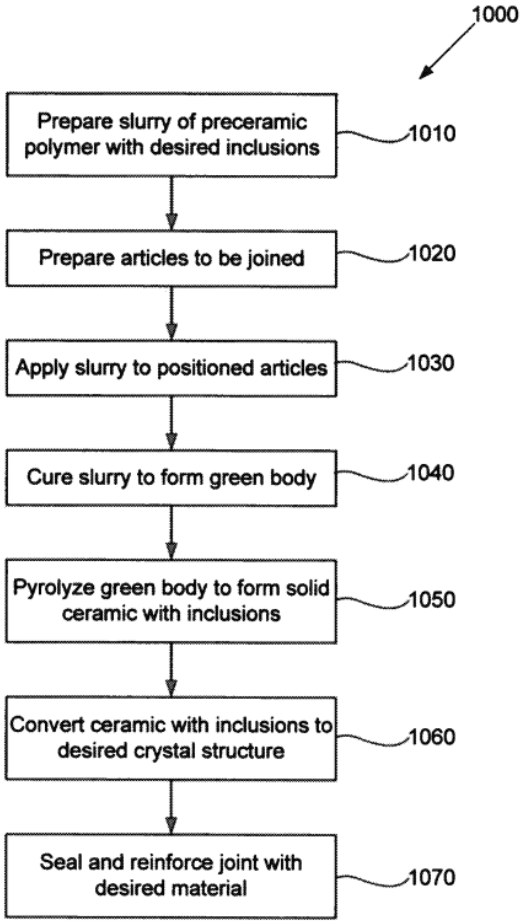

Figure 2.8: Joint preparation steps [29]

The reinforcement phase can be performed using chemical vapour infiltration (CVI): a layer of ceramic polymorph and infiltrated into the matrix is obtained. In particular, the sealing layer is deposited due to the thermal decomposition of methyltrichlorosilane (MTS) in a hydrogen carrier gas. A broad range of suitable temperatures, pressures and MTS concentration can be considered, but exemplary infiltration conditions can be 800-1400 °C, 3-1000 mbar, and MST partial pressures of 0.01-5.0 mbar. The deposition of the reinforcing layer would concern only the area of the substrates in the vicinity of the joint layer, and not the entire artefact.

The study involves all elements (articles, matrix, inclusions, sealing layer) made of β-SiC due to its strength even at high temperature and neutron fluence, and low thermal and neutron-induced expansion, but may be suitably adapted to prepare joints of other type of materials. The primary interest on this specific material is related to an obtained joined which may exhibit a desirable combination of fracture toughness, shear strength, resistance to neutron damage and impermeability to retain helium and fission products.

The resulting joint obtained is represented in Figure 2.9 due to a schematic illustration of the cross-section.

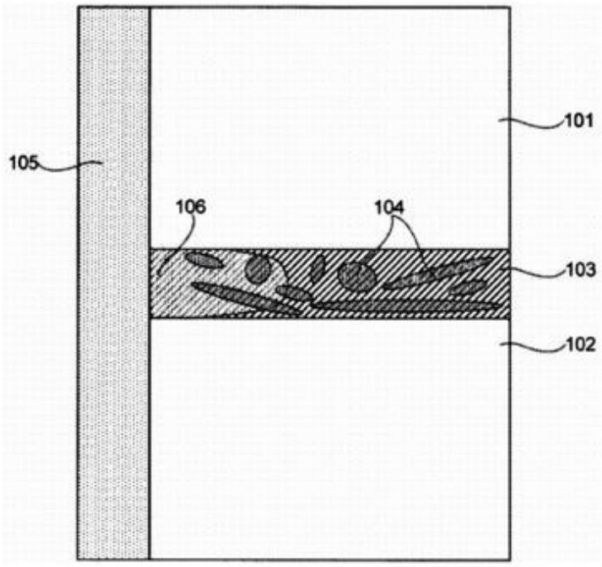

101-102	First and second articles
103	Matrix
104	Plurality of inclusions
105	Sealing layer
106	Sealing penetrated into the matrix

Figure 2.9: Schematic illustration (with references) of a cross-section joint [29]

For nuclear applications a high level of purity is desirable because it may inhibit corrosion, differential radiation-induced swelling, and mechanical stresses caused by thermal expansion coefficient mismatch: so, matrix, inclusions and sealing layer should have a purity as well as possible similar to the articles themselves. For examples, these three elements may be at least about 99% pure or 99.7% pure.

The polycarbonsilane polymer involved is a viscous liquid at room temperature in which inclusions are mixed due to mechanical mixing and ultrasonication, for a good dispersion, in order to form the slurry. Then, the obtained mixture is applied on the articles, to one or both of them, with a brush or a spatula or, alternatively, a dipping technique is used, and then the articles are positioned relative to one another. Subsequently, the conversion to ceramic polymorph is thermally guided and consists mainly of three steps. The first and the second steps are related to the formation of the "green" body: the monomers are polymerized at low temperature (e.g., 100 °C) and then the polymer is crosslinked at higher temperature (e.g., 200-400 °C). Whereas, the third step concerns properly the pyrolysis at a still higher temperature (e.g., 600-850 °C) resulting in the formation of an amorphous ceramic. In order to convert it to a crystalline one, temperature greater than 1100 °C is needed; it is also selected according to the desired result. All the steps illustrated are graphically summarized in Figure 2.10.

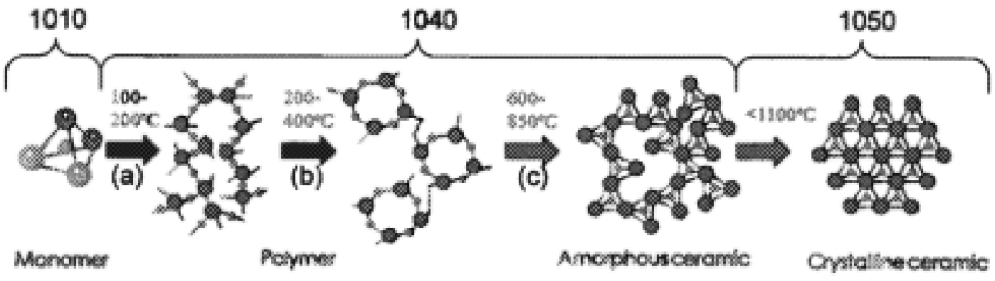

Figure 2.10: Chemical reactions of the intermediate steps [29]

Obviously, the temperatures described may be varied according to the preceramic polymer involved and the result to be achieved.

However, as the polymer-derived ceramic is converted to matrix, the gases generated form voids and cracks which are responsible for the weakness of the joint. Inclusions are needed to occupy these voids, inhibit the formation of others and contrast the shrinkage of the polymer.

Another aspect to consider is relative to the high dependence of the process on operating parameters: preferably, all the steps should be performed in an inert atmosphere such as argon or vacuum, and with a slow heating rate, in some embodiments less than about 4 °C/min, in order to avoid or inhibit the formation of gas bubbles. Prolonged process at high temperatures determines the formation of large crystal grain size suited for use in nuclear applications due to the fact that radiation may induce amorphization in finer crystal structures.

In some cases, multiple cycles of slurry application and then pyrolysis are performed in order to improve joint density.

Apart from the nuclear field, there are also applications of this type in the aerospace industry, as one works in harsh environments where joints are subject to radiation, corrosive or oxidizing chemicals, electrical discharge, extreme heat. Complex part geometries have to operate for long periods of time without degradation in performance, such as nuclear fuel cladding, thermal protection systems, heat exchangers, rocket nozzles and turbine blades.

3 Polymer-derived ceramics

Polymer-derived ceramics (PDCs), as the name suggests, refer to the synthesis of ceramic materials through proper thermal treatment (curing and thermolysis processes) of polymeric precursors under a controlled atmosphere. They could be inorganic or organometallic systems.

Even if this kind of precursors have been known since the beginning of the 20th century, industrial production began only in the 1940s with the organochlorosilane (Muller-Rochow process). The interest in polymer-derived ceramics has developed since 1960s. It is in these years that Ainger and Herbert, Chantrell and Popper have achieved the production of non-oxide ceramics for the first time by pyrolyzing polymer precursors. Later, in early 1970s, Verbeek and colleagues have produced small-diameter Si_3N_4/SiC ceramic fibres from precursors, such as polycarbosilanes, polysilanes and polysiloxanes. Later, Fritz and Raabe and Yajima et al. have been able to synthesise SiC ceramics pyrolyzing polycarbosilanes. So, the achievements have led to continued development of the PDC technology and the attainment of some successes in recent years [16], [30], [31].

The PDC approach is an advance ceramic manufacturing technique that designs or controls molecular structures of ceramic products at molecular or atomic levels. Also, they are unique due to the fact that the amorphous ceramics obtained are not achievable with any other synthesis techniques (e.g., power sintering, chemical vapour deposition). The structure is obtained through pyrolysis at low temperature and provide superior creep and oxidation resistance with respect to conventional power-based advanced ceramics, as well as more controlled intrinsic porosity, complex shaping capability, enhanced toughness, and high modulus and strength.

Preceramic polymers are characterised by many degrees of freedom: although they have a basic structure containing light elements such as C, H, O, N, B, the structure can be modified to achieve the desired final result (e.g., to enhance the mechanical and thermal properties, or introduce new ones), and temperatures and process times (cross-linking and pyrolysis) can be easily optimised. Hence, not only can they be produced with significant energy and cost savings and superior properties compared to traditional ceramics, but they can also benefit from all additive manufacturing techniques, such as 3D printing, that were previously unthinkable. However, some problems have to be considered in the polymer-to-ceramic conversion, such as shrinkage, residual porosity, and related defects which significantly reduce the mechanical strengths and moduli of the obtained components [32]. All these aspects will be covered later in the discussion.

It is therefore clear how such PDCs can be used for high temperature applications such as coatings, membranes and adhesives, reinforcements, sensors, fibres and matrices. The percentages for each of these are shown in Figure 3.1 below. Anyway, further advancements are expected to be in CMCs and advanced manufacturing.

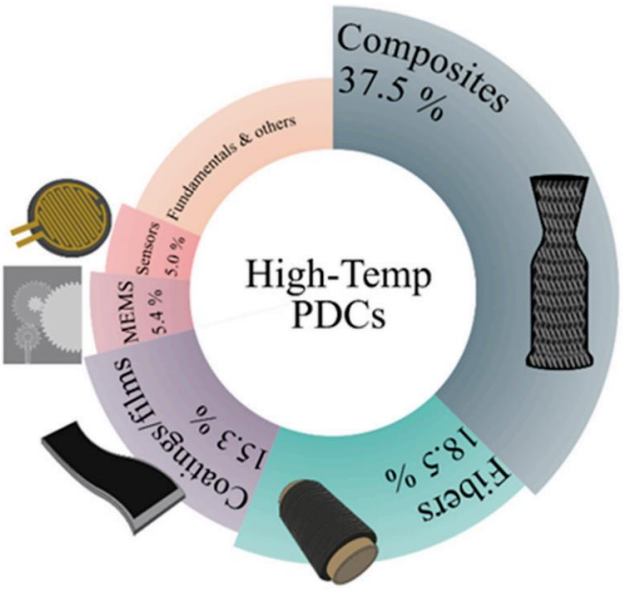

Figure 3.1: High-temperature PDCs for different applications [32]

3.1 Classes and general aspects

Preceramic polymers are mostly metalorganic compounds, usually based on silicon and additional materials, such as carbon, nitrogen, oxygen, or even metals, like boron or aluminium, in the backbone structure. Side groups, typically hydrogen, alkyl, vinyl, etc. are connected to the backbone. The properties and the composition of the final PDCs depend on both backbone group (X) and side groups or substituents (R^1 and R^2). A general oversimplified representation of the molecular structure is represented in Figure 3.2.

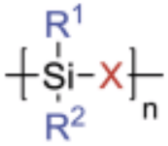

Figure 3.2: General simplified formula of Si-based preceramic polymers [30]

In particular, changing the functional groups R^1 and R^2, psychochemical behaviour can be modified and adjusted: chemical and thermal stability, solubility, electronic, optical and rheological properties are all affected from substituents connected to the silicon atoms. When side groups are organic substituents, they control the carbon content of the resulting ceramic. Formerly, a carbon excess is detrimental with respect to mechanical and high-temperature properties, so resistance to crystallization and oxidation. SiCO and SiCN ceramics are an exception. Furthermore, the modification of the atmosphere in which the process is conducted can lead to different properties. Obviously, air is the most desired atmosphere due to lower processing costs. The presence of moisture can be exploited to convert very moisture-sensitive precursors at lower cost: specifically, the formation of silane groups by hydrolysing Si-H and Si-N bonds is favoured [16]. At the same time humidity can enhance oxygen incorporation. However, oxidative or inert atmospheres are chosen according to the desired result.

The best-known classes are the binary systems such as Si_3N_4, SiC, BN, AlN, the ternary ones SiCN, SiCO, BCN and the quaternary ones SiCNO, SiBCN, SiBCO, SiAlCN and SiAlCO. On the other hand, the best-known group are the polysiloxanes, characterized by the alternation of silicon and oxygen atoms

in the backbone [16], [30]. Although, there are more types of precursors and, in order to have a complete overview of all the possible classes, the Figure 3.3 represents a summary of them.

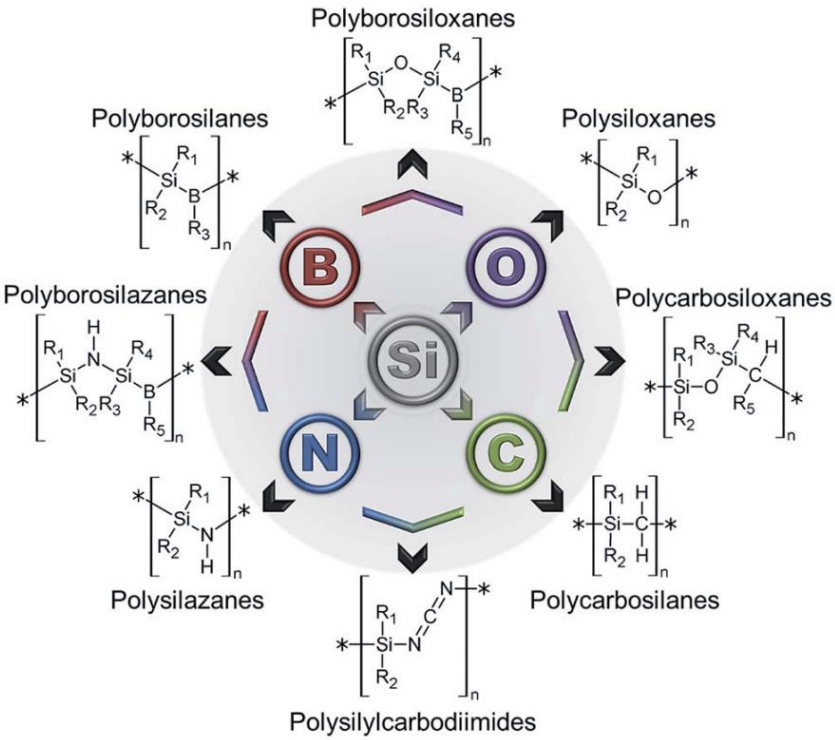

Figure 3.3: Main classes of Si-based preceramic polymers [16]

In particular, PDCs are mainly divided into polysilane, polycarbonsilane, polysilazane and polysilaxane [30], [33].

Polysilanes are characterized by a simple one-dimensional silicon backbone and their specific properties are dependent from the so-called σ conjugation due to the delocalization of electrons on Si-Si bonds. This makes it possible to confer certain properties like optoelectronic and photoelectric ones so that polysilanes can be used for applications in photoresists, photoconductors, semiconductors, and hole-transporting materials. Also, they can be used as precursor for silicon carbide-base ceramics. The most general and common procedure for the synthesis of this type of polymer is the Wurtz-type reductive dehalogenation reaction, even if an alternative method is the catalytically dehydrogenative oligomerization of hydrosilanes in the presence of transition metal complexes.

Polycarbonsilanes have structures containing Si-Si and Si-C bonds whose complexity depends on the different forms of carbon chain in the backbone (e.g., methylene, vinylidene, phenylene, etc.). This results in different ceramic yields: it increases with the increase of the molecular weight and greatly influences the quality of SiC ceramics. Therefore, some kinds of these polymers have an alternating arrangement of a π-conjugated unit, called unsatured polycarbonsilane. They are widely used for electric or photo conductor, photoresist, nonlinear optical materials, as well as precursors for SiC fibres, whiskers, powders, and nanomaterials. There are several methods of synthesis, the most common of which is under high or atmospheric pressure; others include coupling reactions, thermal cyclopolymerization, and a variety of ring-opening polymerisation.

Polysilazane polymers consist of alternating backbone of Si-N bonds with carbon-containing side groups. This is the reason why they are used as SiCN ceramic precursors. Due to the smaller Si-N bond energy with respect to the ones of Si-O and Si-C bonds, the bond can be easily transformed into other ones in some chemical reactions. This kind of polymers are characterized by high thermal stability,

oxidation and corrosion resistance, so that they can be used as barrier for heat exchangers. Other applications are related to precursors for SiN_x dielectrics and antigraffiti coatings. On the other hand, carbon-free polysilazane, perhydropolysilazane, can be used as Si_3N_4 ceramic precursor. The synthesis methods are the ammonolysis reaction of chlorosilanes with ammonia or aminolysis with different primary amines, even if ring-opening polymerization of cyclic polysilanane is used. In order to improve chemical and physical properties, the modification of silazane oligomers with urea or isocyanate-containing compounds can be performed. In addition, depending on the processing conditions, the ceramic composition can change from binary (Si/N) to ternary (Si/C/N) ceramics, or also quaternary systems.

Polysiloxanes, or silicone, are characterised by Si-O backbone: the low intermolecular force between silicon-oxygen-silicon atoms is responsible for the flexibility of the polymer. As a result, the glass transition temperature results low. Many of them have excellent chemical, physical, and electrical properties, shows good resistance to high temperature or ozone, low surface tension and energy, as well as high gas permeability. The main synthesis methods include ring-opening polymerization of cyclic silaethers and polycondensation of linear silanes. Also, dimethyl-dichloro silane is used for industrial synthesis. Moreover, cross-linked polysiloxane is able to achieve a higher ceramic yield and can be synthetized through the modification of thermal or irradiation-sensitive curing chain groups or sol-gel method by hydrolysis and condensation of hybrid silicon alkoxides.

Other PDCs are polysilycarbodiimides and boron-containing silicon polymers such as polyborosilane, polyborosiloxane, polyborosilazane and their derivatives. The first ones, made of N=C=N group and substituents like hydrogen, phenyl, methyl, ethyl, are precursors for fabricating SiCN-based ceramics. In contrast, the second ones are used as precursors for fabricating borosilcon ceramics.

A general overview is summarised in Table 2.

Organosilicon polymer	Backbone structure	Synthesis methods	Applications
Polysilane	$–R_1R_2Si–$	Wurtz-type coupling of halosilanes Anionic polymerization of masked disilenes Catalytic dehydrogenation of silanes Reduction of dichlorosilanes	Photoresists Photo conductors Semiconductors Precursors for synthesis of polycarbosilane
Polycarbosilane	$–R_1R_2Si–C–$	Kumada rearrangement of polysilanes Ring opening polymerization Dehydrocoupling reaction of trimethylsilane Hydrosilylation of vinylhydridosilanes Grignard coupling reaction of (chloromethyl)-triethoxysilane and vinylmagnesium bromide	Precursors for preparation of SiC Electric or photo conductors Photoresist Nonlinear optical materials
Polysilazane	$–R_1R_2Si–N=$	Ammonolysis reactions of chlorosilanes with ammonia or by aminolysis Ring opening polymerization of cyclic polysilanane	Precursors for preparation of Si_3N_4 or SiCN Barrier for heat exchanger or on steel against oxidation
Polysiloxane	$–R_1R_2Si–O–$	Ring-open polymerization of cyclic silaethers Polycondensation of linear silanes	Precursors for preparation of SiOC Medicine Electronics Textile chemistry
Polysilylcarbodiimides	$–R_1R_2Si–N=C=N–$	Pyridine-catalyzed polycondensation reaction of chlorosilanes with bis(trimethylsilylcarbodiimide)	Precursors for preparation of SiCN
Polyborosilazane	$–R_1R_2Si–N(R_3R_4B)–$	Co-condensation reaction of boron trichloride, organodichlorosilanes, and hexamethyldisilazane	Precursors for preparation of SiCBN

Table 2: Summary of backbone structure, synthesis methods and applications of most common preceramic polymers [33]

It is important to underline that the properties of final polymer-derived ceramics are either greatly determined by subsequent processes including shaping, cross-linking, and sintering.

3.2 Characteristics

The growing interest in preceramic polymers is due to the fact that they are cheaper than traditional ceramics and that they can be used to create products with new compositions and exceptional or unusual properties [31].

1. Designability. The structure, composition, and preparation process (temperature and time) can be adjusted in order to control the phase composition and to tune the microstructure of the final ceramic product desired.

2. Good moldability. Ceramics with complex shapes can be produced, including one-dimensional ceramic fibres, two-dimensional coatings, three-dimensional micro-electro-mechanical systems (MEMs), and ceramic composites. At the same time, the solubility of precursors can also be used to obtain dense fibre-reinforced ceramic matrix composite. In particular, the fibre of the precast are impregnated with the polymer which is able to fill the voids in ceramic matrix after all the steps process; the process can be repeated until the desired result is achieved.

3. Low sintering temperature. Unlike conventional ceramics, which require high sintering temperatures, typically above 1600°C, polymer precursors can be sintered at temperatures below 900°C.

4. No sintering additives required. Preceramic polymers make it possible to avoid the use of sintering aids required for traditional ceramics. These are necessary to accelerate the diffusion of atoms and thus promote sintering, but their residues at the grain boundaries undermine oxidation resistance and mechanical properties at high temperatures. Eliminating them makes it possible to achieve good oxidation resistance at high temperatures, as well as high-temperature creep resistance.

5. High-temperature performance. It relates to the achievement of a highly pure matrix through the absence of additives, resulting in good high temperature properties such as creep, oxidation and corrosion.

3.3 Processing

The manufacturing process of a Si-based ceramic consists of five steps: synthesis, shaping, cross-linking, pyrolysis and crystallization. There has already been a brief discussion in section 3.1 of how the various precursors can be synthesised, so this aspect will not be discussed further.

The core of processing is based on shaping processes unthinkable for traditional ceramics and lower temperature than those used in traditional sintering (800-1500 °C vs. 1900-2200 °C), and can be used [34]. Instead, the remaining steps will be discussed in the following sub-sections and a little preview is represented in Figure 3.4 .

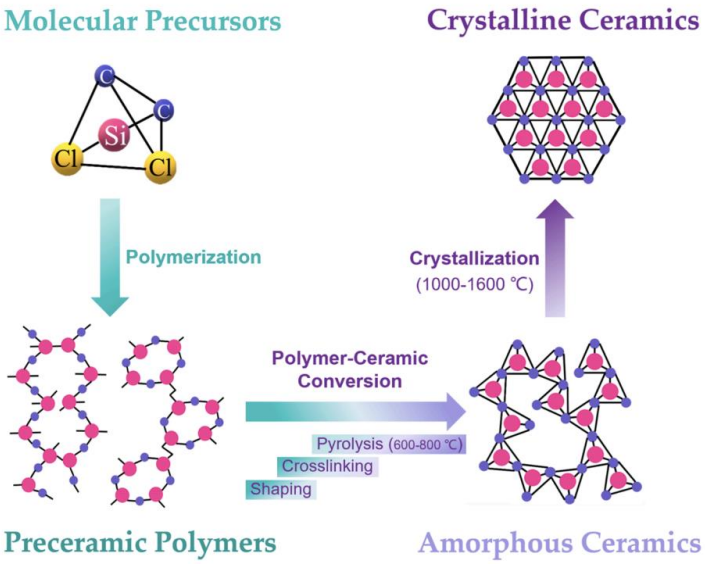

Figure 3.4: Process overview [35]

3.3.1 Shaping

Firstly, the conventional shaping process uses ceramic powders to which a certain amount of polymeric binders is added. These are dissolved in an organic or aqueous solution, which will be burned out during sintering. On the other hand, the process is not straightforward due to the low rheological properties of powders and the need to control the polymer binder [33], [35].

In the case PDCs, this step is simpler as there is no need for preparation and the preceramic polymer can be used directly for shaping as a liquid. The advantages are therefore that slurry processing methods can be used, the viscosity of the precursor can be controlled and, because it is a liquid, it is easier to purify, thus reducing impurities in the final ceramic product [2]. Besides, the technological advantages over powder-based and the sol-gel approaches include no drying problems or long gelation and drying times, and a constant rheology throughout the process window. In addition, their solutions are stable over long periods and can be easily loaded with fillers for the production of ceramic composites. In the case of solid precursors, they can be dissolved in organic solvents or melted at low temperatures below 150 °C [35].

A distinction can be made between more standard technologies such as uniaxial, isostatic and warm pressing [36]–[38], and more innovative technologies such as extrusion, injection moulding, spraying, dip coating, spin coating, chemical vapour deposition, 3D printing and additive manufacturing [31], [35]. The latter in particular make it possible to produce components that would be impossible to achieve with powder processing. A brief summary of the most commonly used technologies is shown in the Figure 3.5 and Figure 3.6 below.

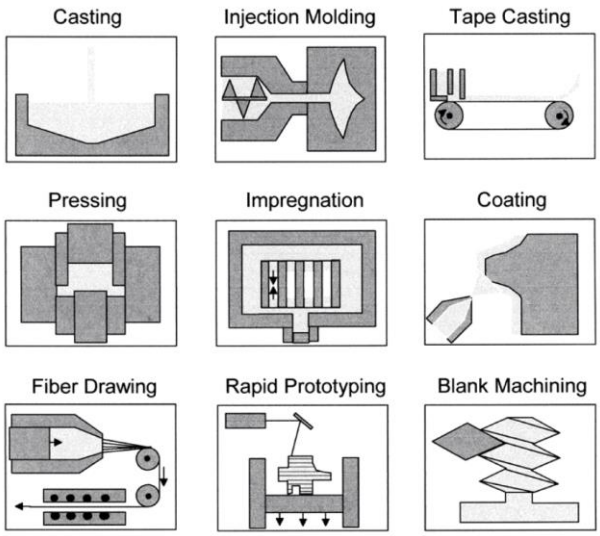

Figure 3.5: Common shaping techniques for PDCs manufacturing [34]

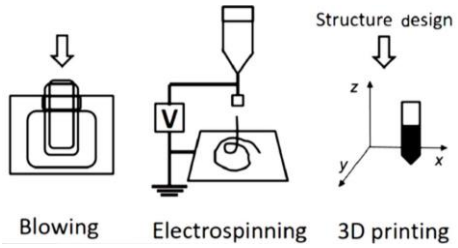

Figure 3.6: Innovative shaping technologies for PDCs manufacturing [31]

The current state-of-the-art includes ceramic fibres, coatings, ceramic tapes and foams, ceramic matrix composites, ceramic joints. In the end, it is clear how the use of precursors enables the design of components with finer details and eliminates the problems associated with tool wear and brittle fracture upon finishing the component.

3.3.2 Cross-linking

After the shaping step, it is essential that the obtained parts retain their shape during the final ceramization process: cross-linking, also known as curing, usually thermal, is therefore the next step, even if in the case of liquid precursors curing takes place at the same temperature as shaping and can be further improved by heating at low temperatures [35]. The cross-linking process consists of a series of reactions that lead to changes in the composition and properties of the starting polymer. In particular, preceramic polymers are transformed into thermosets by thermal crosslinking at temperatures below 200 °C: functional groups, such as Si-H, Si-OH, Si-vinyl functionalities, are incorporated by spontaneous condensation or addition reactions and a 3D polymeric network is formed, turning the precursors into unmeltable and insoluble preceramics [16], [35].

In order to obtain highly cross-linked preceramics, a certain latent reactivity is required due to the composition of the precursors, i.e. a mixture of oligomers and low molecular weight polymers that are easily volatilised and depolymerised. This process therefore allows volatility to be reduced, resulting in an increase in mass yield during polymer-to-ceramic conversion [16].

The cross-linking temperature can be further lowered by using catalysts. Their use has the additional benefit to reduce the evaporation of oligomers, avoiding the formation of bubbles. Even if catalysts are not used, bubble formation can be eliminated due to overpressure application using a silicone oil medium or gas [30] [35].

Obviously, the ideal conditions for cross-linking and the subsequent conversion from polymer to ceramic depend on the chemical structure of the precursors: by changing the main parameters, such as temperature, heating rate and atmosphere, it is possible to obtain materials with different properties, starting from the same polymeric precursor. For this reason, curing must be carefully controlled. In the past, the most common technique was oxidative curing, but the resulting ceramic was characterised by significant oxygen contamination, of around 15 wt.%, leading to a reduction in high temperature stability. Today, many different atmospheres can be used, such as ammonia, thionyl chloride, nitrogen dioxide, nitric oxide, halogenated or unsaturated hydrocarbons; reactive plasmas based on ammonia, methane, nitrogen, hydrogen, water, oxygen, silane or borane gas have also been proposed. [30].

However, another cross-linking option is UV polymerisation, which can be achieved after the addition of photosensitive functional groups to the PDC backbone [30]: curing is realised under illumination at a specific wavelength in order to obtain a non-molten polymer [31]. This approach is suitable for the fabrication of microcomponents and fibres. Other methods involve γ-ray or e-beam irradiation, performed in vacuum or protective atmosphere to produce oxygen free ceramics; moreover, the applicability of the first one is limited to fibres, due to low penetration depth, while the second one is suitable for thicker curing depending on beam energy and material density [35]. It is also possible to add filler particles: these strongly influence the rheology of the preceramic polymer, so that if a large amount is added, curing may not be necessary, as the solid additives are sufficient to maintain the shape of the part during heating.

3.3.3 Polymer-to-ceramic conversion

The polymer-to-ceramic conversion step is also known as pyrolysis or ceramization. It is a heat treatment carried out at temperatures above 300 °C, typically up to 900-1000°C, which leads to an organic-to-inorganic transformation, from a thermoset polymer into an amorphous ceramic [16]. The transformation is caused by rearrangements, condensation and radical reactions, resulting in the formation of new bonds and the removal of organic groups, such as CH_4, C_6H_6, CH_3NH_2, NH_3, and H_2; indeed, CO and CO_2 are eliminated especially in oxidizing environment.

This is the most sensitive part of the process because the phase composition, structure and properties of the amorphous ceramics obtained are strongly dependent on it, so on the all parameters that have an influence [31]. The most important ones are heating rate, reaction temperature, dwell time and reaction atmosphere [30], [33], [35].

About reaction atmospheres, inert or reactive gases, can be used and, as a result, different ceramic yields and chemical/phase composition can be obtained [39]. The most widely used are argon or nitrogen, due to the fact that gradually eliminate the gases emitted from the precursors, while oxygen and vacuum are used for the formation of silicate ceramics and to promote crystallization via carbothermal reduction reactions, respectively [35]. However, the chosen atmosphere will not react with any fillers that may have been added to the polymer. In terms of heating rate, this influences the formation of cracks and pores as a result of the release of gas during the transformation: a low value, e.g. less than or equal to 2

°C/min, must be kept constant at least in the temperature range where the polymer-to-ceramic transformation takes place [30], [35].

Suitable processes to perform ceramization are hot pressing, spark plasma sintering, chemical vapour deposition, plasma spraying, rapid thermal annealing, laser pyrolysis, and microwave deposition [35].

On the other hand, Si-based ceramics derived from organosilicon polymers often suffer from the cracks, forming pores and large shrinkage [2], [16], [30], [31], [33]–[35], [38], [39]. Usually, a mass loss in the range of 10-30% [34] is associated to the conversion. In addition to the change in mass, a change in volume is found due to the densification of the polymer: the density varies from about 1g/cm^3 as a precursor to >2 g/cm^3 as a ceramic (e.g., SiO_2, 2.2-2.6 g/cm^3, Si_3N_4 and SiC, 3.0-3.2 g/cm^3 [34]), so density increases together with the mass loss. As a result, the volume of the material decreases during the ceramization process and thus does not leave the material unaffected. The effects are related to shrinkage and porosity formation. The first one is the most evident and can be approximated as linear, reaching values up to 40%, while the second one is caused by the release of gaseous products in the early stages of the process. At temperatures above 400 °C, an open-pore channel network is formed that, upon further heating up to 800-1000 °C, can diminish [34]. In particular, it is known as residual porosity due to the fact that the open pores formed may disappear through thermal treatment and shrinkage, but a residue is always present [16].

It is easy to see that these effects are negative, since shrinkage in particular leads to the formation of residual stresses in the resulting ceramic. Stresses will occur when different parts of the system shrink at different rates and this can lead to cracks formation. Cracks are responsible for the reduced mechanical performance of the component, as well as dimensional accuracy and structural integrity, sometimes leading to component collapse during pyrolysis. A solution is represented by adding active or passive fillers and carefully choosing heat treatment to minimise shrinkage. However, the discussion on fillers is further elaborated in the section 3.5.

Of course, all process choices depend on the desired result: sometimes the processing is terminated once the amorphous ceramic has been obtained, since crystallization is not necessary or even undesired for a great number of applications.

3.3.4 Crystallization

The crystallization step is the last one of the polymer-to-ceramic conversion, in which the amorphous ceramic is transformed into crystalline one. The crystallization happens when the heat treatment temperature increases above 1000 °C, so a suitable temperature range is 1200-1800 °C [16], [31]. However, the PDCs majority, and especially ceramics containing oxygen, may crystallize at temperature as low as 1000-1200 °C, while some others have the capability to avoid crystallization at temperatures up to 1700 °C.

In particular, the amorphous-crystalline transition is characterised by a rearrangement of the structure as a result of the breaking of relevant chemical bonds with increasing temperature. The result is a separation of the ceramic and carbon phases to form a multiphase ceramic system, which in turn promotes nucleation. Finally, the crystalline nuclei formed gradually increase with increasing temperature and time. the whole process is accompanied by decomposition reactions, together with the formation of small amounts of gaseous products [31].

A parameter used to measure the efficiency of the conversion from preceramic polymer to ceramic material is the ceramic yield α_c, defined as the ratio between the residual mass after the complete transformation and the initial mass of the polymer [16]. Typical values are in the 70-90 wt.% range, although even higher ones have been reported when reactive atmospheres are used [34].

The whole process is illustrated in the following figures. In detail, Figure 3.7 shows the mass loss related to the temperature increase during the different process steps in the case of a polycarbosilane under inert atmosphere. As expected from the previous descriptions, the pyrolysis step is the one where the greatest mass loss occurs.

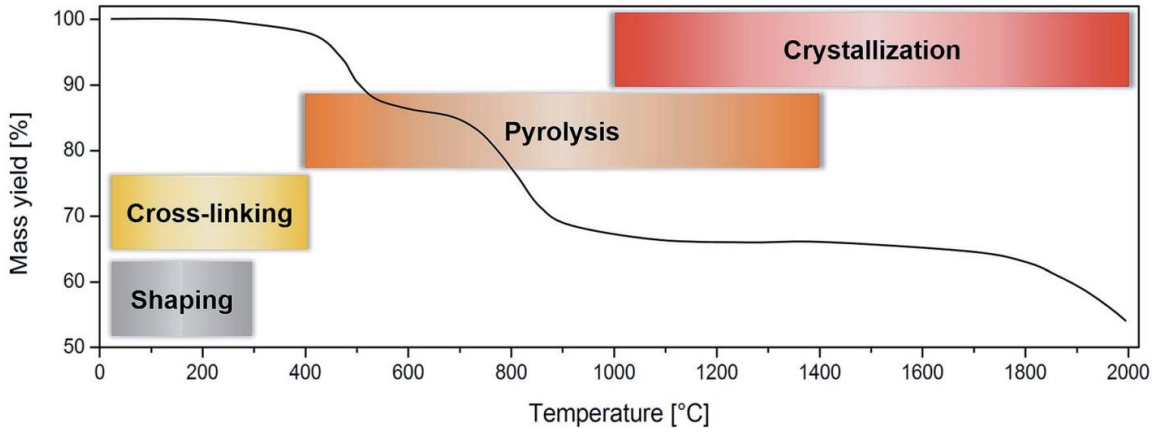

Figure 3.7: Mass changes with temperature in case of a polycarbosilane under inert atmosphere [16]

Similarly, it is possible to correlate the density increase during conversion with the temperature increase. Figure 3.8 shows the density increase related to the temperature increase during the different process steps in case of conversion of a poly(organo)silazane into SiCN, when pyrolysis is performed under protective atmosphere.

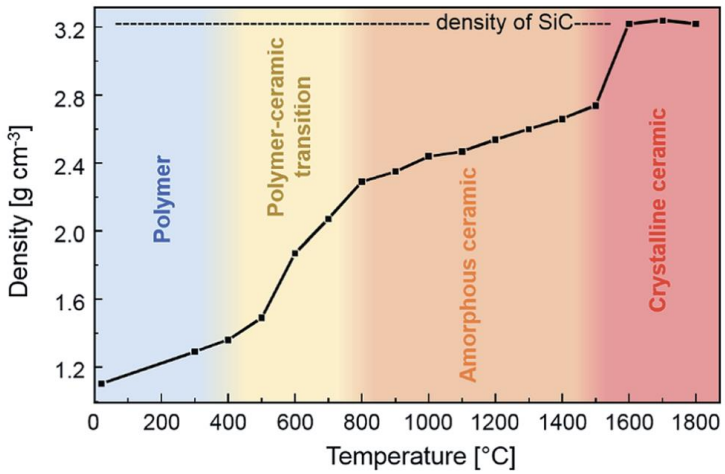

Figure 3.8: Density increase with temperature in case of poly(organo)silazane into SiCN under protective atmosphere [16]

3.4 Properties

3.4.1 Mechanical properties

Due to the fact that PDCs release a large amount of small molecule gases, such as CH_4, H_2, CO, CO_2, in the polymer-to-ceramic conversion creating a porous structure and shrink during pyrolysis, the resulted ceramics have lower mechanical properties than traditional ones. So, this shortcoming severely limits their applications in fields like aerospace, turbine, and leads to the need to improve to broad the scope.

In addition, the mechanical properties study is limited by the fabrication of suitable bulk test specimens. Nowadays, two methods have been developed: power route and liquid route. They lead to the formation of dense, crack-free, monolithic PDCs, and fully dense, small rods or thin plates suitable for flexural strength and fracture mechanics measurements, respectively. It has been possible to measure the values of the mechanical properties of the Si-C-O and Si-C-N systems at different pyrolysis temperatures [30]. The elastic modulus (E) range values is well below the one of crystalline SiC or Si_3N_4, reflecting the open structure of the PDCs networks. The range identified is of ≈57-113 GPa for SiOCs and ≈80-155 GPa for SiCNs. Again, due to the open amorphous structure, low values of the density are measured. As a general trend, they increase with pyrolysis temperature due to the increase in network connectivity as a result of hydrogen stripping of C-H bonds. Also, the Poisson's Ratio (ν) values are quite low: from 0.21 to 0.24 for SiCN system, while an equal value to 0.11 for SiCO one; this last value is attributable to the low atomic packing density and high cross-linking degree of silicon carbide. In terms of Vickers hardness (HV), since SiOC and SiCN are open-structure, low-density systems, the deformation mechanism has a greater contribution from the densification volume, leading to the formation of circumferential Hertzian cone cracks around the indenter impressions. The range values measured are ≈5 to 9 GPa and ≈8 to 15 GPa, respectively. The ways to increase the hardness are to increase the pyrolysis temperature or to increase the concentration of C in the amorphous silica network. In addition, Si-based PDCs exhibit a remarkable creep resistance, but the property that sets PDCs apart from other known ceramics is their viscosity, which is two to three orders of magnitude higher than vitreous silica and is certainly the highest measured for a high-temperature glass. The inelastic behaviour of these amorphous materials is due to stress transfer from the silica, which experiences viscous flow over a range of high temperatures, and the graphene network. When the stress is relieved, the elastic energy stored in the graphene regions is the driving force for strain recovery.

At the present, two are the main common methods to improve the mechanical properties: doping and densification. The first method involves the use of a second phase of particles that strengthen and toughen PDCs through crack deflection, detouring, branching, pinning and other effects. Usually, Al-salt, Zr-salt, and Ti-salt are the most commonly used [38] and significant improvements have been achieved. On the other hand, the second one involves three different processes such as polymer impregnation pyrolysis (PIP), chemical vapour infiltration (CVI), and liquid silicon infiltration (LSI). The purpose is to fill the defects like pores and cracks, although they have different mechanism and densification levels.

In addition, the oxygen content is an important factor to be considered due to the fact that has a significant influence on the mechanical properties, especially at high temperatures. Specifically, as the oxygen content increases, the density of the resulting amorphous ceramic decreases. If the content is too high, it accelerates the carbothermal reduction reaction, releasing a large quantity of small molecular gases and making it difficult to densify the matrix. A specific case is represented by SiC with an excessive oxygen content: it is responsible for the formation of SiOC phase which decomposes above 1200 °C, resulting in weight loss and strength reduction. To avoid this phenomenon, the oxygen content should be limited to less than 1.30 wt.%.

3.4.2 Chemical properties

In high-temperature applications, oxidation resistance and chemical durability are of primary interest [30]. With regard to the former, a parabolic oxidation rate can be observed for PDCs pyrolyzed at temperatures high enough to completely remove hydrogen from the system. In this case, the polymer-to-ceramic conversion results in a dense, continuous oxide layer, free of bubbles and cracks, with a sharp oxide-ceramic interface. More in detail, the values for the parabolic constant and the activation energy are the same as those for pure SiC and Si_3N_4. Also, studying the oxidation kinetic, it has been found that Si-based PDCs exhibit higher stability than their crystalline counterparts due to the role of mixed SiC_xO_{4-x} units at the interface between the amorphous SiO_2/Si_3N_4 clusters and graphene layers. This demonstrates the role of mixed bonds in the atomic structure on the enthalpy of formation: if present, the energy of formation tends to be negative. The addition of extra elements plays a role in the oxidation behaviour: the addition of boron, for instance, reduces the oxidation rate, though it is still close to that of SiC/ Si_3N_4, while the addition of Zr reduces the oxidation rate in conjoint with a reduction in the C-activity of Zr-free system.

With regard to the second one, a study by Sorarù et al. examined the behaviour of silicon oxycarbide glasses containing different amounts of "free" C in highly basic or acidic (HF) solutions. In particular, due to the bonding properties and higher rate of compositional disorder and cross-linking of the carbon network, the SiCO network has a higher durability than pure silica glass, SiO_2, in both basic and acidic solutions. The explanation lies in the fact that Si-C bonds are less available for nucelophilic attack and that the presence of free or Si-bonded carbon prevents local transport of the reactants. On the other hand, if SiCO is pyrolyzed at temperatures equal to or higher than 1200 °C, the chemical durability decreases since there is a phase separation into SiO_2, SiC and carbon regions [40].

3.4.3 Thermal properties

Thermal properties are essential for high temperature applications, too. They mainly include parameters such as thermal conductivity (K), coefficient of thermal expansion (CTE), specific heat capacity (Cp), thermal diffusion rate (α), thermal shock resistance (TSR). Thermal conductivity is of most concern and is controlled by phonon transmission, so it is important to consider the microstructure of the materials, i.e. impurities, crystallinity, grain boundaries, microcracks and micropores, as they have a major influence on phonon scattering [38] and, generally, they tend to aggravate it in the phonon transmission process, reducing the thermal conductivity.

In particular, when talking about impurities, it is necessary to consider two different parts: on the one hand, the phase generated during the heat treatment, which refers to free carbon, and on the other hand, the dopants introduced to adjust the thermal properties. Depending on the type of PDC considered, precipitation of free carbon can increase or decrease thermal conductivity, the former being SiOC and the latter being SiC.

Moreover, thermal conductivity is modified by doping phases, in which boron-containing compounds are very important. One example is the addition of boron nitride nanotubes (BNNTs) to PDC and it has been shown that the thermal conductivity actually increases as the amount of BBNTs increases. Also, when the content exceeds the percolation threshold (36 vol%), a percolation network is formed, leading to a jump in thermal conductivity [38], [41].

3.4.4 Electrical properties

The main electrical parameter of interest is the direct current (DC) electrical conductivity: usually, it varies from 10^{-10} to 1 S·cm and depends on temperature, phase composition, microstructure, and porosity.

About the microstructure, the main conductive phase in PDCs is the precipitated free carbon. In particular, when the free carbon content increases also the electrical conductivity increases and when the last one has a sudden change in the increasing process, the percolation threshold appears. The conducting regimes can be explained through three different models, as it is possible to see in Figure 3.9. Specifically, in order to understand the figure, (1), (2), and (3) represent SiC-based nanodomains, free carbon ribbons, and α-SiC nanoparticles, respectively.

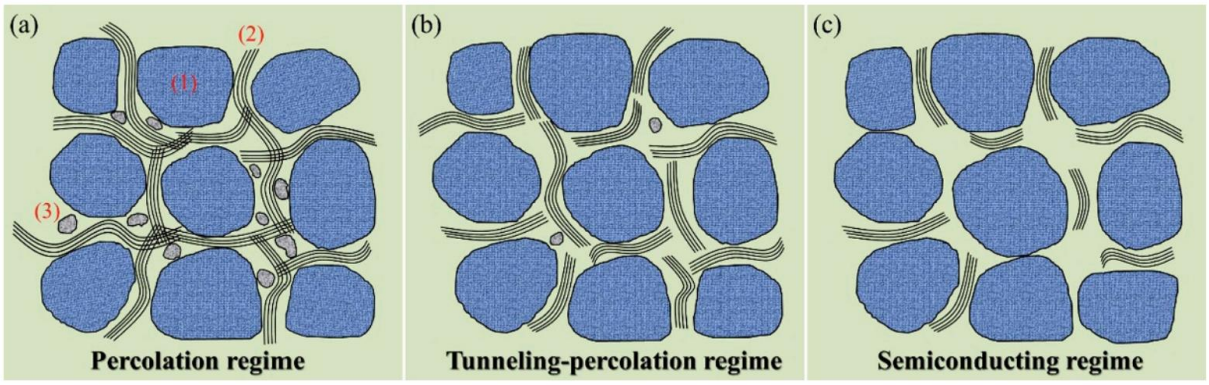

Figure 3.9: Models for conducting regimes of PDCs [38]

The percolation regime checks when the free carbon content exceeds the amount required to form a percolation network and thus current conduction is achieved by direct transport of charge carriers. While, the tunnelling-percolation regime happens when the free carbon content is only higher than the threshold value of the tunneling process, so a percolation network is not formed. In the end, semiconductors regime verifies when the free carbon content is lower than the tunneling percolation threshold.

However, in order to increase the electrical conductivity, a way is to add conductive phases. One such example is the addition of a doped boron phase to SiOC: the result is an increase in electrical conductivity by two orders of magnitude (from 10^{-5} to 10^{-3} S·m) [38], [42].

In addition to microstructure and phase composition, also pores have a great influence, in a negative way: as PDCs porosity increases, the electrical conductivity decreases.

Furthermore, the temperature effect is due to the fact that it affects the microstructure evolution. In particular, the increase in temperature during the various stages of the sintering process first allows the growth of so-called carbon clusters, which then split into nanocrystallised carbon and then migrate towards the grain boundaries of the ceramic component formed. When grain boundary formation is complete, the carbon that has segregated along them forms a network of turbostatic carbon. The Figure 3.10 illustrates all these phases, taking the effect of temperature on the microstructure of SiC, studied by Xu et al. [43].

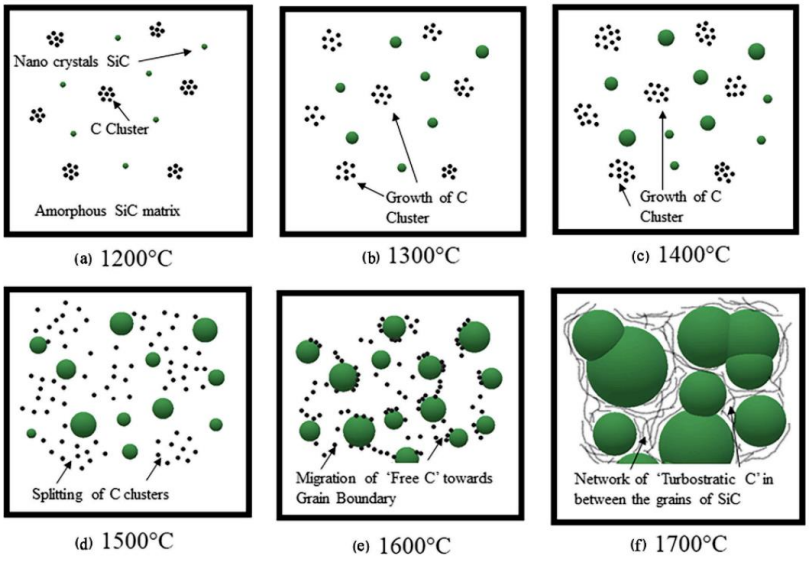

Figure 3.10: Temperature effect on microstructure evolution [43]

3.4.5 Electromagnetic properties

PDCs are attractive because of their broad absorption characteristics, combined with their controllable microstructure and light weight. Generally, the use of dopants is common practice so that the ceramic precursors have a more powerful electromagnetic wave adsorption capability. The electromagnetic wave loss mechanism is often a combination of magnetic loss and dielectric loss [38], according to the dopants used. So, magnetic materials, such as Fe, Co, Ni, are able to dissipate electromagnetic waves through natural resonance or eddy current loss, while dielectric materials, such as carbon, graphene, dissipate through conduction and polarization losses. Therefore, in order to enhance the electromagnetic performance, special structures can be developed with peculiar microstructures, including porous structures, core-shell structures, and heterostructures, promoting interface polarization, multiple reflection, and synergistic effects.

When considering the incorporation of metallic iron atoms into the backbone of the polymer precursor, ferrocene is the most prominent example of organometallic species [30].

On the other hand, the magnetic properties of the resulting ceramics depend not only on the structure but also on the pyrolysis conditions: in fact, pyrolysis of Si-containing polymers in the same nitrogen atmosphere leads to the formation of ceramics containing mainly α-Fe nanoparticles, whereas Ge- and Sb-containing polymers are completely converted into their iron alloys [30].

3.4.6 Optical properties

Optical properties are the least considered of all, because PDCs are generally black: the colour is given by the presence of sp^2-hybridised C atoms in the ceramic structure forming absorbing graphene layers. However, the ability to control the chemical composition of a precursor makes it possible to produce transparent ceramics that minimise the presence of free carbon. In this respect, SiCO systems are of great interest. In particular, Sorarù and colleagues used precursors with Si-H functionalities to prove their thesis [30], [44]. These groups not only reduce the C content, but also provide a reactive motif

during pyrolysis to create new Si-C bonds. This made it possible to produce very small transparent discs of SiCO glasses. The most transparent glasses obtained exhibit an optical absorption edge at 500-550 nm. Also, the photoluminescence spectra show a luminescence band centred at about 500 nm due to the sp^2 C clusters presence. This result is an excellent example of a trade-off: the concentration of the clusters is high enough to give intense luminescence, but low enough to make the glass transparent.

In the end, other studies could be proposed about SiCO glasses doped with Eu or Er, or synthesis of SiCO thin films containing Si, SiC, and C nanoclusters. In the first case, Eu^{3+}-based luminescence was observed up to 400 °C, and a broad blue emission band, centred at 450 nm, was identifies at higher pyrolysis temperature, due to the reduction of Eu^{3+} to Eu^{2+}. In the second case, however, it was observed that the pyrolysis temperature affects the luminescence: low temperatures (800-1000 °C) produce blue UV luminescence, while high temperatures favour green-yellow luminescence.

3.5 Fillers

Fillers represent an innovative approach to manage shrinkage and to reduce porosity during the polymer-to-ceramic conversion; in addition, microstructure and properties of ceramics can be tailored [16]. In particular, they can be added before the shaping step in order to achieve:

i) Relatively dense and crack-free ceramics with low shrinkage;
ii) Ceramics containing specific amount and features of porosity;
iii) Ceramics with desired functionalities.

Subsequently, the cross-linking step allows to bind the fillers together at low temperature making the materials easy to handle before the heat treatments [35].

They can be of different nature (e.g., ceramic, polymeric, metallic), various morphologies/dimensions (e.g., powders, platelets, fibres in nano/micrometer scale) and various kinds (e.g., passive, active, meltable, sacrificial) [30], [34], [35]. Of course, a different result may be obtained depending on the type of filler chosen. The Figure 3.11 shows not only the different fillers used, but also how they behave after pyrolysis.

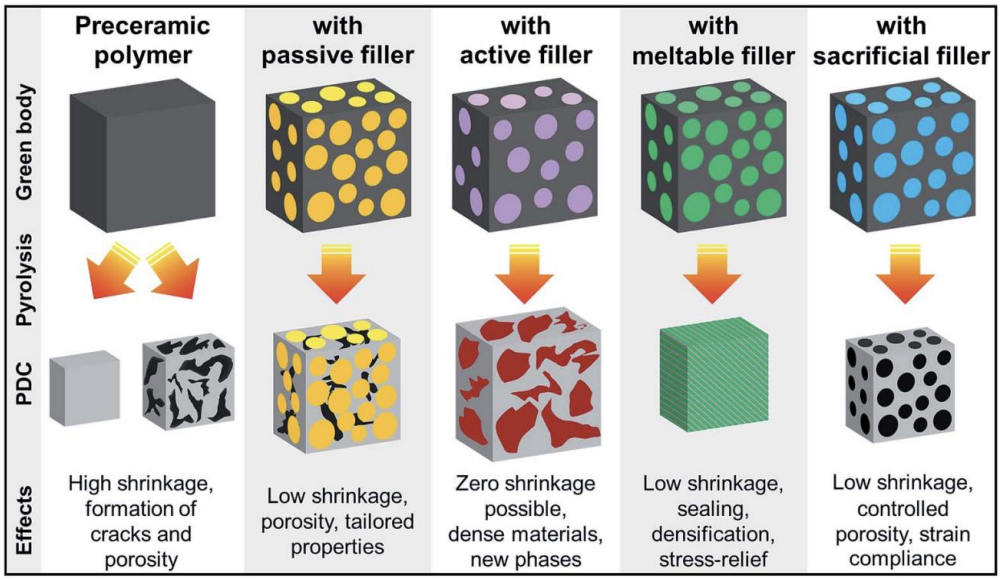

Figure 3.11: Effect of different types of fillers on PDCs [16]

The different results that can be achieved with passive and active fillers are well illustrated in Figure 3.12 below. In particular, the interaction between the polymer, in this case a polysiloxane, and the filler of interest is highlighted. In the case of the passive filler, there is a simple physical bond, whereas in the case of the reactive filler, there is the formation of primary bonds, such as oxygen bridges, which are responsible for the generation of interconnected filler network microstructure [45].

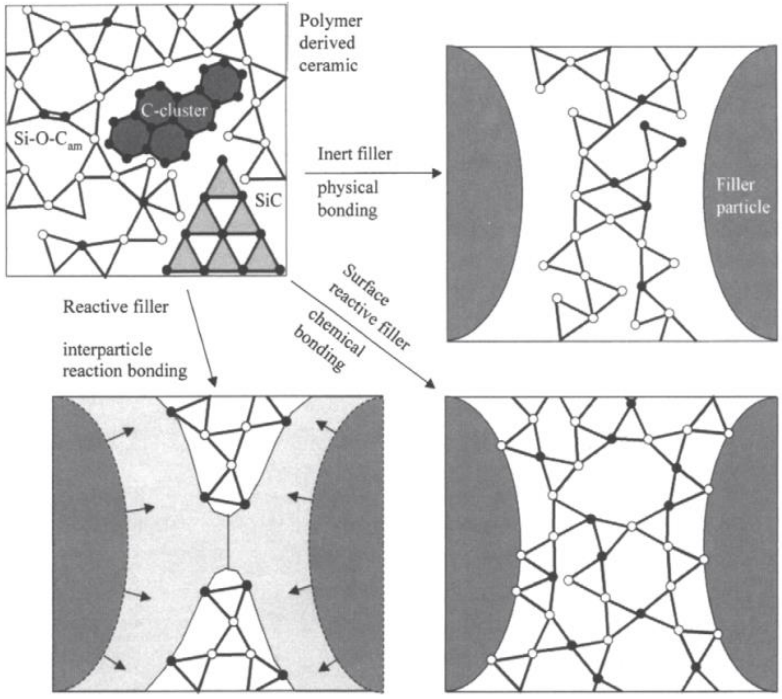

Figure 3.12: Polymer/filler interaction in case of a polysiloxane [45]

The content of fillers introduced is a variable, depending also to the desired result: they can be added in small quantities or can be the main fraction compared to the precursor, making it a simple binder. In any case, such an addition makes it possible to achieve higher density values. In the end, the result is a composite material composed by a phase derived from the pyrolysis of the preceramic polymer and one or more secondary phases related to the incorporation of fillers.

Furthermore, as the mechanical properties of the resulting ceramic are primarily dependent on the amount of residual porosity present, they can be improved by the addition of filler.

Independent on the type of filler, a good dispersion of the filler particles, and so a uniform distribution in the polymer precursor, is essential to improve the ceramic yield and the mechanical properties of the final ceramic. At the same time dispersion represents a major problem because the particles used, which are only a few nanometres to a few micrometres in size, have a tendency to agglomerate. In order to overcome the problem, suitable dispersing agents and/or adequate technologies, such as ultra-sonitication, ball-milling and mechanical stirring, can be used. In some cases, depending on the reactivity of the polymer precursor, high-energy methods (e.g. ultra-sonication, ball-milling) may not be the more appropriate choice, as they can cause premature cross-linking of the polymer [16].

3.5.1 Passive

The special feature of passive fillers is that they are inert in the system, i.e. the initial composition, mass and particle size remain unchanged during the polymer-to-ceramic conversion process. However, some

filler materials are inert only under certain conditions, such as non-oxidative atmosphere or lower temperature.

In terms of the function of these passive fillers, shrinkage is reduced because the addition of filler reduces the volume fraction of the shrink phase, mainly resulting in a macroscopic reduction. From this it can be concluded that there will always be a residual porosity (typically <10 vol%), especially when medium to high volume fractions of fillers are used. On the contrary, porosity increases as the volume fraction of filler added to the PDC increases, especially if the filler has a narrow particle size distribution. Also, crack formation may still occur due to localized stresses, such as around filler particles.

Typical examples of passive fillers are ceramic materials such as SiC, Si_3N_4, ZrO_2, TiO_2, BN, Al_2O_3, SiO_2. This kind of fillers helps the escape of gas generated during pyrolysis via forming a rigid skeletal structure and hence eliminating the macro-defects. The advantage of using a ceramic filler is that the passive behaviour can be maintained over a wide temperature range without the need for a protective atmosphere. Of course, they are able to tailor the functionality of the final ceramic. An example is represented by electrical conductivity: it does not depend linearly on the percentage of electrically conductive filler introduced in the polymer, but it is subjected to an abrupt increase only when a critical value is reached. This one is known as 'percolation threshold' and coincides with the transition dispersed-isolated particles to an interconnected particles network, as can be seen in Figure 3.13 (right).

In general, mechanical properties increase with increasing filler content up to a maximum of 40-50 vol%, with a marked decrease with further increases in filler content due to porosity formation. On the other hand, even if small fractions of filler (<10 vol%) are introduced in the system, the toughening mechanism (crack-tip bridging) is caused by localized high residual stress around the filler particles [34]. This phenomenon can be observed in Figure 3.13 (left).

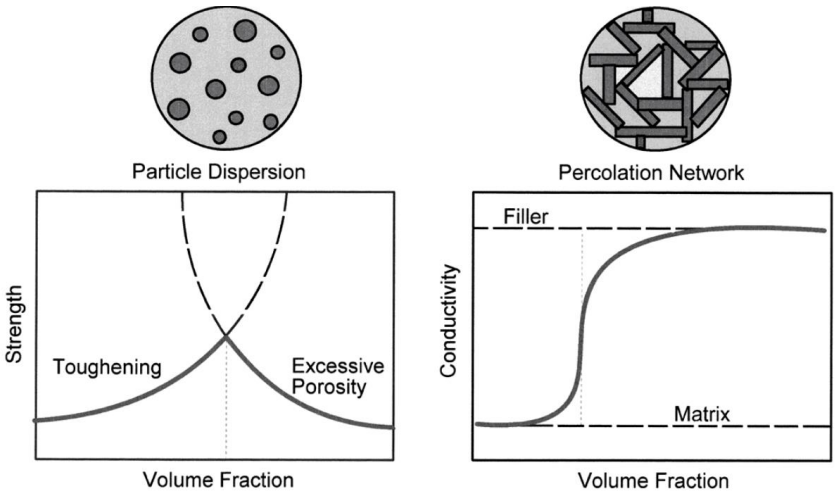

Figure 3.13: Filler effects on mechanical properties (left) and field properties (right) [34]

In addition, the CTE of the filler is of paramount importance as it determines the overall CTE of the final composite. Obviously, a high mismatch between the value of the post-pyrolysis ceramic and the filler can lead to microcracking, which is detrimental to the final mechanical properties.

3.5.2 Active

Active fillers are also known as reactive fillers due to the fact that they are able to react with the carbon containing gaseous products generated during the polymer-to-ceramic conversion process, the heating environment, and the ceramic residues [30], [34], [35]. It is possible to achieve near-net-shape conversion by compensating for polymer shrinkage with filler expansion (up to 50 vol%), or a maximum shrinkage of less than 1-5 vol% can be observed [45]. Obviously, to avoid excessive expansion and therefore failure due to over-expansion of the system, the amount of filler must be carefully chosen. Moreover, they can also be used to introduce new phases into a PDC system, modifying functionality and performance, or obtain completely new materials. A schematic representation of active filler action is shown in Figure 3.14, in which R^f represents the initial particle radius.

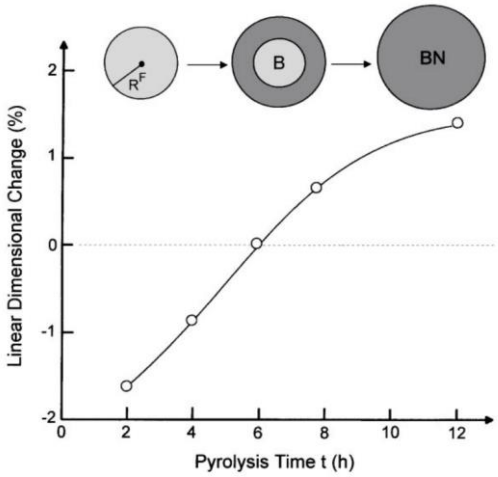

Figure 3.14: Linear dimensional change of polysiloxane 40 vol% boron mixture pyrolyzed at 1480 °C in nitrogen, as function of filler reaction time [46]

It can be seen that time is a key parameter influencing the filler response: as the particle size decreases, the filler response time is reduced, so that within a given reaction time, a higher proportion of smaller particles are converted compared to larger particles, and therefore the reduction in overall shrinkage is greater [46]. Also, a prolonged annealing time results in reduced shrinkage.

Typical grain sizes are 1-10 μm and suitable examples of active fillers are metallic (B, Ti, Cr, V, Mo) or intermetallic ($MoSi_2$, $CrSi_2$) filler particles which lead to formation of metal carbides, nitrides or silicides during pyrolysis due to reduction reaction. The final ceramic is characterized by tailored electrical conductivity, magnetic properties, CTE, and also mechanical properties and hardness are improved.

3.5.3 Meltable fillers

Meltable fillers are generally glasses. The use of this type of filler makes it possible to significantly improve various properties of the ceramic resulting from the polymer transformation. In particular, the ability to melt in the pyrolysis phase, or simply to soften if the temperature is high enough, allows the filler to seal the porosity and densify the resulting ceramic, providing improved protection against corrosion and oxidation. In addition, by softening at high temperature, meltable fillers enhance the relaxation of thermomechanical stresses caused by the thermal expansion mismatch between fillers and

polymer matrix. While, after cooling below the softening point, hardness and abrasion resistance can be increased. Their special feature is that they can behave as reactive fillers so, in certain cases, they can react with the other components of the system.

There are some drawbacks related to the type of glass used: if it is unsuitable, pyrolysis temperatures may cause an excessive reduction of the glass melt's viscosity or crystallization/decomposition of the glass, whereas at low temperatures the filler may simply behave passive and not result in softening/melting [16].

3.5.4 Sacrificial fillers

Sacrificial fillers are mostly organic compounds [16]. The special feature is that they can be added to the precursor and then removed by thermal decomposition or dissolution in a solvent to create porosity (as in gas separation membranes, for example). This approach can be used for stress control, as porosity reduces the effective modulus of elasticity of the resultant ceramic and increases strain compliance. However, depending on the size and shape of filler particles, it is possible to tailor pore shape, quantity, size and distribution.

They are also used as additives to achieve the required properties for application. A good example is the thermal expansion behaviour of coatings and joints: if there is a thermal expansion mismatch between the substrate and the polymer precursor, problems can occur during processing and use at high temperatures. One solution is to reduce the Young's modulus by introducing porosity.

4 Materials, instruments and experimental methods

4.1 Polymer precursors

The study involves three different polymer precursors: two polymer-derived ceramics are silica precursors, while the third one is a silicon carbide precursor. Due to the different applications, silica precursors are used for the same substrates (Al_2O_3-coated Al and CMC substrates) while the silicon carbide precursor is used for CVD-SiC substrates. However, all the precursors characteristics are reported in the following subparagraphs while substrate specifications will be explained in section 4.2.

4.1.1 Durazane 1800

Durazane 1800 is a commercially available preceramic polymer, an organopolysilazane (OPSZ), produced by Merck KGaA company (Germany). It is a liquid low-viscous, solvent-free polysilazane resin, which appears like a clear liquid, colourless with possible yellow trace. Properties of particular interest are density (0.950-1.050 g/cm^3 at 25 °C) and viscosity (10-40 cP at 20 °C) [47]. Also, it is characterized by good adhesion, hardness, hydrophobicity and barrier properties and applicable on metal, glass and ceramic substrates. For these reasons, Durazane 1800 is suitable for industrial applications high temperature coatings in order to protect metals from corrosion.

The polymer consists of a silicon and nitrogen backbone functionalized with different side groups, usually hydrogen, methyl (CH_3) and vinyl ($CH=CH_2$) groups which contribute to crosslinking by vinyl polymerization [48] [49]. Due to the presence of organic side groups, the reactivity of the polymer is slightly reduced. The molecular structure is represented in Figure 4.1.

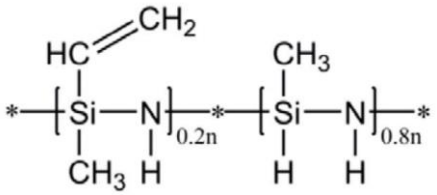

Figure 4.1: Durazane 1800 molecular structure [50]

Crosslinking pathway is different if the process involves the polymer in inert atmosphere o in air; at the same time properties also depend on the atmosphere. In particular, the case of interest is the ambient condition and the crosslinking reactions are mostly hydrolysis and polycondensation reactions. Thereby, the ≡Si-NH-Si≡ group reacts with a water or oxygen molecule, resulting in the formation of silanol groups. These ones polymerize to polysiloxane via polycondensation [48]. So, the reaction scheme is reported in Figure 4.2.

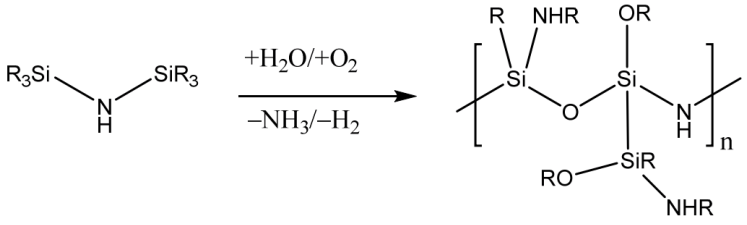

Figure 4.2: Durazane 1800 crosslinking reactions [48]

Typically, curing is performed with radical initiators, what allow a reduction of curing temperature or time, although catalysts can be avoided. Then, pyrolysis takes place at temperatures above 500 °C and the pyrolyzed ceramic material obtained shows excellent high temperature stability at least until 1000 °C. High ceramic yield can be obtained in the range 80-90%, depending once again on the atmosphere. Nevertheless, the reaction of Durazane 1800 with oxygen leads to the formation of a passivating SiO_2-scale, which prevents the complete elimination of C and N [51].

4.1.2 PHPS

The perhydropolysilazane Durazane 2250, known also as PHPS, is an inorganic polysilazane, commercially supplied by Merck KGaA company. It is delivered as transparent liquid 20 wt.% solution in di-n-butylether. Due to the presence of the solvent, it is characterised by low density (0.82 g/cm^3) and viscosity (<5 mPa·s at 20 °C) [52]. In the same way as Durazane 1800, main properties are chemical and thermal resistance, as well as oxidation and corrosion resistance, so it can be used as coating for different kind of substrates.

The polymer consists of a silicon and nitrogen backbone functionalized with hydrogen as side groups. The molecular structure is represented in Figure 4.3.

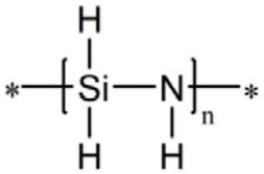

Figure 4.3: PHPS molecular structure [50]

Both Si-N and N-H bonds are reactive, especially with -OH groups, resulting in an enhanced crosslinking during thermal treatment in air [49]. Due to the higher number of reactive groups, the reactivity of this perhydropolysilazane is higher compared to the organosilazane.

PHPS can be converted to silica without lattice defects and having a density of 1.3 g/cm^3 at about 90 °C. Otherwise, low-temperatures (100-300 °C) for curing and cross-linking are preferable to avoid the formation of deficiencies (e.g., voids, pinholes, cracks) due to the shrinkage in the polymer-to-ceramic conversion. In order to lower the process temperature and to favour the advancement of the process, promoting agents such as amine, acid compound and peroxide, and moisture can be used, respectively [53]. Otherwise, UV radiation can be used to accelerate the process.

In the conversion process, the first step is represented by the hydrolysis with water, resulting in the formation of silanol groups as short living intermediates. Then, silica formation is obtained through condensation and cross-linking reactions [53]. So, the reaction scheme is reported in Figure 4.4.

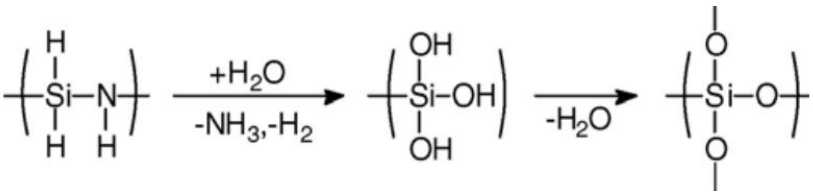

Figure 4.4: PHPS reaction transformation [53]

Silazane adhesion mechanism

Adhesion requires the substrate to be wetted to ensure intimate contact between the surface and the polymer. Then, the adhesion of silazanes to most surfaces occurs through chemical mechanisms involving the formation of oxygen bridges between the silazane polymer backbone and the surface. The formation consists in three different mechanisms [49].

1. The reaction between Si-H groups of the polymeric chain and -OH groups at the surface of the substrate. The Figure 4.5 a illustrates how the oxygen bridge is formed without the rupture of the main chain, with only the elimination of hydrogen gas.
2. The rupture of the main polymeric chain ≡Si-NH-Si≡. The three steps are shown in Figure 4.5 b. So, Si-N bond in the chain is broken due to the interaction with -OH groups at the surface of the substrate. The hydrogen of the hydroxyl group at the surface of the substrate is transferred to the resulting ≡Si-NH_2 group, while the oxygen atom bonds to the silicon separated from the nitrogen. Then, even the bond between the silicon and the nitrogen in the ≡Si-NH_2 group is broken and due to the transfer of another hydrogen from an adjacent hydroxyl group, ammonia (NH_3) is formed and released. Silicon bonds the remaining oxygen forming a second oxygen bridge.
3. Hydrolysis of the sylazane polymeric chain. The resulting silanol groups Si-OH react with -OH groups at the surface of the substrate leading to the formation of oxygen bridges and release of water. This process step is depicted in Figure 4.5 c.

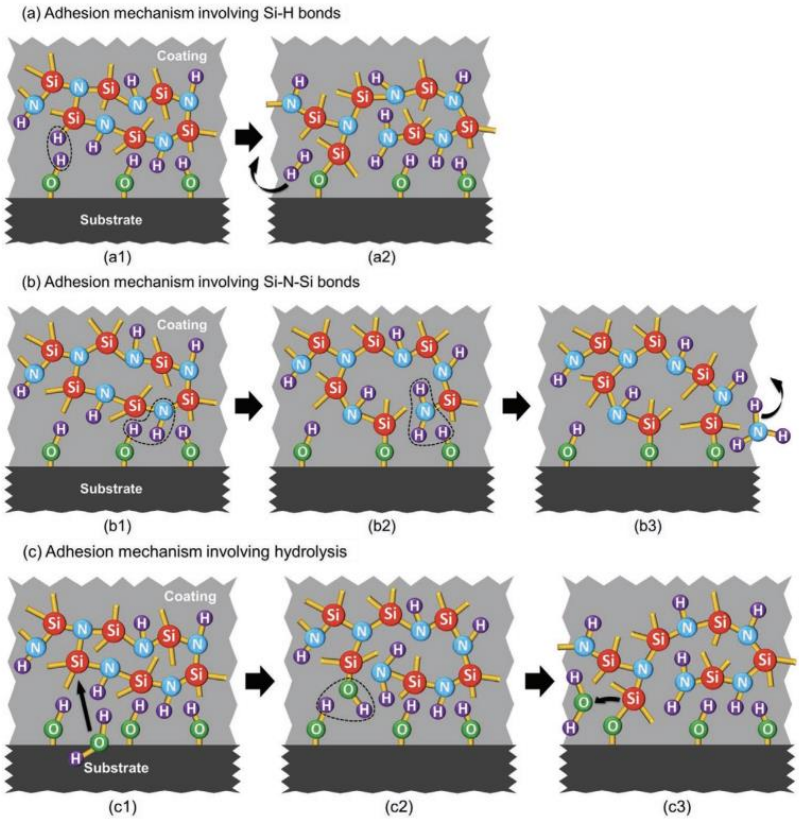

Figure 4.5: Silazane adhesion mechanism [49]

These reactions occur at the interface with the substrate as well as at the surface and within the coating. Also, water molecules adsorbed at the surface of the substrate lead to the formation of oxygen bridges by hydrolysis reactions.

4.1.3 SiC precursor

The polymer precursor was made and supplied by the American company Tethon 3D (Nebraska, USA), specialised in producing photoreticulable powders and precursors for 3D printing of ceramic materials. The resin was specially made to join silicon carbide substrates in order to achieve a 'total-SiC' joint. Despite the fact that the exact composition of the resin is proprietary and therefore unknown, it is almost composed of three elements such as pre-ceramic polymer substance, solvent and SiC nanoparticles equal to 60 wt.%. The material has the appearance of a very viscous grey suspension.

The company provides guidelines in order to use the polymer precursor in the correct way. The material solidifies between 80 °C and 150 °C so, first of all, it is preferable to operate a thermal setting between 80 °C and 100 °C. Then, the material has to be pyrolyzed in argon at 800 °C for 1 hour, even if the hold time is dependent upon the size of the geometry. Since SiC densifies at temperature higher than 1450 °C, the final sintering temperature is 1500 °C or above, according to the desired final result.

4.2 Substrates

Three different kind of substrates are involved in the project study. The main specifications are stated in the following subparagraphs.

4.2.1 Alumina-coated aluminium substrates

The first type is an Al panel of dimensions 100 x 100 x 1,5 mm with aluminium oxide coating on one side. The nanocrystalline oxide ceramic contains gamma (γ) and alpha (α) phase of alumina. The main goal is to bond two aluminium panels ceramic-to-ceramic using something low organic or without organic groups, with curing below 200 °C for various mechanical and electronic applications. A low temperature solution enables to avoid the deformation of ceramic on Al structures due to the difference in the thermal expansion coefficients, and the alloy strength loose as a consequence of certain heat treatments.

Regarding the automotive and energetic point of view, the combination of aluminium light weight and hard ceramic surface can substitute steel and is beneficial for fast moving parts and/or for those that suffer from wear. Moreover, aluminium is about three times lighter than steel, so the reduction of mass for moving parts allows to reach higher speed of movement, lower energy consumption and reduction of friction losses, lower inertia and less impacts on components. Therefore, the abrasion resistance is suitable for turbocharger wheels, the corrosion resistance for transport vehicles such as automotive, marine and aerospace and the heat resistance for engine components like pistons and powertrain. An example is shown in Figure 4.6.

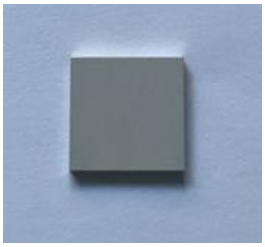

Figure 4.6: Alumina-coated aluminium substrate

4.2.2 CMC substrates

The second type of substrates considered is an oxide/oxide ceramic matrix composite (Ox-CMC) composed of oxide fibers with an oxide matrix. The Ox-CMC was supplied by the Chair of Ceramic Materials Engineering at the University of Bayreuth (Germany). In particular, it is made of an alumina-zirconia matrix (75 wt.% alumina and 25 wt.% zirconia) reinforced with eight layers of Nextel™ 610 alumina fiber fabric DF-19 (8 Hardness Satin, 3000 denier). The fibre volume content is of about 42% while the porosity is of around 27%. The properties characterizing the material are a tensile strength of around 300 MPa and an interlaminar shear strength (ILSS) of 12 MPa with expected 3 point-flexural strength of around 400 MPa. The substrate is shown in Figure 4.7.

Figure 4.7: CMC substrate

4.2.3 SiC substrates

Two types of silicon carbide substrates are used in this study. The first one is a plate Boostec® SiC (former SiC100®) produced by Mersen (Bazet, France): it is a polycrystalline alfa-SiC (>98.5 wt% SiC with no traces of free silicon) obtained by pressureless sintering. In particular, due to the very strong covalent Si-C bond, exceptional physical properties stable over time are obtained. At the same time, SiC does not present sub-critical cracking phenomenon and no sensitivity to mechanical fatigue. Mechanical properties such as bending strength, modulus of elasticity and toughness hardly change with temperature, from cryogenic environments close to absolute zero up to 1450 °C [54]. On the other hand, the second one is a cylindrical substrate of SiC/SiC, produced by CEA (France), through chemical vapour infiltration. The cylinder was cut in order to investigate the adhesion of the polymer in the internal surface due to the fact that the objective is to join it with a plug. They are represented in Figure 4.8.

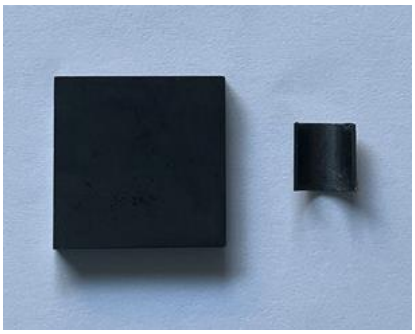

Figure 4.8: SiC substrates

4.3 Preparation

The starting point of the experimental activity is the identification of all the materials, tools and procedures required, after which preparation can begin.

4.3.1 Substrate cutting

Due to the large dimensions of the Al panel, it must be cut to obtain usable substrates of the size of 15 x 15 mm. This was done using the Brillant 220 cutting machine, QATM. It is a precision wet abrasive cut-off machine, suited for precise cutting of small part of different geometries [55]. Specifically, the diagonal cutting mode was used with a rotational speed of the wheel of 2500 rpm and a low feed rate of 0.017 m/s to avoid damaging the alumina coating. The Figure 4.9 shows the cutting apparatus and the cut substrates obtained.

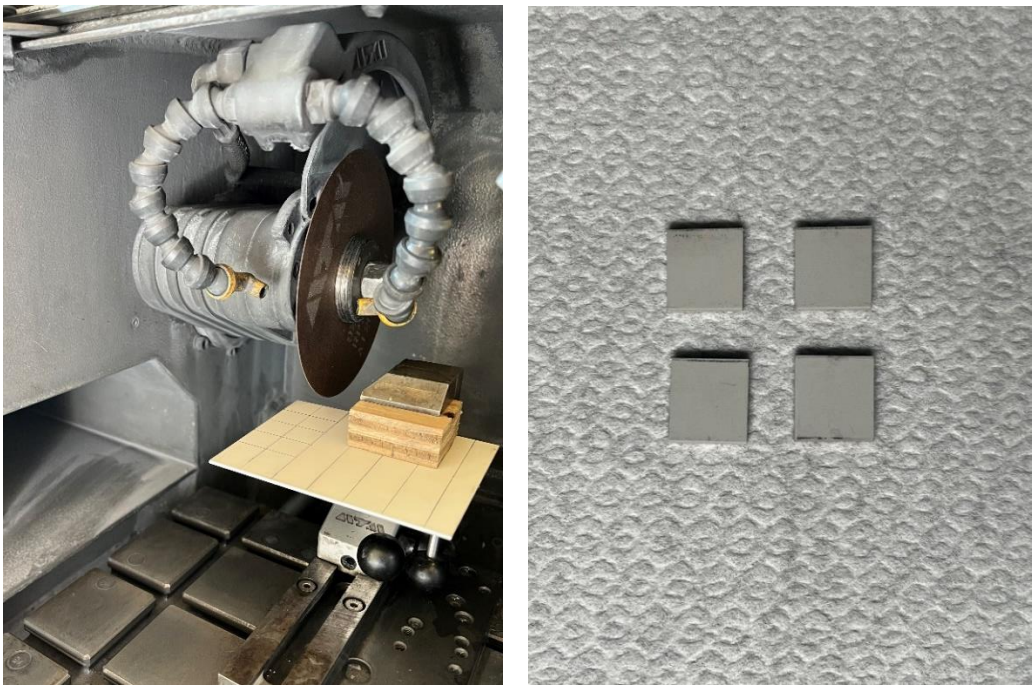

Figure 4.9: Cut of Al panel in suitable substrates with Brillant 220 cutting machine

Then, all substrates were measured using a digital caliper (precision of 0.01 mm), in order to proceed with the polishing procedure.

4.3.2 Substrate cleaning

Before using any type of substrate for coating and/or joining, they were ultrasonically cleaned in ethanol in order to remove dust particles, grease and other contaminants. The operation was carried out through the ultrasonic cleaner Proclean 4.5S, Ulsonix, and involves a 10-minute cycle at 40 °C; in case of the Al_2O_3-coated Al substrates it was repeated twice to ensure that all the cut-off grease was removed. This procedure is of fundamental importance to have a good adhesion between the polymer precursor and the substrate. In the case of alumina, which is a porous material, it is necessary for all of its active sites to be free for the polymer to bind to it. In particular, PHPS is usually bonded covalently to the surface of the substrate.

4.3.3 Polymer preparation

Each polymer requires a special preparation procedure before actual use. All polymers were stored in a refrigerator (at temperature between 0 and 4 °C), so to prevent condensation, it was therefore necessary to allow the polymer to reach room temperature before opening the container. In contrast, the SiC precursor required at least one night out of the fridge to reach a suitable viscosity and had to be shake before the deposition. After using them, the bottle was flooded with nitrogen in order to prevent oxygen contamination.

As far as PHPS is concerned, the commercial product cannot be used to make joinings as it is 80 wt.% solvent and has an extremely low viscosity. The most effective method of removing the solvent was to use a rotary evaporator also known as rotavapor. The instrument used was the Bibby Scientific RE300 Rotary Evaporator, showed in Figure 4.10.

Figure 4.10: Bibby Scientific RE300 Rotary Evaporator

The rotatory evaporator is a distillation unit that incorporate an efficient condenser with a rotatory flask system and uses low pressure evaporation to evaporate the solvent of the desired compound. In particular, as the flask containing the polymer is rotated continually, it transfers a thin layer over the entire inner surface. The result is a very large area for evaporation. In addition, an accessory heating bath can be used [56].

So, it is possible to understand that it is constituted by six main elements:

- Evaporating flask containing the solution from which the solvent will be removed;
- Receiving flask in which the condensed solvent is collected;
- Diagonal condenser to break down the developed vapours;
- Heating bath into which the evaporation flask is immersed in order to keep the solution at the appropriate temperature;
- Motorised mechanism which allows the rotation of the evaporation flask;

- Membrane pump to keep the system in vacuum.

Also, flasks, condenser and all connection elements are made of glass and all the system has to assure a perfect vacuum seal.

The application of a suitable vacuum lowers the boiling temperature of the solvent, allowing it to evaporate at a much lower temperature than that required working at atmospheric pressure; so, the vacuum pump is fundamental. The solvent vapours condense when meet the condenser surface cooled and the droplets are collected in the receiving flask. The condenser is a coil condenser, in which cold water circulates. In addition, at the base of the condenser, a tap allows air to be introduced to break the vacuum at the end of the process. The result is a solvent-free compound.

4.3.4 Fillers addition

About the filler, amorphous silicon (IV) oxide powders produced by Alfa Aesar are used. They are nanopowder, about 80 nm of average diameter, 99.9% metals basis and characterized by a density of 2.4 g/cm^3 [57]. The quantity needed was measured through a precision balance, by Orma model bc, with a precision of 0.0001 g.

The basic idea is to add the maximum amount of filler that can be absorbed by the silica precursor polymer in order to minimise volume shrinkage, as well as and porosity and cracks formation, during the polymer-to-ceramic conversion. From literature, the optimal values range is between 40 and 50 % with respect to the polymer weight. In this experimental case, it was possible to reach up to 48 wt.%. Mixing was done mechanically using a metal rod in a graduated Eppendorf tube. Obviously, this type of process has two main problems: the incorporation of air and the agglomeration of particles.

The result was a highly viscous polymer, with a gel-like consistency. As the pure polymer is transparent, the addition of the particles gives it a white colour, as it is possible to see in Figure 4.11.

Figure 4.11: Pure transparent silica precursor (left) and white coloured silica precursor filled with silica particles (right)

4.3.5 Substrate surface modification

Last but not least, the PlasmaTEC-X OEM – Atmospheric Plasma, by Tantec, was used when the surface needed to be modified, i.e. functionalised, in order to remove pollutant residues and increase surface energy to solve the wettability problem and promote adhesion between the polymer and the substrate. The treatment involves only the surface layers of the material and leaves the mechanical properties

unaltered, adopting low process temperatures. The system, shown in Figure 4.12, is built around the concept of a high voltage DC plasma discharge in atmospheric air and, to ensure proper plasma discharge from the nozzle, the compressed air must not exceed a certain level of pressure and volume [58].

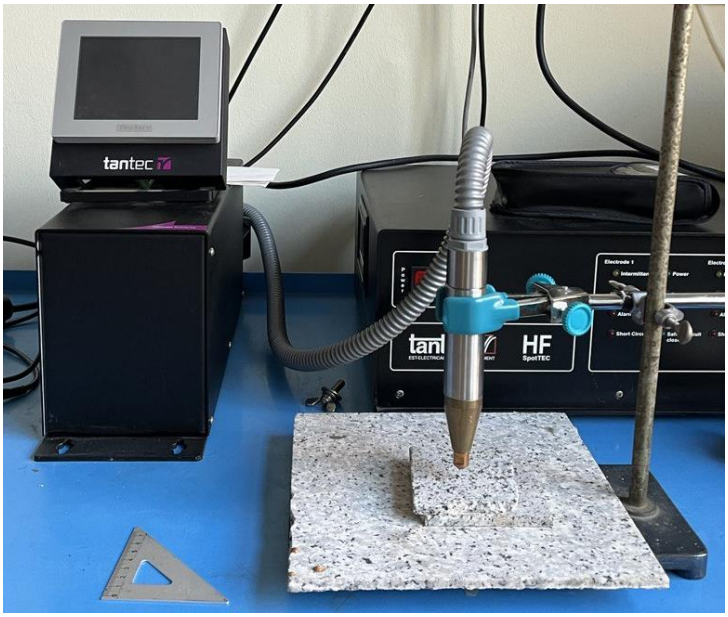

Figure 4.12: PlasmaTEC-X OEM – Atmospheric Plasma

For ox-CMC substrates, the technical parameters used are 1500 l/h of compressed air, a suitable distance between the substrate and the nozzle of about 15 mm, and an operation time of 120 s (specifically, 60 s for each zone of the substrate according to the dimensions). It is important that the treatment was carried out a short time in advance with respect to the deposition in order to ensure its effectiveness.

4.4 Process

Once the polymer and substrates have been prepared, it is possible to proceed with the production of the elements of interest, i.e. coatings and joints.

Before using any oven or furnace, a calibration has been carried out to ensure that the process could be carried out accurately, with a correct match between the required temperature, the temperature red by the thermocouple inside the instrument and the temperature red by the thermocouple used for calibration.

4.4.1 Curing

The first phase of the process was represented by the curing step. The heat treatment was performed into the Binder ED 23, a drying and heating chamber with natural convection [59], shown in Figure 4.13.

Figure 4.13: Binder ED 23 drying and heating chamber

A homogeneous temperature condition inside the oven was necessary to assure the same conditions in case of the preparation of multiple samples; the process was performed in air.

On the other hand, the cross-linking procedure is both an important and sensitive procedure: the volatilization of oligomers is reduced, as well as the shrinkage in the subsequent polymer-to-ceramic transformation, and so the ceramic yield increases.

For each polymer, a different temperature and residence time were used. The corresponding values, collected in the Table 3, were taken from technical data sheets or information received from the manufacture company.

Polymer	Temperature [°C]	Residence time [h]
Durazane 1800	180	4
PHPS	180	1
SiC precursor	100	1

Table 3: Cross-linking process specification

4.4.2 Pyrolysis

The pyrolysis process was conducted in different ways and with different machinery depending on whether silica precursors or SiC precursor was used. In the first case, the Carbolite CWF 1300 furnace was used due to the fact that the process had to be conducted in air. It is a laboratory chamber furnace with a maximum operating temperature of 1300 °C, equipped with a controller with single ramp to set-point and process timer [60]. It is possible to see the system in Figure 4.14.

Figure 4.14: Carbolite CWF 1300 furnace

In the second case, the Carbolite Gero STF 16/180 tubular furnace, was used in order to have argon flux during the entire process, as required. The tubular furnace is characterized by a single zone in which the heated length is of 180 mm, the tube is in alumina bulk, the maximum operating temperature is 1600 °C, and the maximum power is 2.5 kW [61]. In addition, a controller Eurotherm 3216 was fitted. A figure of the system is shown in Figure 4.15.

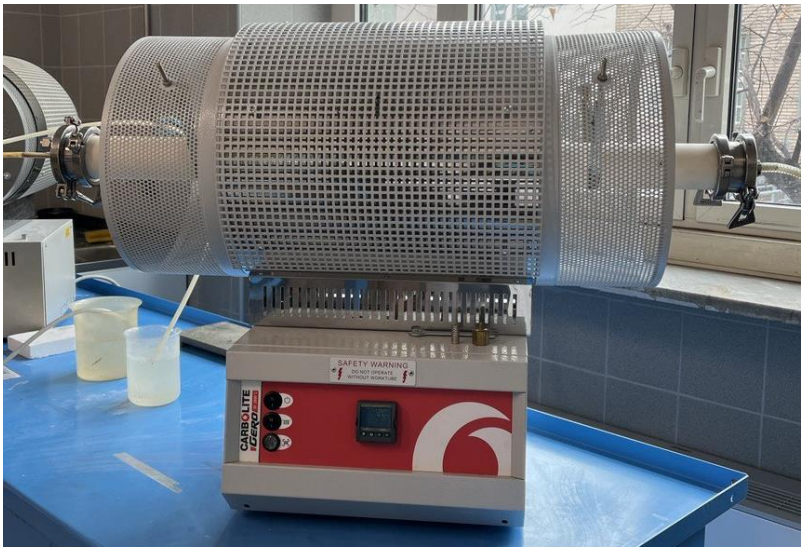

Figure 4.15: Carbolite Gero STF 16/180 tubular furnace

Obviously, for each polymer a specific heat treatment was performed and will be discussed in more details in the section 5.

4.5 Analysis

Once the samples of interest have been obtained, it was possible to move on to analysis. The different types used are explained in detail below.

4.5.1 Scanning Electron Microscope (SEM)

Scanning electron microscope is an instrument through which it is possible to conduct a non-destructive investigation thanks to the interaction between an electron beam and the sample of interest. The instrument used were the JEOL JCM-6000 PLUS, equipped with Energy Dispersive X-ray Spectroscopy (EDS) analyser, and FESEM- ZEISS Supra 40 with EDS- SW9100 EDAX detector.

SEM analysis allows to obtain information about the morphology and the structure of the samples; also, chemical quantitative analysis can be conducted due to the presence of an X-ray spectrometer. Both the electron beam and the sample are under vacuum condition in order to avoid contaminations and vibrations, and the interaction of the electron beam with air particles, respectively. It is possible to set three different values of power, 5, 10, 15 keV, and to reach high magnification. In terms of operation, an electron probe is focused on the sample surface while the electron beam is controlled through electromagnetic lenses: the released electrons from the area of the sample close to the surface are detected to generate an image based on the surface topography; the high resolution is attributable to the vacuum condition. The detectors used include Secondary Electron Detector (SED), Backscattered Electron (BSE) Detector, and X-ray Detector. In particular, secondary electrons are originated from a surface area of the sample and give exclusively morphological information, while backscattered electrons come from a deeper zone of the sample and give mainly information of composition, as well as morphological one. X-rays allow elemental analysis of the sample, providing qualitative and quantitative information on the chemical species present.

4.5.1.1 Sample preparation procedure

Before the analysis can take place, samples must be prepared. First of all, it was necessary to polish them using a semi-automatic Struers polishing machine. SiC grinding foils used were P600, P800, P1000, P1200, P2500, in sequence, and the rotational speed was set to 150 rmp. This operation allowed to get a mirror-like surface.

After cleaning the samples from residues with ethanol, they were placed on stabs using conductive carbon tape. Then, samples were platinum coated, with a treatment of 20 s, in order to make them conductive. It was necessary to analyse them, since both polymers and ceramic substrates are not conductive.

4.5.2 X-Ray Diffraction (XRD)

X-ray diffraction is an analytical non-destructive technique used to identify structure and phase of a crystalline material. The facility used for the analysis was the X'Pert Philips diffractometer with hot stage, then the software X'Pert Highscore was used to investigate the spectra obtained.

In terms of operation, the X-ray source is held stationary while the sample and the detector rotate, so the sample is scanned through a range of 2θ angles. The sample is analysed in powder form to expose as

many crystalline planes as possible, if present. The X-rays are generated by a cathode ray tube, filtered to produce monochromatic radiation, with λ wavelength, collimated to concentrate them, and directed toward the sample. The interaction of the incident rays with the sample produces constructive interference and the diffracted X-rays are detected, processed and counted. The image obtained is called diffractogram, which is characteristic of each type of material and from which information about structure and phases can be obtained from the angular position, structure, preferred orientation and phase abundance from the peak intensity and crystallinity, disorder, stress state and grain size from the peak profile. The appearance of the diffractogram depends on the surface structural characteristics of the sample, such as degree of crystallinity (amorphous, semi-crystalline, crystalline), surface roughness (coarse, fine, lustrous) and purity.

The specific parameters used were: K-Alpha1 wavelength equals to 1.5405980, K-Alpha2 wavelength equals to 1.5444260, the ratio K-Alpha2/K-Alpha1 equals to 0.500, fixed divergence slit of 0.38 mm, generator voltage equals to 40 kV and tube current equals to 40 mA. XRD analysis was performed between 10° and 80°, with scan step size and time per step equal to 0.0131303° and 148.90 s, respectively.

4.5.3 Thermal Gravimetric Analysis (TGA)

The thermal gravimetric analysis (TGA) was performed in order to verify the thermal stability of PDCs. For definition it is an experimental technique which enhances the continuous recording of mass loss over time when the sample under study is subjected to a constant temperature or a temperature gradient. This analysis was performed in case of heating of the sample.

The facility used was the NETZSCH STA 2500 Regulus, made of refractory material, which enables to reach temperatures up to 1600 °C with a heating rate between 0.001 and 100 K/min [62]. It is equipped with a tailor-made ultra-micro balance with a resolution of 0.03 µg. The self-compensating differential balance operates with two symmetric balance arms on which the crucibles with the sample to be analysed and the reference one are placed. Protective gas flushing (argon, 40-50 ml/min) is necessary to protect the balance from contamination and condensation. Then, the analysis can be performed in inert or oxidative atmosphere or in vacuum. The schemes are shown in Figure 4.16.

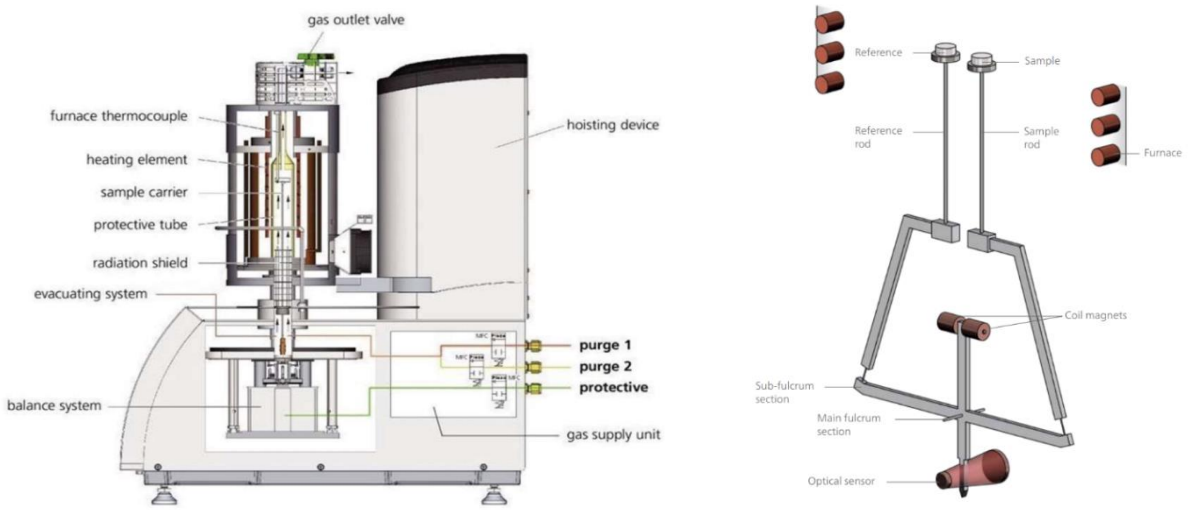

Figure 4.16: NETZSCH STA 2500 Regulus operation scheme

Depending on the specific case to be investigated, TGA was performed on liquid or post-cured samples. In addition, all tests on silica precursors were performed on a post-cured flake sample in air, while tests on the liquid SiC precursor were performed in air to investigate the curing and in argon to verify the thermal stability; the flow rates of both argon and air were always 40 ml/min. The results obtained were then processed with Matlab.

4.5.4 Tensile Mechanical Test

Mechanical tests are performed whenever it is necessary to investigate the strength characteristics of the material under examination. In particular, tensile strength is the easiest and fastest characterisation test. The test is carried out using with a machine equipped with a load cell which applies a tensile load at a constant speed and at regular intervals to a specimen clamped between two grips. The tensile test ends with rupture, i.e. the physical separation of the two ends of the specimen, so it is a destructive analysis.

The facility used was the MTS Criterion model 43, equipped with a 5 kN load cell which was the lowest available in order to be consistent with the loads the material was expected to withstand and that will probably be small. Similarly, a low load feed rate of 0.5 mm/min was adopted. The unit consists of a 2-column load frame with an integrated table with a single zone test area. The samples must be properly prepared so that they can be inserted into the machine, locked in place with two pins (one at the top and one at the bottom) and then the test can be started. In Figure 4.17 it is possible to see the machine and the sample layout.

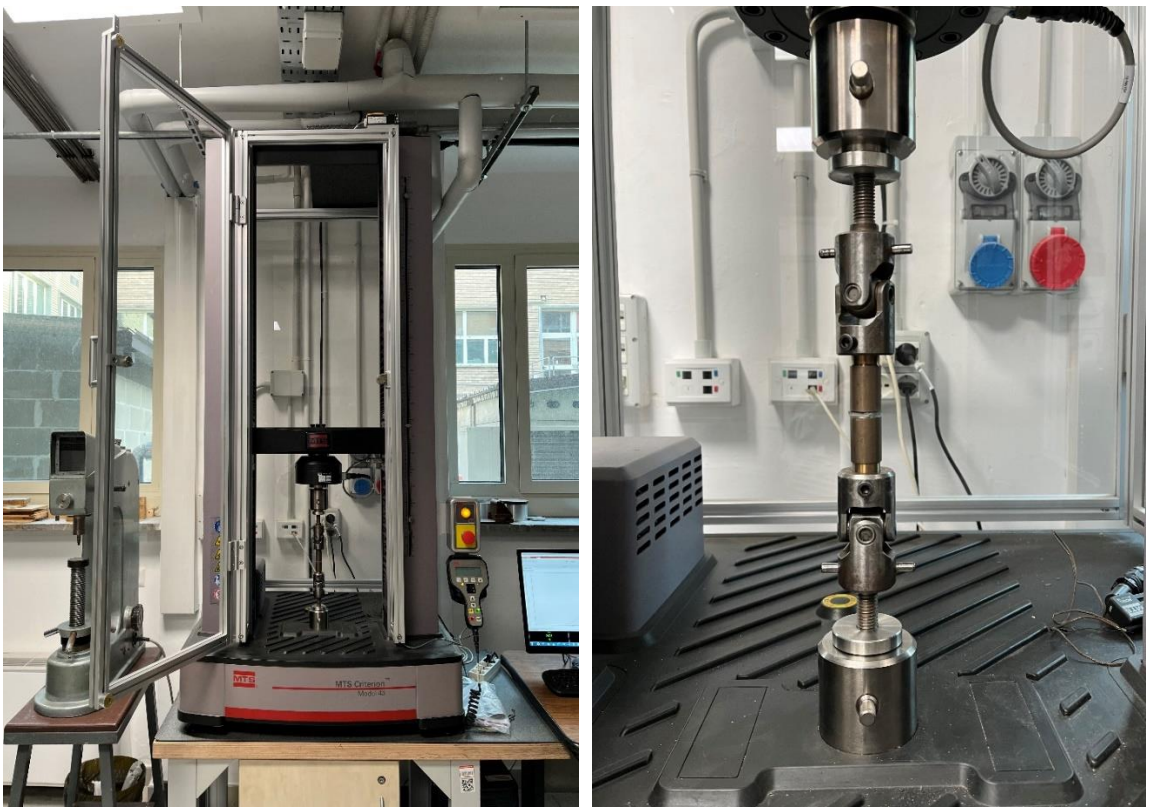

Figure 4.17: MTS Criterion model 43 tensile test machine (left) and locked in place sample (right)

4.5.4.1 Sample preparation procedure

For be inserted into the machine, the specimens must first be mounted on steel cylinders. To do this, it was necessary to use an adhesive, commonly known as VESTRA (DP 490). This is a two-component epoxy adhesive with filling properties and excellent application characteristics, providing stability under static and dynamic loads. Since the tensile tests were performed on the Al_2O_3-coated Al substrates, the adhesive is applied to both the cylinder and the specimen (on the aluminium side) using a spatula. This ensures better adhesion between the two parts. After bonding one side of the joint to a cylinder and applying the adhesive to the other side and another cylinder, this second part of the bonding was carried out using a horizontal guide to avoid misalignment. These operations require a high degree of precision as it is important that the joint is well centred on the cylinders in order to perform the tensile test with uniform stresses throughout the specimen. Then, the drying process was performed in air for at least 48 hours. All the elements needed are represented in Figure 4.18.

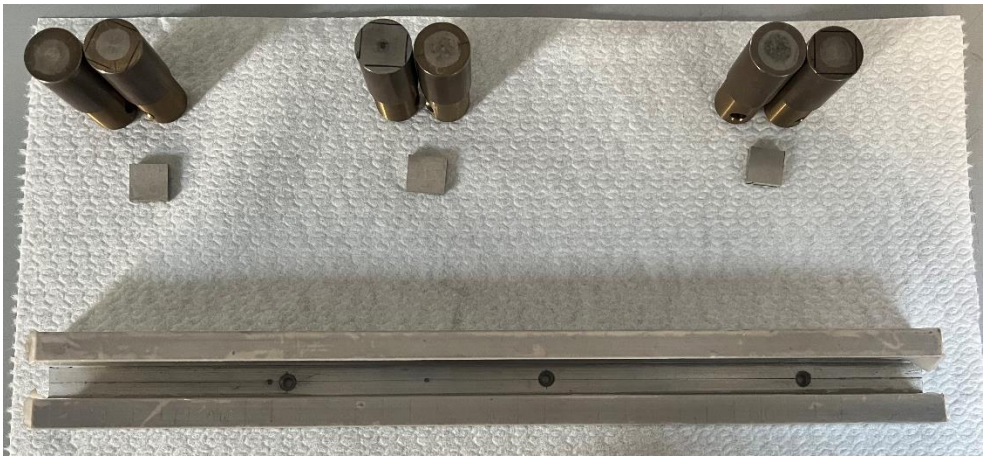

Figure 4.18: Elements needed for samples preparation

4.5.5 Computed Thermography Scan (CT-scan)

The computed thermography is a non-destructive analysis in which the X-rays emitted by the X-ray tube pass through the component being analysed, which is rotating, and are collected and converted into images by software. The machinery used was specially designed by Fraunhofer IKTS for J-Tech@PoliTo. The main features were related to the maximum operating voltage of 300 kV, the max operating current of 1000 µA and the 4-axis manipulation system which allows to manipulate sample xyz and to rotate it full range 0-360° with a continuous rotation.

The specific parameters used in the analysis were an operating voltage of 250 kV, an operating current of 120 µA, from which consequently derived a power of 28 W, the source distance (between the X-ray tube and the detector) equals to 1500 mm, the distance between the tube and the component of 90 mm and the resolution of 12 µm. In addition, a copper filter of 0.6 mm and a beam hardening correction were used to shield low radiation and to avoid fading of the beam as it passes through the component being analysed, respectively.

5 Discussion and results

The aim of the experimental work is to obtain a joint using preceramic polymers. In order to better understand the processes, a coating and a joint were always made at the same time, because it was not possible to look at what is happening inside the joint without some kind of analysis.

The silica precursors used, being commercial products, were not intended to be used as joining material, so the work was a technical feasibility study. Most of the work was carried out using the alumina-coated aluminium substrates and the silica precursor polymer Durazane 1800. As high temperatures could not be reached with these types of substrates, they were used to form a joint with the polymer in the cured state. In this way, it was possible to study a preliminary case with polymer alone as joining material and an improvement that included the addition of filler to the polymer to reduce volumetric shrinkage and the formation of porosity and cracks. Subsequently, the polymer-to-ceramic conversion phase of the silica filled polymer for ox-CMC substrates was investigated. Whereas, the inorganic silica precursor PHPS was used to carry out a single preliminary test, leaving the possibility to evaluate its behaviour in the future.

On the other hand, the work involving silicon carbide precursor was an early stage investigation of the precursor behaviour and the adhesion on the specific substrate, with the aim of being able to realise nuclear grade 'total-SiC' joints.

5.1 Silica precursors

5.1.1 Durazane 1800

Preliminary case characterization

The preliminary case involves the alumina-coated aluminium substrates and the pure polymer, cured at 180°C for 4 hours in air.

A preliminary test was carried out in order to investigate the curing time on a coating, as thin as possible: first of all, a coating sample was checked every hour in order to understand the polymer behaviour. Already after one hour the coating appeared solid and no longer liquid, and very compact. Moreover, it was found to be very sensitive to temperature variations, as evidenced by the formation of macrocracks at each inspection, as shown in Figure 5.1. As it was not possible to control the cooling rate, all subsequent samples were left to cool naturally in the oven before being removed and analysed.

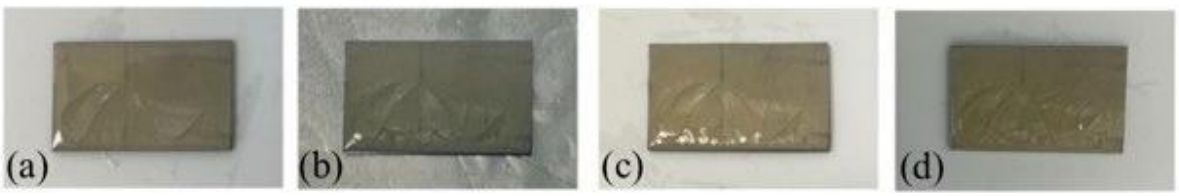

Figure 5.1: Pure Durazane 1800 coating appearance during the 4 hpurs of curing. (a) Aftern 1 hour (b) After 2 hours (c) After 3 hours (d) After 4 hours

The pure polymer is transparent in its liquid state, while after the cross-linking it appears light yellow due to the presence of organic side groups in the backbone. In addition, the polymer is brittle, as the coating tends to peel off from the substrate at the points where it is thickest. Despite this, a partially good adhesion is observed with respect to the alumina coating of the substrate.

Subsequently, the test was repeated to take a post-curing polymer sample on which TGA could be performed. In this case, an aluminium substrate was used to take the polymer in flakes. In fact, it was found that the polymer did not adhere well to the metal, but tended to become very brittle and spall as a result of the curing process, as it can be seen in Figure 5.2.

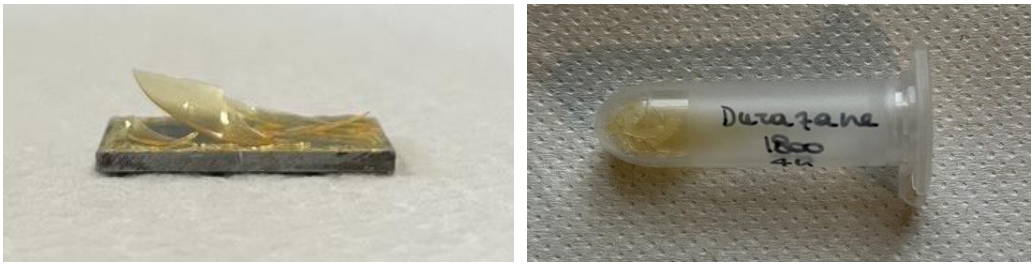

Figure 5.2: Pure Durazane 1800 coating on aluminum (left), post-curing flakes sample of pure Durazane 1800 (right)

The thermal gravimetric analysis had two different objectives: to verify the curing time and to investigate the conversion process from polymer to amorphous ceramic. To perform the first test, a quantity of 14.7 mg of sample was brought to an initial temperature of 20 °C, which was kept constant for 5 minutes so that the sample reached a uniform temperature. Then, a heating rate of 10 °C/min was used to reach the curing temperature of 180 °C, at which the sample was kept for 1 hour. This first result, shown in Figure 5.3, represents the mass loss with respect to time.

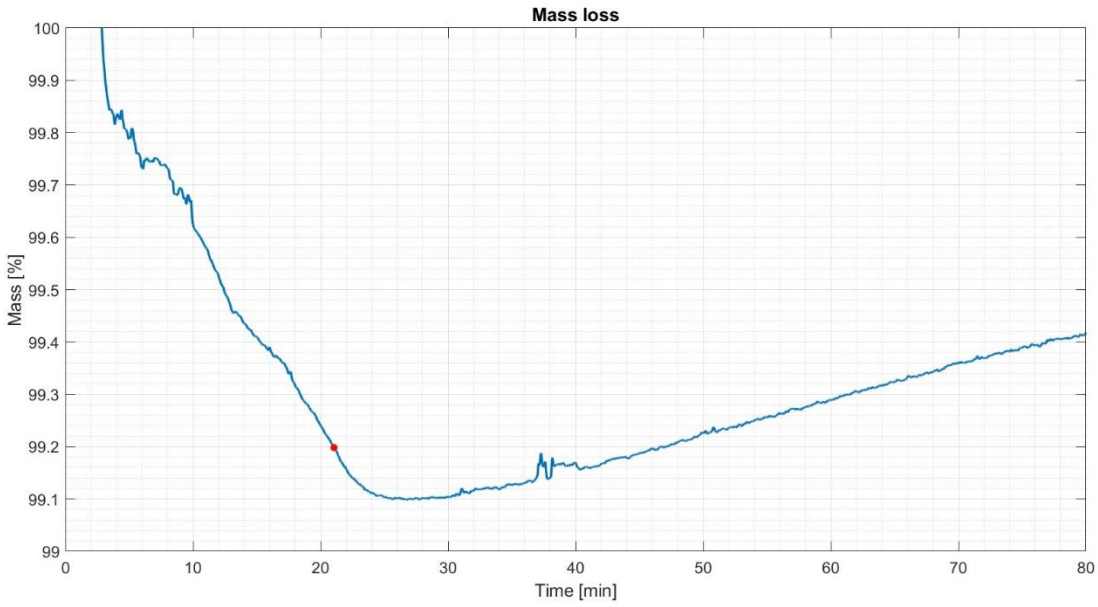

Figure 5.3: Durazane 1800 curing time verification

The red dot identifies the time when the sample reached the temperature of 180 °C; from that point, an isotherm of 1 hour was considered. A weight loss of 0.8% is observed up to 180 °C, then a further loss of 0.1% and a subsequent increase of 0.3% due to the reaction of the polymer with the air. Overall, the weight loss is of 0.6%, so it can be assumed that the curing time chosen was adequate.

The second part of the analysis involved the same sample, but it was heated up to 1200 °C, always with a heating rate of 10 °C/min. In this case, the mass loss variation with respect to the temperature was investigated. The result is shown in Figure 5.4.

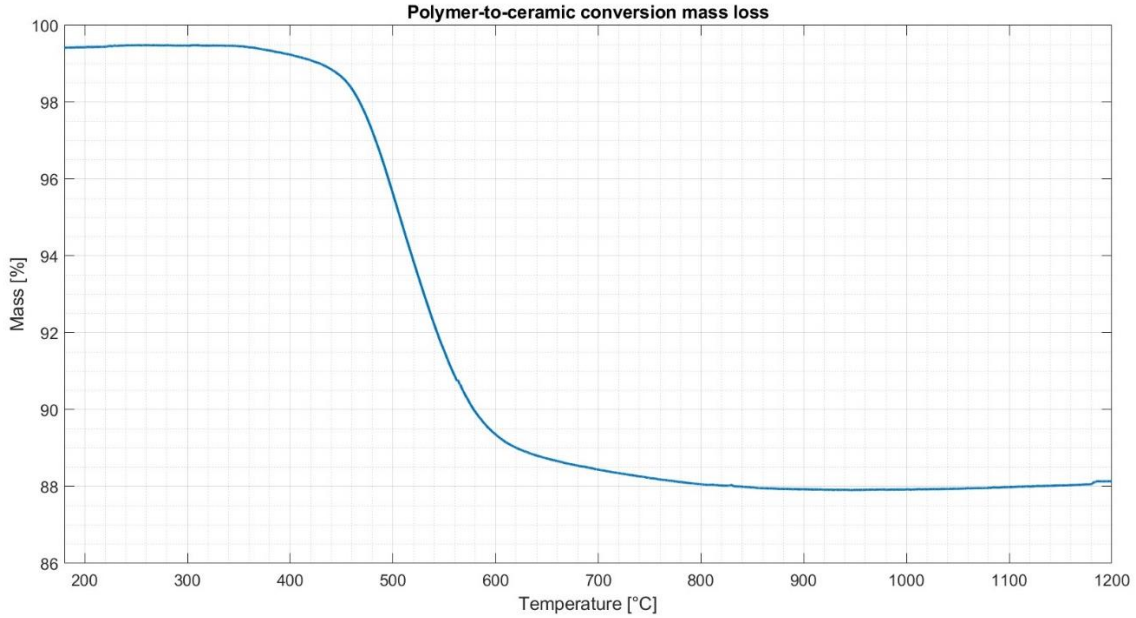

Figure 5.4: Durazane 1800 mass loss in polymer-to-ceramic conversion

The result obtained is consistent with the information found in the literature. Two steps can be distinguished: the first is related to the temperature range 100-400 °C, while the second is related to the temperature range 500-750 °C [48]. In particular, at temperatures above 100 °C, the mass loss is due to the degradation of non-crosslinked volatile oligomers, while at temperatures above 200 °C, the thermoset polymer is obtained by further radical polymerization of residual vinyl groups. So, up to 400 °C, further dehydrogenation and transamination reactions occur, although the total mass loss is negligible, as can be seen from the flat curve. Between 500 °C and 750 °C, however, a significant mass loss is associated to the organic-inorganic transformation of the thermoset polymer into an amorphous ceramic. The mass loss of 11.4% is found between 400 °C and 800 °C, while at 800 °C a plateau is reached and no further mass loss is found.

Considering the first and the second tests, the total mass loss of the process is of 12%.

With the confirmation of the TGA on the curing time, it was possible to proceed with the realisation of a coating and a joint as samples for SEM analysis. In particular, a force of 1.21 N was applied to the top of the joint, using a mass of 123.06 g; considering that the average area of a substrate is 2.25 cm^2, a pressure of 5.38 kPa was applied. The two samples are shown in Figure 5.5.

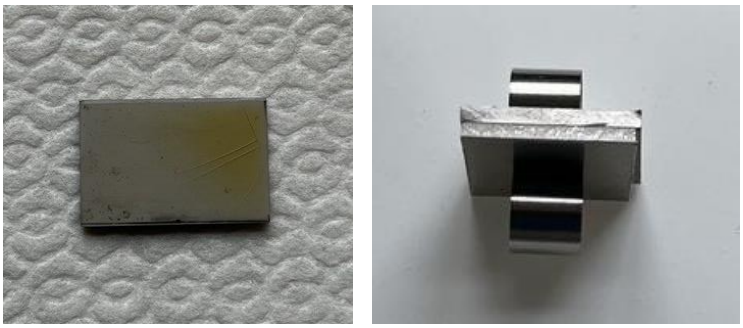

Figure 5.5: Durazane 1800 samples, coating (left) and joint (right)

The coating obtained is thinner than the first one, in fact two-thirds of the substrate remain transparent, showing the colour of the underlying alumina, while only one-third shows a concentration of polymer, as can be seen from the yellow colour. Such a thin coating made it possible to observe the shrinkage due to the cross-linking process, which was not evident in the previous sample. This sample confirmed the theory that a thicker coating is more prone to fracture. Indeed, three macro-fractures can be found in this area. Otherwise, the joint appears to hold together despite the fact that there is a very thin layer of polymer joining the two substrates; it also proved resistant to both a cut-off machine test and polishing. A schematic representation of the joint is represented in Figure 5.6; the main elements are not to scale with those in reality.

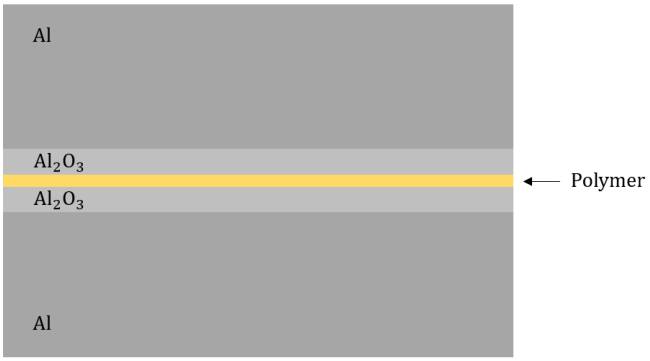

Figure 5.6: Schematic representation of the joint

The SEM images, Figure 5.7, shows that the coating is compact and homogeneous, in some areas the surface appears rough, probably due to densification of the polymer, but no micro-cracks are observed. Only the macro-fractures mentioned above, which can be observed with the naked eye, are found.

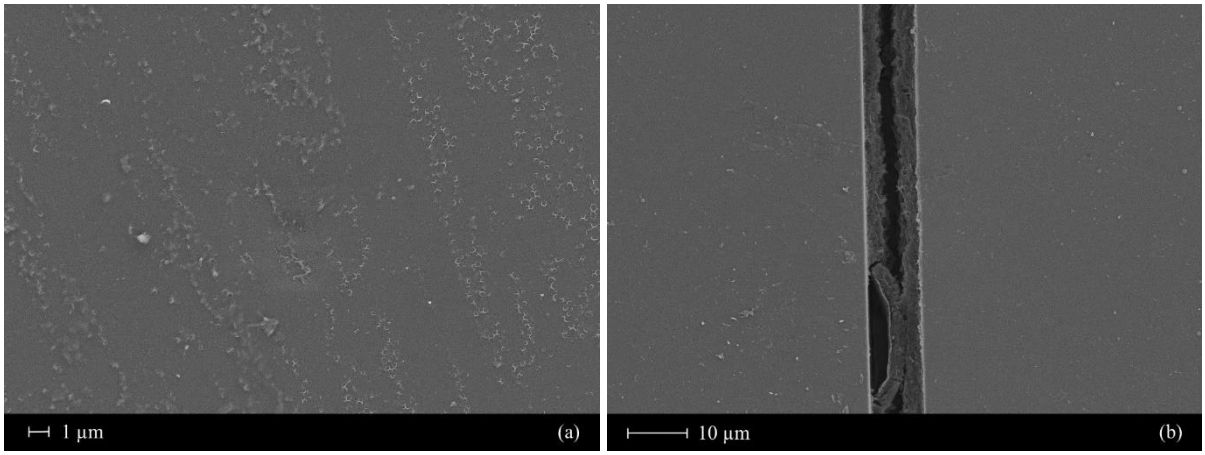

Figure 5.7: Pure Durazane 1800 coating SEM images. (a) Coating detail, (b) Macro-fracture detail

On the other hand, the joint, in Figure 5.8, is very discontinuous, with many holes and cracks; also, the adhesion is not so good, with only a few points of continuity between the two substrates. The joint is of about 20 µm thick: such a thin layer is obtained because the deposited polymer has a very low viscosity and also tends to infiltrate the porous alumina coating. However, the result obtained is in line with expectations given the brittleness of the post-cured material in the coating and the information on cracking and pore formation following the removal of low molecular weight volatile species and the densification and volume shrinkage.

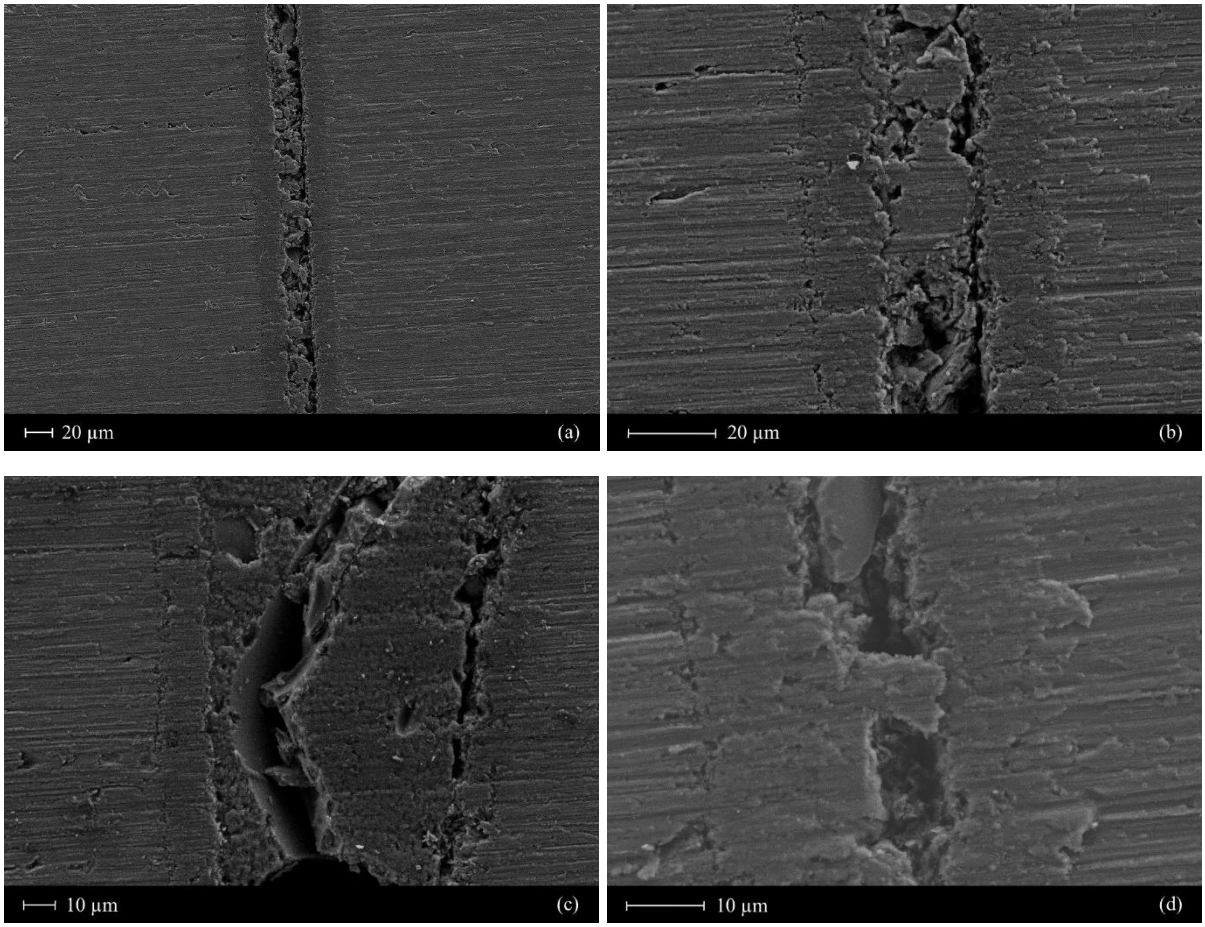

Figure 5.8: Pure Durazane 1800 joint SEM images. (a) Joint overview, (b) Joint detail, (c) Interface detail, (d) Continuity element between the substrates

It is important to note that in the case of the coating, the entire surface is available for the elimination of volatile species, thus inducing less stress in the thermoset polymer obtained by crosslinking, unlike the joint, where the species have only the edge area.

Mechanical test

Once the characterization was complete, the samples for the tensile mechanical test could be prepared. In particular, six specimens had to be made in order to establish statistics in the behaviour of the material. Low tensile strength was expected due to the brittleness of the material and from what could be seen from the SEM images.

In Figure 5.9 is reported the diagram which illustrates the load carried by each joint as a function of the elongation. Each test was stopped when the joint reached failure, which was definitely a brittle fracture.

All tests were successful with the exception of sample 5, which is not in the figure due to sample breakage during insertion into the machine.

The stress was then calculated on the basis of the peak load and the average area values, as follows:

$$\sigma = \frac{F}{A} \tag{1}$$

In which:

- σ [MPa] is the ultimate tensile stress (UTS);
- F [N] is the peak load;
- A [mm^2] is the surface area.

The fracture occurred under quasi-static conditions as the load was applied slowly at feed rate of 0.5 mm/min.

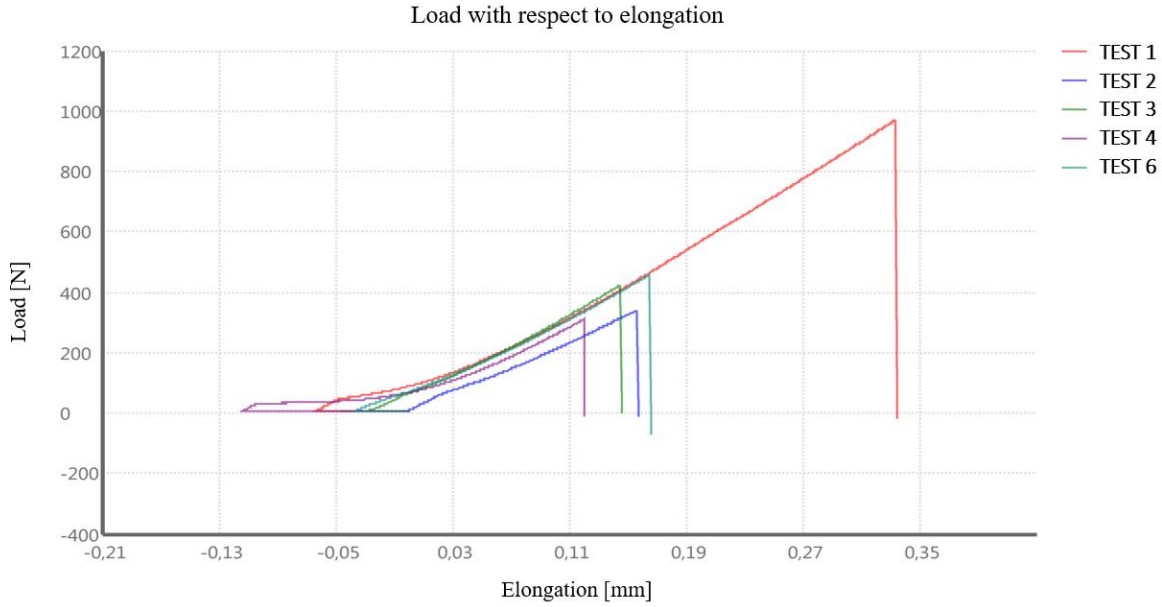

Figure 5.9: Pure Durazane 1800 tensile mechanical test, load with respect to elongation diagram

As the substrates used were cut individually, it was difficult to ensure that they all had the same dimensions, so an average area was calculated for each pair of substrates forming a joint to determine the ultimate tensile strength. At the same time, the approximation that the polymer was uniformly deposited on the substrate surface was made. In the Table 4, all the values of interest are reported.

Sample	Average area [mm^2]	Peak load [N]	UTS [MPa]
1	222.22	970.60	4.37
2	198.23	337.70	1.70
3	215.09	422.40	1.96
4	207.58	310.40	1.50
5	210.32	-	-
6	219.44	458.00	2.09

Table 4: Tensile mechanical test results for pure Durazane 1800

The results were coherent with the expectations, the only exception was represented by the sample 1 which was able to withstand double and even triple the peak load of the other samples. However, the case history is referred to samples 2-3-4-6, whose average UTS value is 1.81 MPa.

It was then possible to observe and analyse the fracture surfaces: the fracture is cohesive because the polymer is present on both sides of the joint in a perfectly mirrored fashion. On the other hand, the fracture surfaces have three main aspects, in fact those of the specimens 4 and 6 can be assimilated to those of specimens 2 and 1, respectively. They are shown in Figure 5.10.

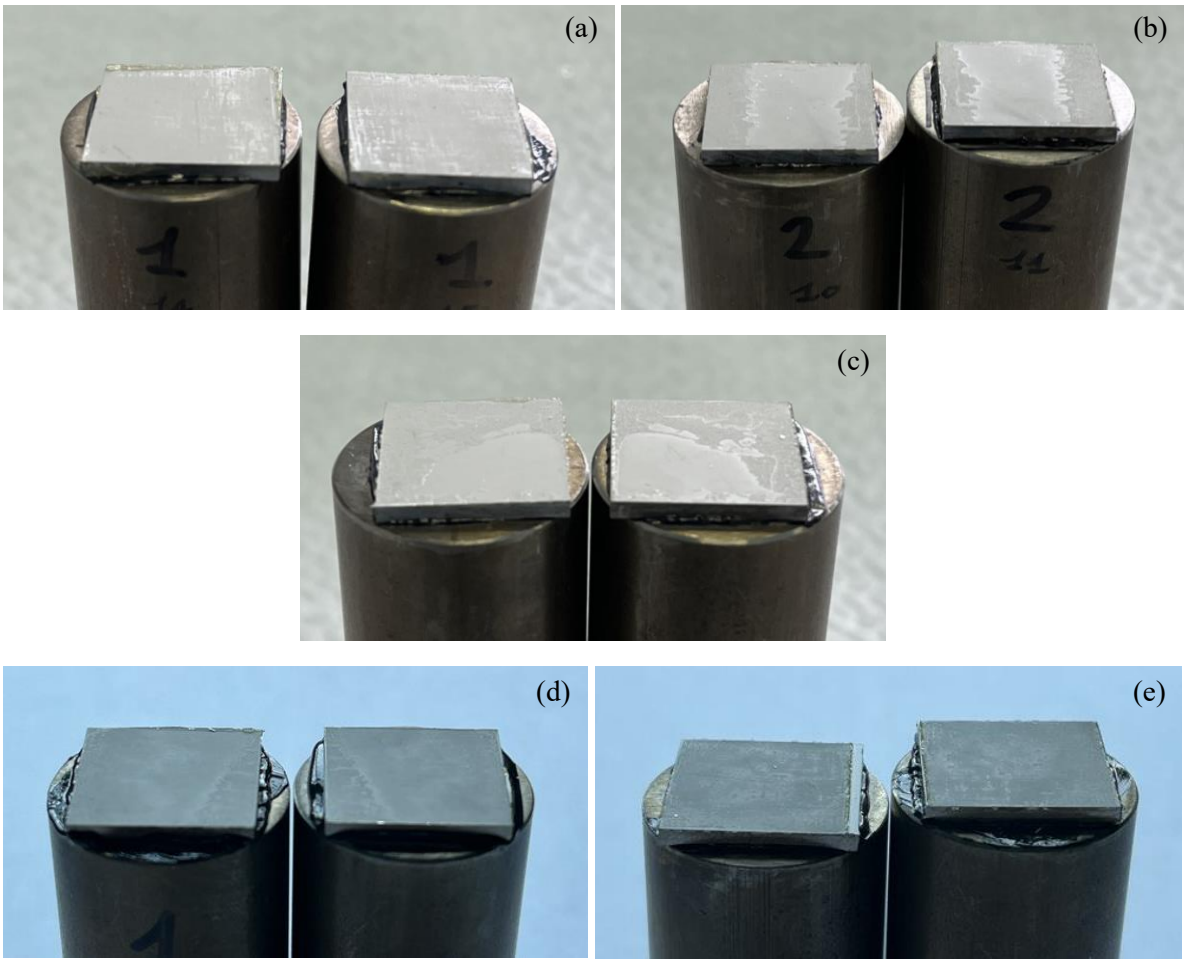

Figure 5.10: Fracture surfaces of pure Durazane 1800. (a) Sample 1, (b) Sample 2, (c) Sample 3, (d) Sample 4, (e) Sample 6

In the case of sample 1, the polymer is evenly distributed over the surface, in sample 2 it is mainly distributed towards two outer edges, while in sample 3 the polymer appears to cover two-thirds of the surface (leaving an area comparable to a quarter of the circumference uncovered). In samples 2-3-4 the polymer can be identified by its darker grey colour compared to alumina.

For a more detailed and comprehensible analysis, the surfaces were examined by SEM, in Figure 5.11.

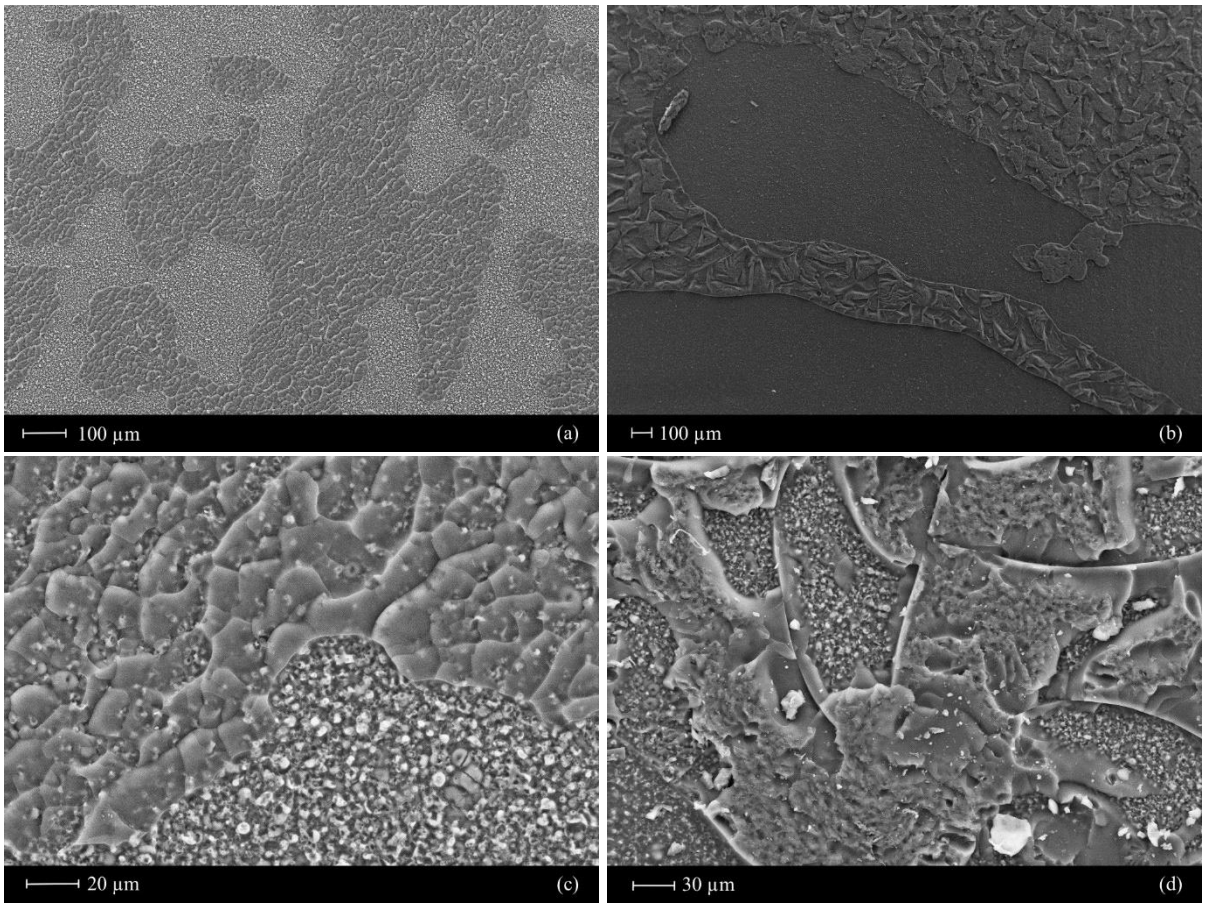

Figure 5.11: Fracture surfaces of pure Durazane 1800 at SEM, progressive magnifications from (a) to (d)

It is possible to distinguish the polymer from the alumina substrate because it appears to be jagged rather than smooth, as shown by the dark grey wavy bands in Figure 5.11 a. The flake pattern is also evident in all the other images. From the figure d, it can be seen that the thermoset polymer has some porosity.

A punctual EDS analysis was performed in order to verify the distinction between the polymer and the alumina coating of the substrates, providing compositional information. Spectrum 1 represents the point where the analysis was carried out for the polymer, while Spectrum 2 is the point examined for the alumina coating, as it is possible to see in Figure 5.12.

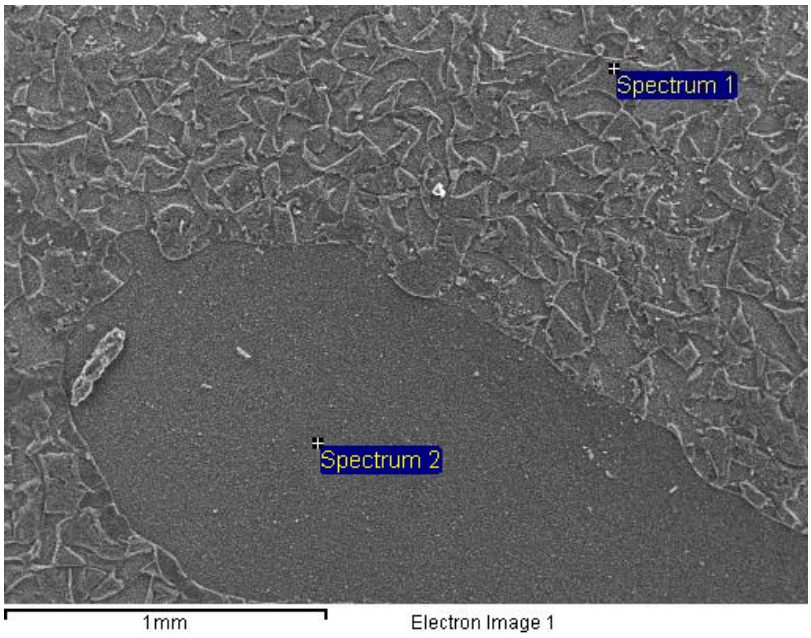

Figure 5.12: EDS punctual analysis on fracture surface of pure Durazane 1800

The results are summarized in Table 5 for Spectrum 1 (thermoset polymer) and in Table 6 for Spectrum 2 (alumina coating). Obviously, the EDS of the polymer reveals the main components of the chain, i.e. Si, C and O, as a result of the cross-linking reaction. However, it is interesting to note the presence of Si and C in the EDS of the alumina, indicating that the polymer has infiltrated the alumina porosity after deposition, although no layer formation can be detected; on the other hand, as expected, the largest shares concern Al and O.

Element	Weight [%]	Atomic [%]
C K	33.09	48.50
O K	20.22	22.24
Si K	46.69	29.26
Totals	**100.00**	

Table 5: EDS punctual analysis for pure Durazane 1800 in fracture surface (Spectrum 1)

Element	Weight [%]	Atomic [%]
C K	13.07	20.69
O K	37.95	45.11
Al K	37.88	26.69
Si K	11.10	7.52
Totals	**100.00**	

Table 6: EDS punctual analysis for alumina coating of the substrate in fracture surface (Spectrum 2)

XRD analysis

The last analysis performed on the pure Durazane 1800 was an XRD analysis on a pyrolyzed sample of polymer, in flakes, in order to verify the polymer-to-ceramic conversion. Once pyrolyzed, the polymer converts to amorphous ceramic and appears white in colour, as it is possible to see in Figure 5.13.

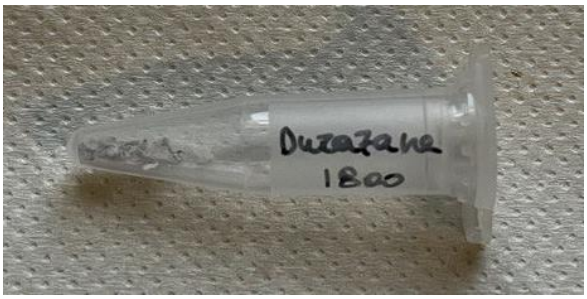

Figure 5.13: Pyrolyzed pure Durazane 1800 sample

The analysis confirmed the presence of only amorphous ceramic, as it can be seen from the halo in Figure 5.14.

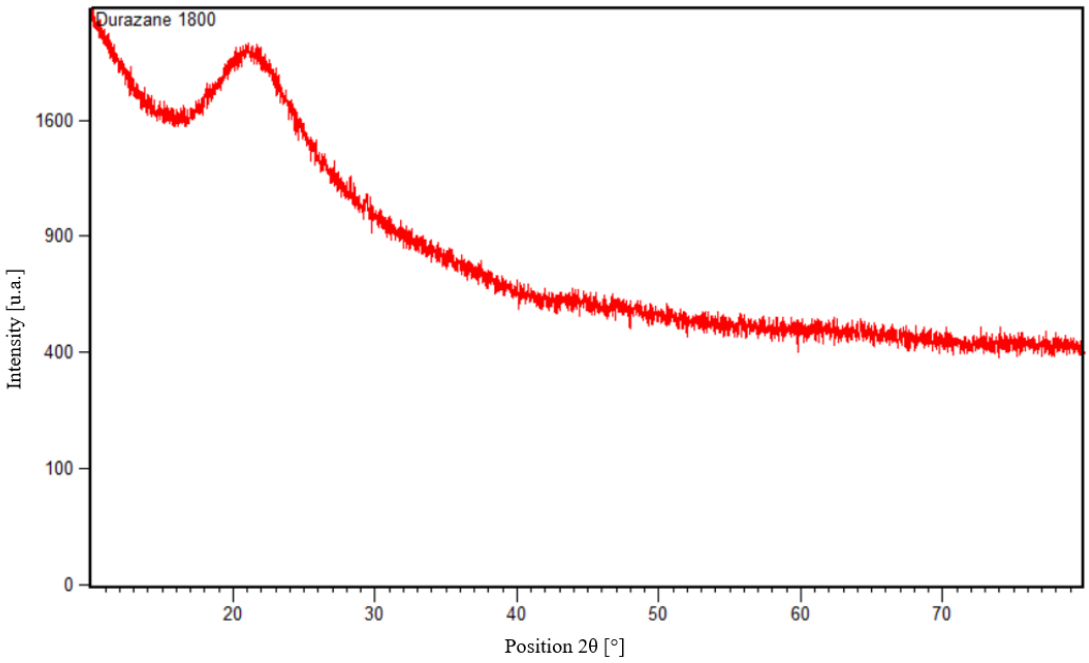

Figure 5.14: XRD spectrum of a pyrolyzed sample of pure Durazane 1800

Results in the literature, such as the study by Lenz Leite et all. [51], have confirmed that pyrolysis at certain temperatures only leads to the formation of an amorphous phase.

Improved case with fillers

Once the preliminary case analysis was complete, it was possible to proceed with the addition of filler, up to 48 wt.%, so that the effects could be studied. Based on the information gathered from the literature, an improvement in both the morphology of the joint material and the mechanical strength was expected. The same procedure (curing at 180 °C for 4 h in air) as for the preliminary case was repeated, with the realization and characterisation of a coating and a joint, followed by the preparation of specimens for the tensile mechanical tests.

Since the addition of filler increases the viscosity of the polymer, it was much more difficult to spread the material to obtain a thin, uniform layer, especially since a metal spatula was used for the deposition. In fact, there are two things to note: despite the addition of filler, the coating appears to be very cracked due to the thicker layer, while in the case of the joint it is possible to see that there is material that has

leaked out. This is because when the polymer is heated, even if it is very viscous, it begins to fluidise before it hardens and becomes a thermoset polymer. Therefore, the application of weight results in the leak out of the excess material, as long as it is fluid. The samples are shown in Figure 5.15.

Figure 5.15: Filled Durazane 1800 samples, coating (left) and joint (right)

In this case, the thicker polymer layer makes the resulting coating very brittle, much more than in the preliminary case, so that it tends to peel off the substrate very easily. In fact, it is possible to see how in some areas the coating is no longer present. On the other hand, similarly to the previous case, the joint appears to hold together and proved resistant to both a cut-off machine test and polishing.

The SEM images of the coating, in Figure 5.16, show that the coating is very compact, except for the macro-fractures. However, unlike the preliminary case, the coating is not uniformly coloured, but 'clouds' and corpuscles are visible. These can be assimilated to the added nanosilica particles. In particular, the already agglomerated particles cannot be separated by mixing, as they have only been mechanically dispersed. Instead, tend to agglomerate further.

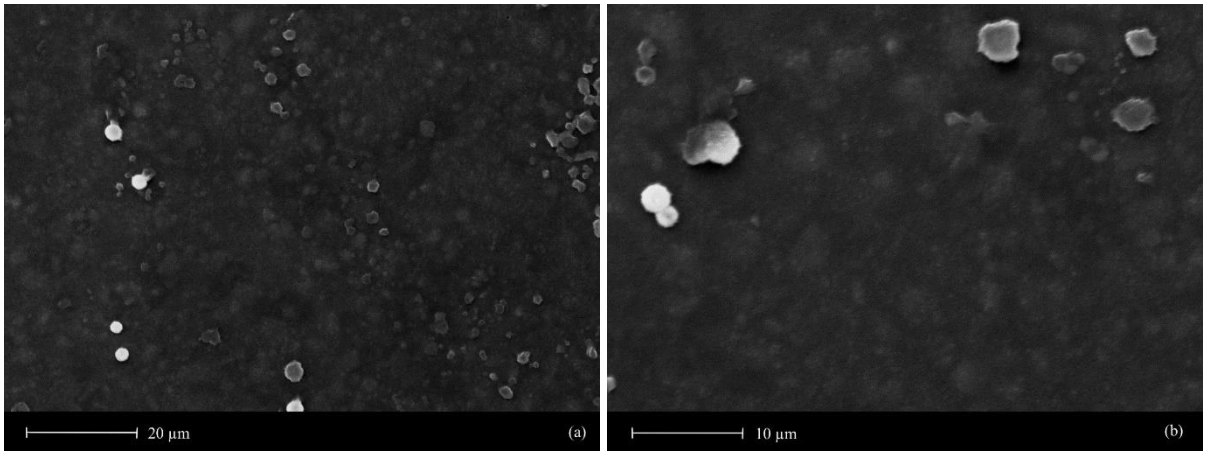

Figure 5.16: Filled Durazane 1800 coating SEM images

The joint, in Figure 5.17, is completely different from the one obtained in the preliminary case. Obviously, some holes are still present, as well as some cracks, but the joint appears dense and compact. Porosity and cracking can always be attributed to the removal of volatile species and the stresses induced by the densification of the cross-linking reaction, but inhomogeneous filler dispersion can also contribute to cracking by creating regions with different filler percentages and thus subjecting them to locally induced stresses of different magnitudes. The interface between the thermoset polymer and the substrate also appears to be improved, there are good adhesion and continuity, although these are found more on one substrate (the top) than the other (the bottom). The joint is about 30 µm thick, so it is thicker than the previous one.

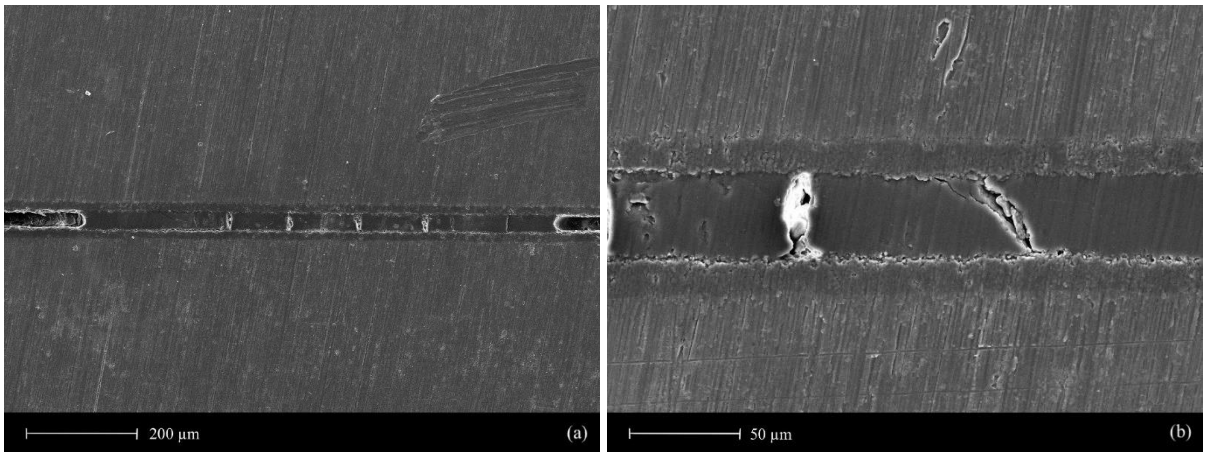

Figure 5.17: Filled Durazane 1800 joint SEM images

Due to the improvements in joint adhesion and compactness, an improvement in mechanical performance in tensile tests was expected.

Mechanical tensile tests

Six further samples were prepared and tested under the same conditions as the previous ones. In particular, in Figure 5.18 the diagram load-elongation is shown. The peak load for each sample is significantly higher than the average for the preliminary case. In the preliminary case the average value is around 500 N when all specimens are considered (if only the statistically valid specimens are, it does not reach 400 N), compared to around 1500 N of the improved case (considering all the specimens or only the statistically valid ones).

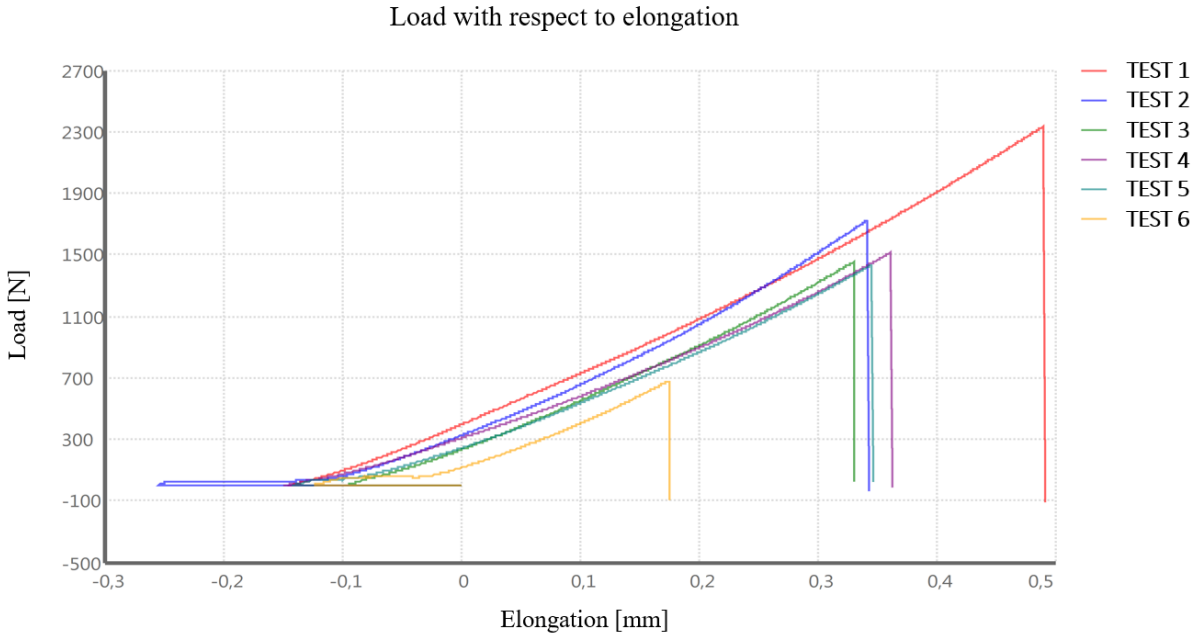

Figure 5.18: Tensile mechanical test of filled Durazane 1800, load with respect to elongation diagram

Of the six samples, four have very similar values (tests 2-3-4-5), one sample (test 1) is characterized by the highest value of all, while the last sample (test 6) has the lowest value. From a statistical point of view, the four samples with similar values are considered to be reliable. All the values, including the

ultimate tensile strength, are given in Table 7. In this case, the average value is of 7.22 MPa, about four times higher than the one obtained in the preliminary case.

Sample	Average area [mm^2]	Peak load [N]	UTS [MPa]
1	219.64	2331.10	10.61
2	212.36	1722.50	8.11
3	204.60	1452.10	7.10
4	207.98	1513.80	7.28
5	223.95	1431.70	6.39
6	232.25	677.20	2.92

Table 7: Tensile mechanical test results for filled Durazane 1800

Another aspect to consider is the fracture surfaces, shown in Figure 5.19: the fracture is always cohesive and the surfaces are all similar, especially in the pattern detected and thus in the way the polymer infiltrates the porous alumina coating. So, the polymer is identified by the shiny pattern on the grey aluminium oxide. Sample 1 is the one with the greatest amount of material and the most even distribution, so it has the highest strength value. On the other hand, sample 6 is the one with a thicker layer of joint material, probably less infiltrated, so it is characterized by the lowest strength value for these reasons.

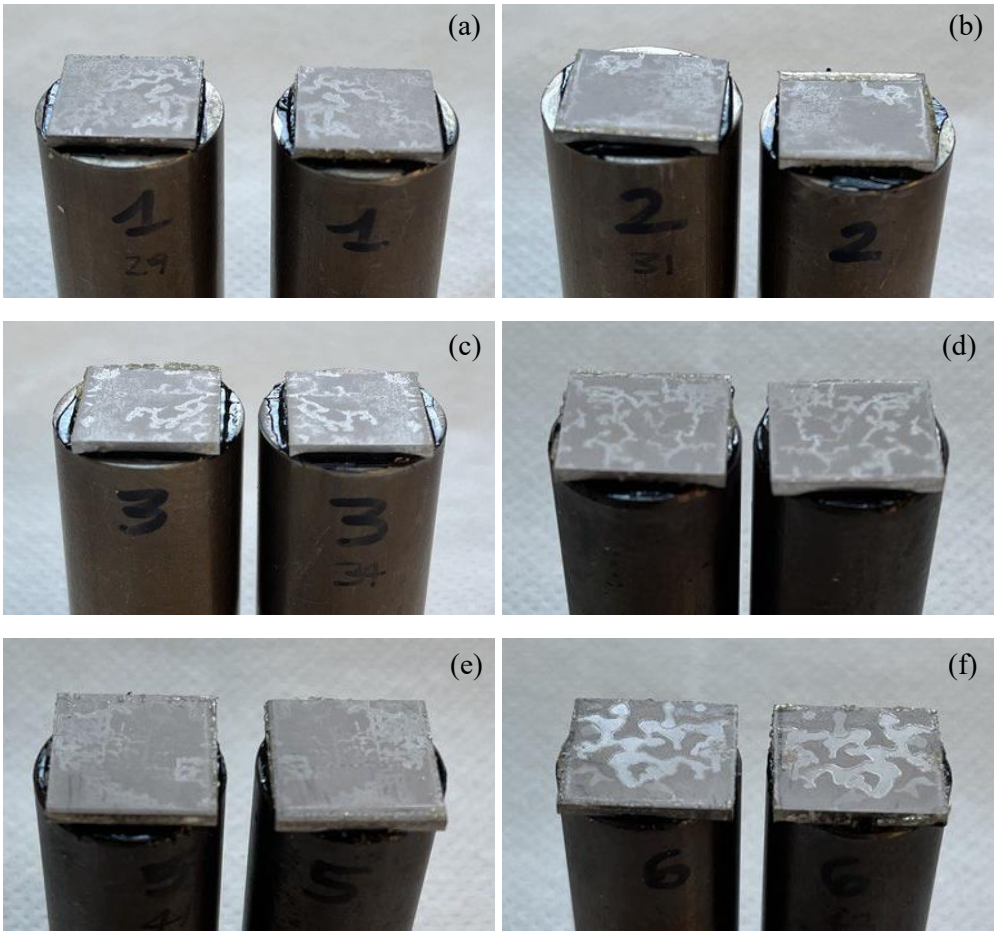

Figure 5.19: Fracture surfaces of filled Durazane 1800. (a) Sample 1, (b) Sample 2, (c) Sample 3, (d) Sample 4, (e) Sample 5, (f) Sample 6

Therefore, the differences between the fracture surfaces of Sample 1 and Sample 6 were investigated through SEM analysis; the images are shown in Figure 5.20**Errore. L'origine riferimento non è stata**

trovata., left column and right column, respectively. The subsequent magnifications show that the two fracture surfaces are in fact very different (not really noticeable at lower magnifications in the micrometre range), in particular the porosity of the joining material. In figure c, the nanometric detail of the two samples can be seen, with sample 6 being much more porous than sample 1, which appears denser and more compact.

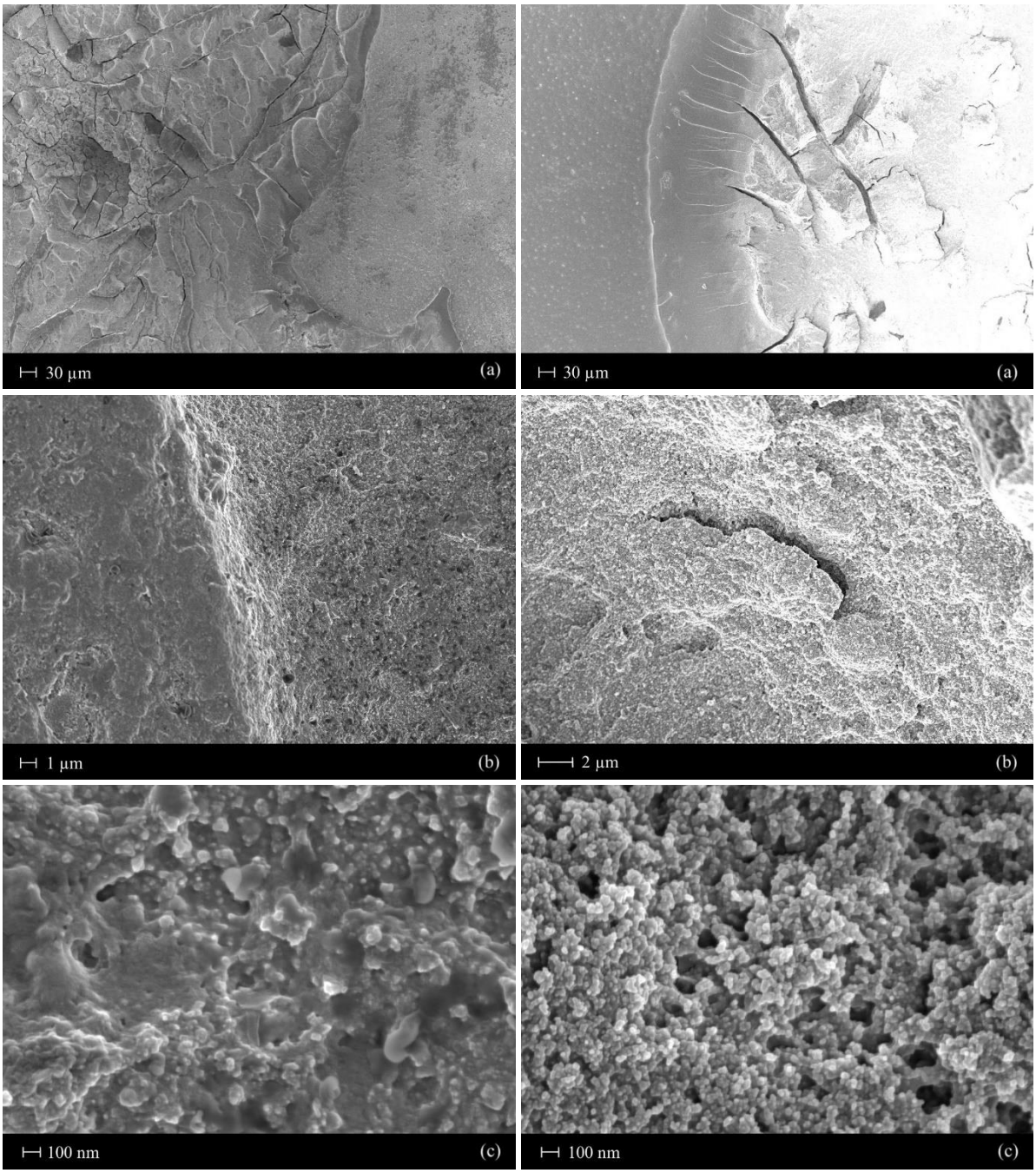

Figure 5.20: Comparison between fracture surfaces of filled Durazane 1800. Figures (a), (b), (c) on the left are related to Sample 1 while figures (a), (b), (c) on the right are related to Sample 6

Even in this case, a punctual EDS analysis was performed on the Sample 1 in order to verify the distinction between the thermoset polymer and the alumina coating of the substrate. Point 2 represents the point where the analysis was carried out for the polymer, while Point 3 is the point examined for the alumina coating, as it is possible to see in Figure 5.21.

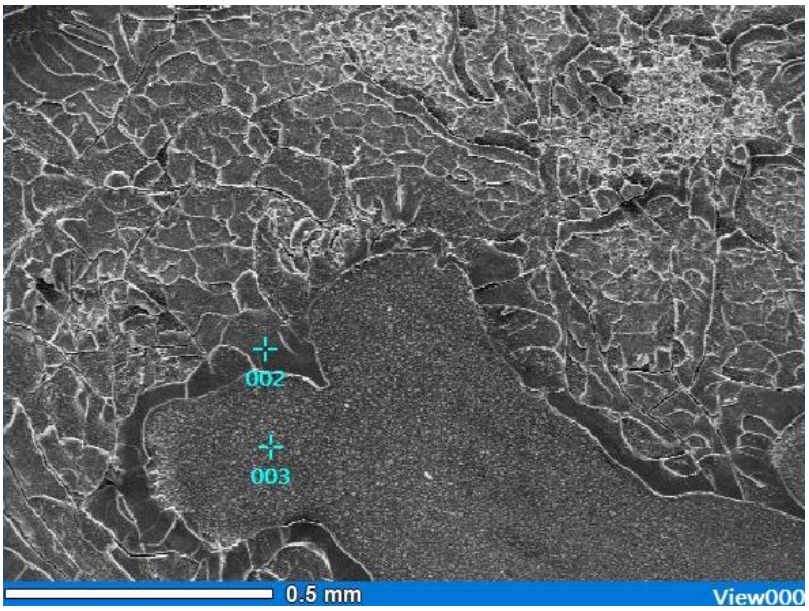

Figure 5.21: EDS punctual analysis on fracture surface of filled Durazane 1800, Sample 1

The compositional information provided are then summarized in Table 8 and Table 9 for the thermoset polymer and the alumina coating, respectively. A higher percentage of Si is detected in the case of the polymer, due to the addition of the silica nanoparticles.

Element	Weight [%]	Atomic [%]
C K	3.03	5.29
O K	39.65	51.94
Si K	57.30	42.76
Al K	0.01	0.01
Totals	**100.00**	

Table 8: EDS punctual analysis for filled Durazane 1800 in fracture surface (Point 2)

The same phenomenon can be observed with the alumina coating. Although the viscous filled polymer is more difficult to deposit in a uniform and controlled manner, it is possible to achieve a thicker layer and allow the material to infiltrate and bind the porosity of the alumina.

Element	Weight [%]	Atomic [%]
C K	13.83	22.01
O K	35.82	42.79
Si K	16.08	10.94
Al K	34.27	24.27
Totals	**100.00**	

Table 9: EDS punctual analysis for filled Durazane 1800 in fracture surface (Point 3)

TGA on the polymer with fillers after curing

As was done for the preliminary case, a thermogravimetric analysis was performed on a post-curing sample of filled polymer. The aim was to study the polymer-to-ceramic conversion and, in particular, to

determine the temperature range at which the greatest mass loss occurs in order to understand how to manage the pyrolysis phase. The result is shown in the diagram in Figure 5.22.

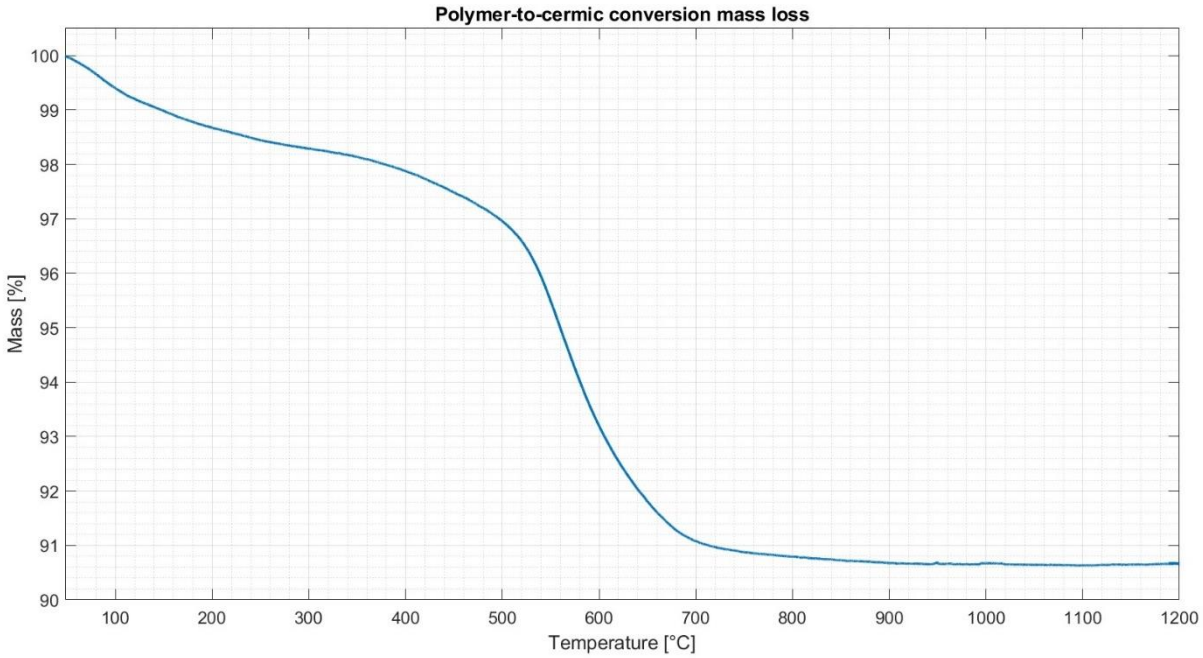

Figure 5.22: Filled Durazane 1800 mass loss in polymer-to-ceramic conversion

It can be seen that the total mass loss of the process is of 9.40%, slightly lower than the value found in the case of pure polymer. The trend is very similar to the preliminary case, although for temperatures below than 400 °C there is a higher mass loss of 2.2%, associated with the most volatile species. The significant mass loss of 6% then occurs between 500 °C and 700 °C, corresponding to the conversion to amorphous ceramic. Again, a plateau is reached around 800 °C, so that no further mass loss occurs at higher temperatures.

This information was the starting point for the realisation of joint pyrolysis, using substrates that can withstand high temperatures.

Joint with ox-CMC substrates

After completing the study on aluminium substrates coated with alumina, it was possible to study and characterise the behaviour of the filled polymer on ox-CMC substrates. As the substrates were different from the previous ones, an adhesion test was carried out with the pure polymer before proceeding with the filled one. The main objective of the preliminary test was to understand if the polymer could infiltrate between the alumina fibres of the alumina-zirconia matrix.

The pure polymer, due to its viscosity similar to water, was able to infiltrate completely. In fact, in the case of the coating, the substrate appeared yellowed compared to the untreated one, as can be seen in Figure 5.23, and the same was true for the joint, which in reality was not obtained.

Figure 5.23: Pure Durazane 1800 on ox-CMC substrates. Coating (left), not-formed joint (right)

Believing that the problem might be the low viscosity, it was decided to try again with the filled polymer. An immediate problem was found with the deposition of the polymer on the substrate due to the low wettability. This was translated into an adhesion problem after the curing process. In fact, as shown in Figure 5.24, the cured polymer appears to be completely cracked and non-adherent.

Figure 5.24: Filled Durazane on ox-CMC substrates, joints attempt

So, a surface modification treatment with plasma at low temperature was carried out on the substrates in order to improve wettability and adhesion. With the naked eye, it was not possible to detect any macroscopic differences between the treated and untreated substrates, but they could be seen in the ease of deposition. In this case, a positive result was obtained: although the coating is cracked, it also adheres to a large extent, but splits when touched with a metal rod, while the joint seems to stay together and proved resistant to the polishing test. The samples obtained are shown in Figure 5.25.

Again, it is possible to see that material is leaking due to the weight placed on the joint during the curing phase. In addition, due to the irregularity of the substrate surfaces, there are areas where the joint is thinner and others where it is thicker.

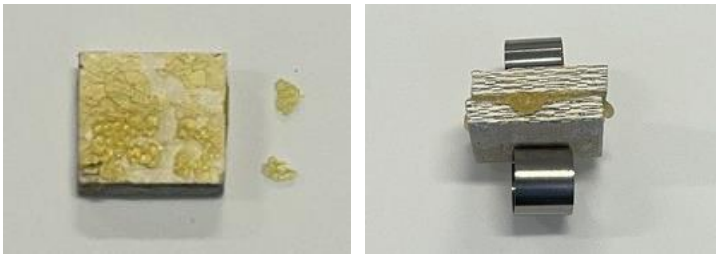

Figure 5.25: Filled Durazane 1800 samples with ox-CMC substrates, coating (left) and joint (right)

From the SEM characterization, Figure 5.26, it was found that the thicker part of the joint is approximately 55 µm thick. Even in this case the joint appears dense and compact, with few cracks and voids. In addition, the joint appears much more uniform along the entire cross section analysed than that obtained with alumina-coated aluminium substrates. Although there are some areas where there are problems with the adhesion at the interface (detail in figure b), good adhesion can be found along almost the entire cross section analysed (detail in figure c). An interesting feature is the polymer's ability to infiltrate the alumina-zirconia matrix, as shown in figure d.

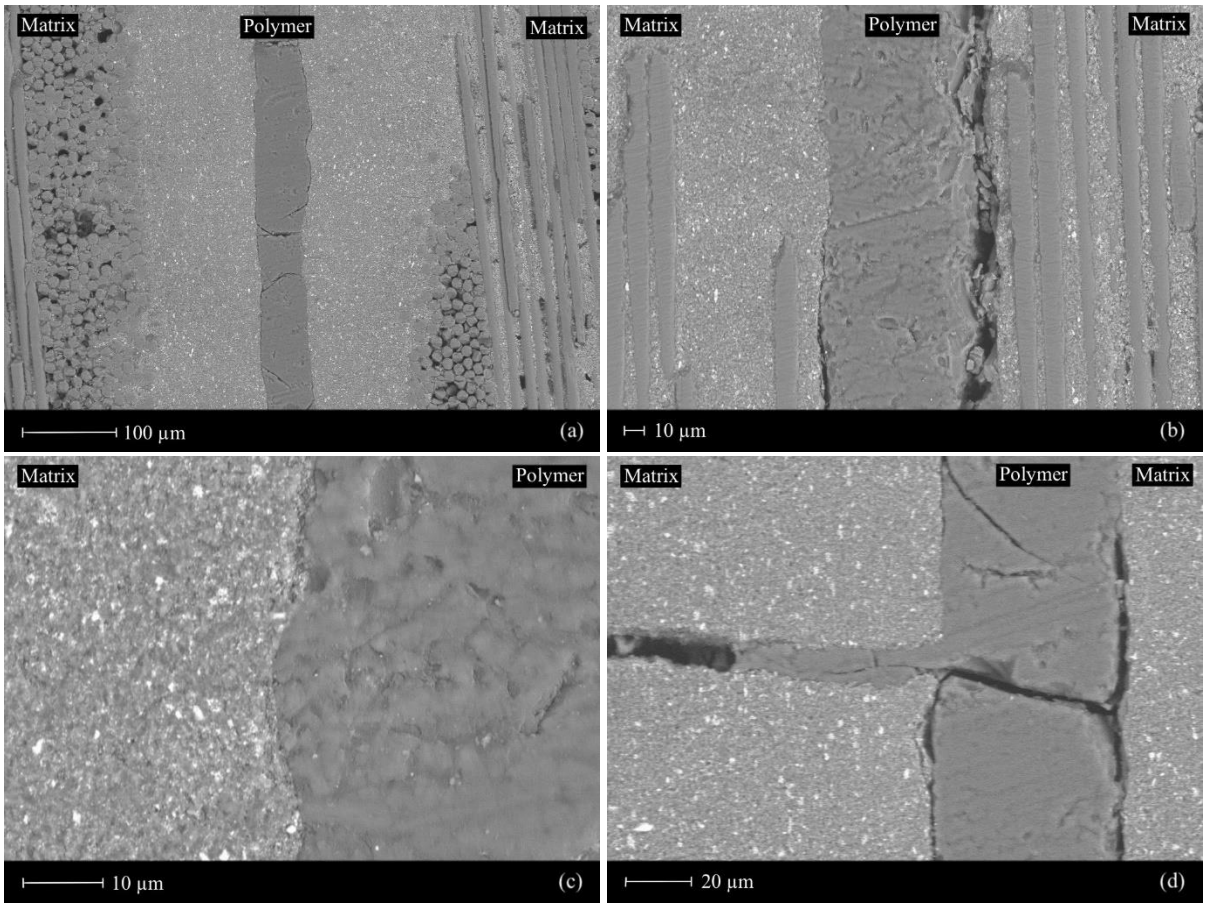

Figure 5.26: Filled Durazane 1800 joint with ox-CMC substrates SEM images. (a) Joint overview (b) Interface, (c) Interface detail, (d) Infiltrated polymer in the matrix

As these substrates can be heated up to 1200 °C, a pyrolysis test was carried out on the joint. In order to minimise the formation of pores and cracks as much as possible, a slow heating rate was used, particularly in the temperature range where the conversion from polymer to amorphous ceramics takes place. The procedure followed for the pyrolysis and the subsequent substrate resistance test was:

i) Up to 400 °C: heating rate of 5 °C/min;
ii) 400-800 °C: heating rate of 2 °C/min;
iii) 800-1200 °C: heating rate of 5 °C/min;
iv) 1200: one-hour isotherm.

The result was a completely pyrolyzed joint that still held together. Visually, the yellow thermoset polymer has now changed to white amorphous silica, and the Figure 5.27 shows a continuous structure due to the pyrolysis of the joint.

Figure 5.27: Pyrolyzed joint with ox-CMC substrates

In addition, any organic groups present in the polymer were also removed by pyrolysis. The presence of cracks and pores was therefore inevitable. A computed tomography (CT) scan of the joint was performed to determine the morphology of the joint's plane and the results are shown in Figure 5.28.

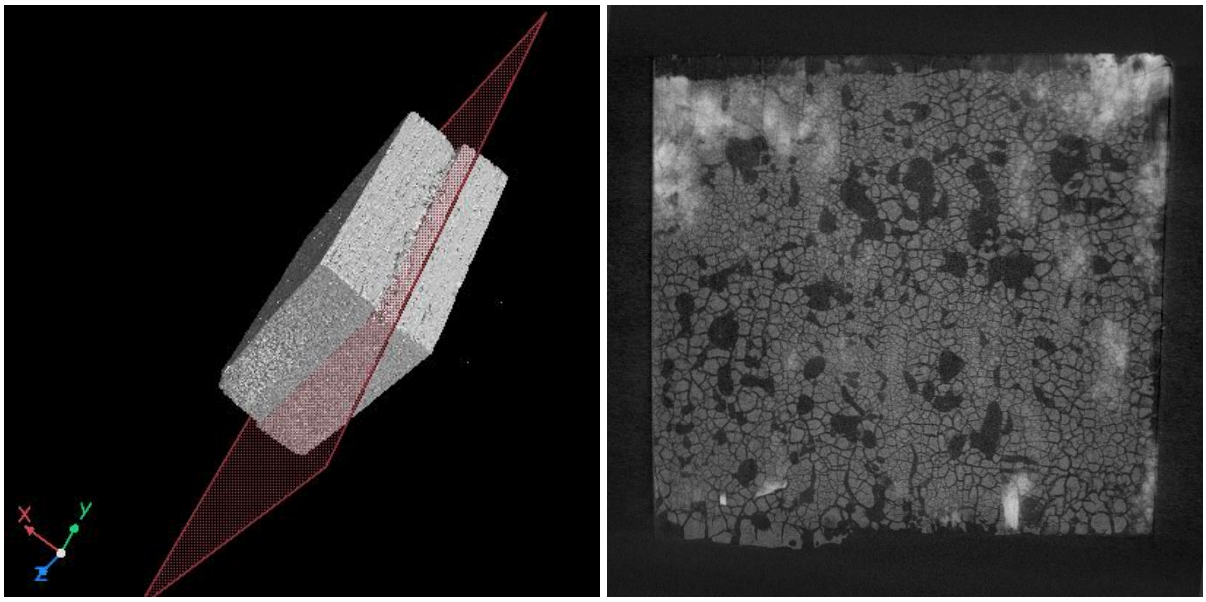

Figure 5.28: CT-scan of the pyrolyzed joint. 3D model with the individuation of the joint plane (left), joint plane representation (right)

5.1.2 PHPS

The inorganic silica precursor, PHPS, was used in a single preliminary test to evaluate its future use in the same way as Durazane 1800. The alumina-coated aluminium substrates were used.

First, the rotavapor was used to remove the solvent: it took about 50 minutes to remove 95% of the solvent. The result was a polymer with a gel-like consistency, viscous enough to be used as an adhesive, but still fluid enough to be applied with a metal spatula to realise a uniform coating without too much difficulty. Then, the samples were cured in an oven at 180°C for 1 hour in air and subsequently allowed to cool naturally in the instrument, as in the case of the Durazane 1800. The curing time was taken from the technical data sheet of the material, but refers to the polymer with the solvent, so it is an initial value to be optimised later.

The results are shown in Figure 5.29. In the case of the coating, a test was also carried out on the substrate on the aluminium side. While there is no obvious difference between the joint made with PHPS and that made with Durazane 1800, there are a number of differences in the coating. Firstly, PHPS has a good adhesion on both the aluminium and alumina sides. Secondly, the coating appears compact and crack-free, with some ridges in the areas where the coating is thicker. Finally, the cured polymer appears transparent due to the absence of organic groups.

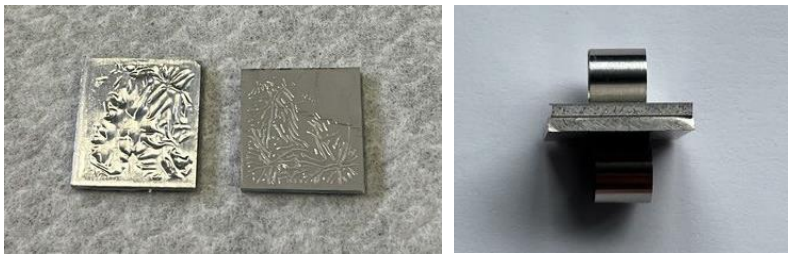

Figure 5.29: PHPS and alumina-coated aluminium substrates. Coatings (left), joint (right)

As the coating was not brittle and did not tend to detach from the alumina, it was possible to analyse the cross-section by SEM, as shown in Figure 5.30. It has a thickness of about 30 µm where it is thinner (i.e. not at a ridge), looks compact and shows a better adhesion than the Durazane 1800.

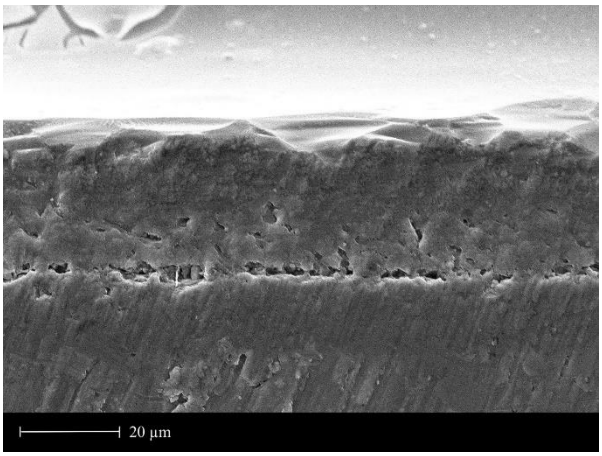

Figure 5.30: PHPS coating at SEM

The same considerations can be made for the joint in Figure 5.31, which is about 13 µm thick, so it is thinner than the one obtained with the other polymer. Although there are areas characterised by pores and cracks, it is interesting to note that along the entire joint there are more or less extensive areas characterised by compactness and absence of cracks; others are characterized by good adhesion of the polymer to both substrates or, most commonly, to one of them. This result with Durazane 1800 was obtained only after the addition of the silica nanocarriers.

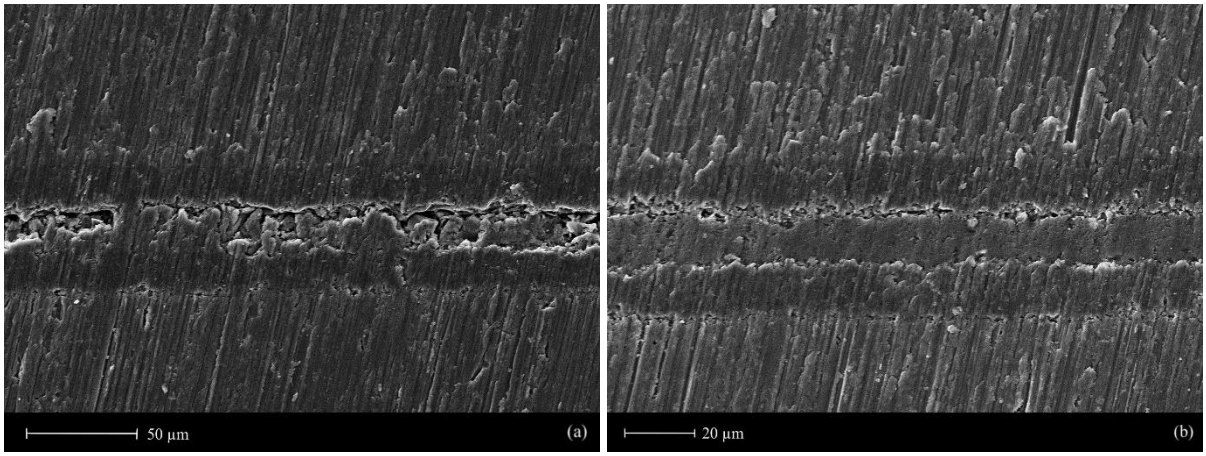

Figure 5.31: PHPS joint at SEM

5.2 SiC precursor

The work on the silicon carbide precursor has the aim to investigate the behaviour of the experimental resin, in terms of the process and the adhesion to the specific substrates, in order to be able to produce nuclear grade 'total-SiC' joints. A preliminary study is required as the product was specifically designed for this type of joint, and as it is not a commercial product there is no information available.

A three-step process was followed to achieve full densification of the precursor.

1. Thermal setting at 100 °C in oven for 1 hour. This part of the process is the only one carried out in air;
2. Heating process until 800 °C in argon atmosphere with a heating rate equals to 10 °C/min, followed by 1 hour hold to complete the pyrolysis;
3. Heating process until 1500 °C in argon atmosphere with a heating rate equals to 10 °C/min, followed by a 30 minutes hold to complete the sintering.

In particular, the steps 2 and 3 are performed in a tubular furnace in order to guarantee the argon fluxing.

Once the polymer had been prepared, a first test was carried out. The precursor was very viscous, which made it difficult to deposit it homogeneously on the substrate, resulting in a coating that was not thin and, above all, varied in thickness over the entire surface of the plate. In fact, Figure 5.32 shows the lines resulting from the deposition with the spatula.

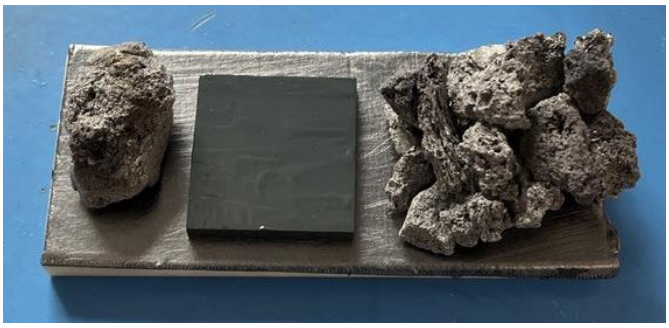

Figure 5.32: Cured SiC precursor, assembly before pyrolysis

The sample shows the result after the curing and also the assembly (complete with titanium sponges) before the pyrolysis is shown. Titanium sponges are used in order to not compromise the process in the case of small oxygen infiltrations.

To investigate the curing phase, a TGA was performed on the liquid polymer in air. A quantity of 67.54 mg of sample was brought to an initial temperature of 20 °C, which was kept constant for 5 minutes so that the sample reached a uniform temperature. Then, a heating rate of 10 °C/min was used to reach the curing temperature of 100 °C, where the sample was kept for 1 hour, in order to reproduce the curing step. The mass loss versus time obtained is shown in Figure 5.33.

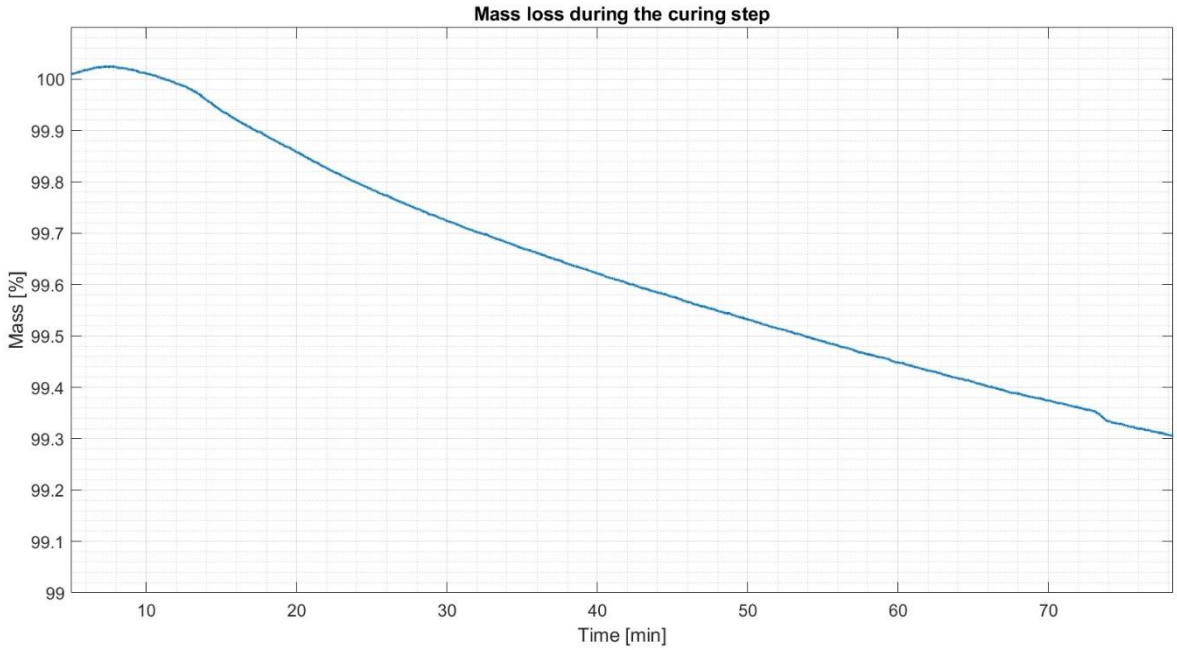

Figure 5.33: SiC precursor mass loss during curing step

The graph shows a mass loss of 0.7% and therefore the curing can be considered effective.

Then the step 2 and 3 are performed and the obtained samples can be seen in Figure 5.34.

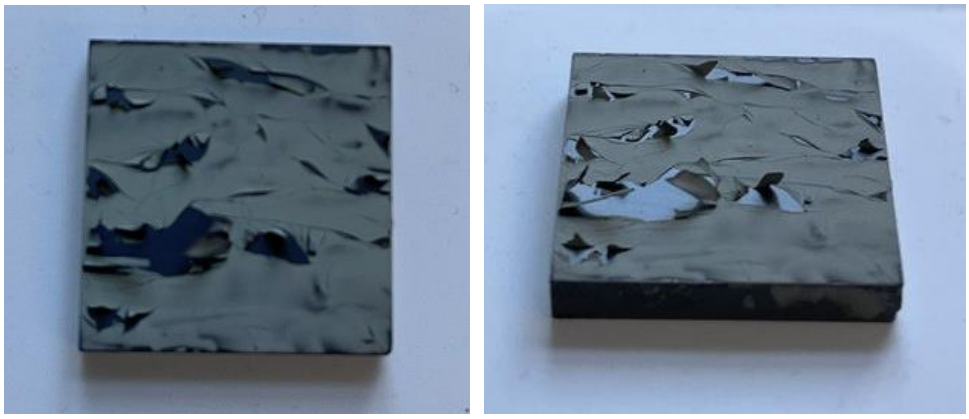

Figure 5.34: Result of Pyrolyzed SiC precursor

After the pyrolysis and the sintering steps, the precursor was converted to SiC. A very thin layer, characterized by a light grey colour, remains of the original thick, dark-coloured coating, with a few cracks in places. So, it is evident as some adhesion problems need to be solved. The same problem was also found on the cylinder, which is made of the same material as the plate.

A TGA was carried out to investigate also the thermal conversion of the SiC precursor. In this case, the liquid polymer (98.72 mg) was heated up to 1500 °C at a heating rate of 10 °C/min under argon flux. The curve which illustrates the mass loss as a function of the temperature is shown in Figure 5.35.

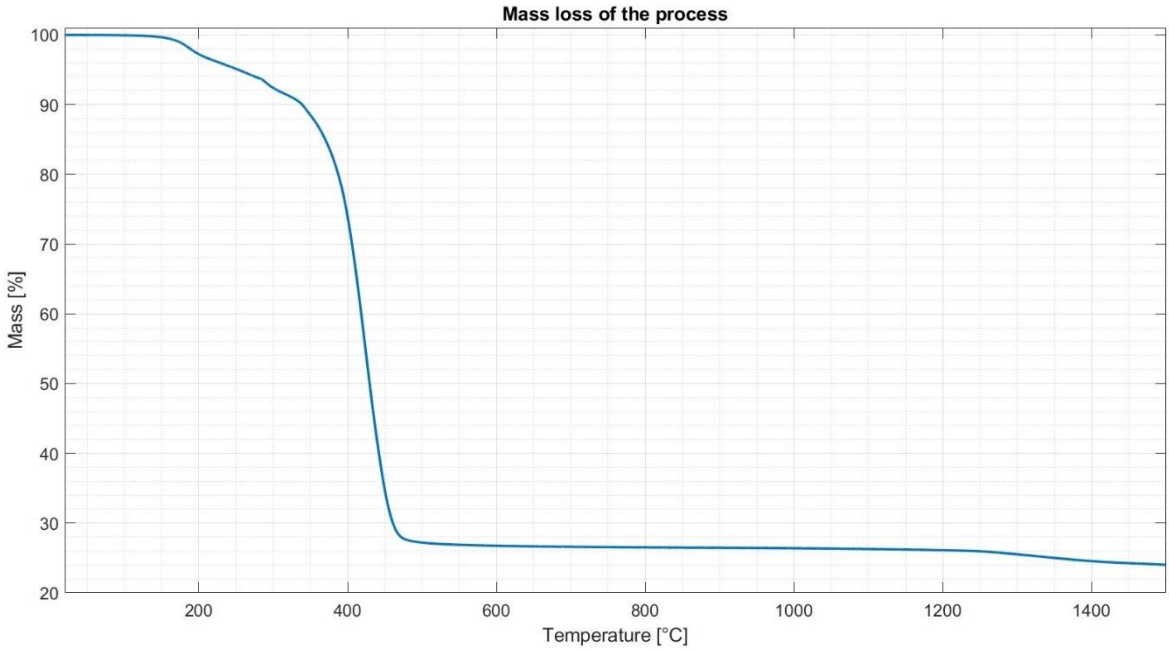

Figure 5.35: SiC precursor mass loss during the polymer-to-ceramic conversion

In particular, a mass loss of 72.80% was observed in the temperature range 200-500 °C. This result is considered abnormal due to the fact that the polymer is filled with the 60 wt.% of SiC nanocarriers.

Further studies will have to be done in the future to further investigate the behaviour of the precursor and to establish the technical feasibility of a 'total-SiC' joint.

6 Conclusions and perspectives

The goal of achieving effective joints with ceramic and CMC materials is now a serious technological problem at a universal level. Solving this problem would allow the realisation of high-performance components with complex rather than standard shapes, widening the range of applications in areas such as energy conversion and efficiency, space exploration and aeronautics, where high-performance materials are required but still have significant production and energy costs. Among the new technologies being developed, preceramic polymers represent a bridge between technological fulfilment and energy saving, given the advantages of being able to use additive manufacturing techniques and low process temperatures, and ultimately obtain a ceramic material with tailored properties.

In this work, it has been possible to carry out a preliminary study in order to evaluate the technical feasibility of ceramic joints made with ceramic precursor polymers. Although the study presented represents a first stage of research, the in-depth bibliographical research has made it possible to understand the processes involved in the polymer-to-ceramic transformation and thus to define guidelines and repeatable procedures in order to obtain reliable results also from a statistical point of view. At the same time, the critical aspects of the process could be addressed: volumetric shrinkage, residual porosity due to the elimination of volatile species and cracks formation due to residual stresses are all phenomena that undermine the integrity and strength of the resulting component and must be minimised.

In particular, the study carried out on the Durazane 1800 silica precursor in its cured state and the alumina-coated aluminium substrates has allowed to fully understand the possibilities of the pure material, its mechanical strength and its criticalities in order to improve performance. The solution represented by the addition of passive filler, such as nanometric amorphous silica fillers, has made it possible to control the critical aspects of the crosslinking process and achieve significant improvements in both joint morphology and mechanical strength. It was possible to move from a joint characterised by many voids and cracks to a very dense and compact joint, although not cracks-free, better adhered to the substrate, and capable of achieving an average tensile strength of 7.7 MPa, a value four times higher than the one obtained in the preliminary case with the pure polymer. Moreover, the analysis of the fracture surfaces has enabled a better understanding of the adhesion mechanism that occurs between the polymer and the substrate, which is fundamental to achieve an effective joint.

The positive results obtained with this type of substrate have made it possible to extend the study and investigate the pyrolysis step, this time using ox-CMC substrates. Once again, it has been possible to obtain a compact joint that holds together, a result that is by no means self-evident, since the conversion process from polymer to amorphous ceramics is accompanied by a non-negligible loss of mass due to the elimination of the remaining volatile compounds and organic groups, causing further formation of pores and cracks and inducing stresses. This result is a good starting point for further tests in the future: first, the pyrolysis step will be optimized, finding a more suitable and slow heating rate to minimize the criticalities, then the process (both curing and pyrolysis step) will have to be repeated in its entirety to check the actual reproducibility, and finally the samples will have to be prepared for mechanical tests to check the strength of the pyrolyzed material and its adhesion. Surface treatments are used to functionalise the substrate area to promote and enhance the intimate contact between the polymer precursor and the substrate surface: as only the plasma treatment has been tested for the modification of the surface of the substrates, other treatments could be tested in order to try to obtain better results, such as laser treatment and hydrated salts.

Similarly, the preliminary study carried out on the inorganic silica precursor PHPS confirmed the effectiveness of these precursors as joining material and opened up further avenues for the fulfilment of the objective. The joint obtained was compared morphologically with that obtained with pure Durazane 1800, and interesting aspects emerged. In particular, the solvent-free PHPS, characterized by a gel-like consistency, showed better adhesion to the alumina-coated aluminium substrates and a dense structure over more or less extensive areas of the joint's cross-section, results obtained with the Durazane 1800 only after the addition of filler. The test was carried out with a curing time characteristic of the polymer with the solvent, so further TGA analysis will be performed in the future to find the optimum curing time for the solvent-free polymer, keeping the temperature used constant. All the analyses and mechanical tests carried out with Durazane 1800 will have to be repeated, first without fillers in order to have a baseline for comparison, and then the amount of charges to be added will have to be found in order to have an improvement of the properties and performance. The final objective will be to determine if the inorganic silica precursor performs better than the organic one as joint material and to proceed with the ox-CMC substrates study.

The realisation of a continuous joint based on silicon carbide has so far been an ideal goal. From a theoretical point of view, it has been possible to study the achievement of the ceramic material from the precursor, but there is still a lot of work to be done, starting with the adhesion between the polymer and the substrate. Once the surface has been modified with the most effective treatment and the test repeated on a coating, it will be possible to move on to the actual joint. However, even this conversion process could be optimized with respect to the specific desired result.

Other possible general future improvements are related to the modification of the technical parameters, such as curing temperature and time, atmosphere used, addition of catalysts to promote the polymer-to-ceramic conversion. Also, different types of fillers could be used, both passive and active, and the addition of fibres could be considered to create a real cushion within the polymer to limit volumetric shrinkage and minimise criticality during conversion.

It is important to stress that if the results obtained are very satisfactory, it will be necessary to study the industrial applicability of the proposed technology. The operating conditions would concern all the stages of the process. The starting point could be represented by the mixing of the polymer and the filler, then the use of mechanical or microwave mixers with subsequent degassing to facilitate the uniform dispersion of the particles, but also to eliminate any embedded oxygen or gas bubbles formed in them. Then, how to perform the heat treatment, both curing and pyrolysis, due to the fact that in case of large components, large installations would be required, which would involve the use of large amounts of energy, and it would therefore be desirable to also consider on-site joining techniques (e.g. laser).

In conclusion, the positive results obtained demonstrate and confirm the great potential of these precursors also in the joint field, and it will be necessary to continue studying them in order to resolve the criticalities and improve their performance before possibly moving to a pre-industrial scale. Future studies will therefore be of fundamental importance.

Bibliography

[1] L. C. Vieira, M. Longo, and M. Mura, "Are the European manufacturing and energy sectors on track for achieving net-zero emissions in 2050? An empirical analysis," *Energy Policy*, vol. 156, Sep. 2021, doi: 10.1016/j.enpol.2021.112464.

[2] T. Konegger *et al.*, "Ceramics for Sustainable Energy Technologies with a Focus on Polymer-Derived Ceramics," in *Novel Combustion Concepts for Sustainable Energy Development*, Springer India, 2014, pp. 501–533. doi: 10.1007/978-81-322-2211-8_22.

[3] O. Guillon, "Ceramic materials for energy conversion and storage: A perspective," *International Journal of Ceramic Engineering & Science*, vol. 3, no. 3, pp. 100–104, May 2021, doi: 10.1002/ces2.10086.

[4] Cerame-Unie Aisbl (CU), "CERAMIC ROADMAP TO 2050 FOR THE WELL-BEING OF A RESILIENT, CLIMATE NEUTRAL EUROPE." [Online]. Available: www.cerameunie.eu

[5] S. Prakash Pandey and V. Singh, "The Importance of Engineering Materials in Present World," 2015. [Online]. Available: www.ijsr.net

[6] J. Rödel *et al.*, "Development of a roadmap for advanced ceramics: 2010-2025," *J Eur Ceram Soc*, vol. 29, no. 9, pp. 1549–1560, Jun. 2009, doi: 10.1016/j.jeurceramsoc.2008.10.015.

[7] K. Martinsen, S. J. Hu, and B. E. Carlson, "Joining of dissimilar materials," *CIRP Ann Manuf Technol*, vol. 64, no. 2, pp. 679–699, 2015, doi: 10.1016/j.cirp.2015.05.006.

[8] Amanda Allison FdEng, "Prepared by the Joining Sub-Platform 2014." [Online]. Available: www.joining-platform.com

[9] "NOVEL CERAMIC MATRIX COMPOSITES PRODUCED WITH MICROWAVE ASSISTED CHEMICAL VAPOUR INFILTRATION PROCESS FOR ENERGY-INTENSIVE INDUSTRIES." [Online]. Available: https://www.cem-wave.eu/

[10] "Novel Ceramic Matrix Composites produced with Microwave assisted Chemical Vapour Infiltration process for energy-intensive industries." https://cordis.europa.eu/project/id/958170/it

[11] "Innovative cladding materials for advanced accident-tolerant energy systems." https://cordis.europa.eu/project/id/740415

[12] "SiC composite claddings: LWR performance optimization for nominal and accident conditions." https://cordis.europa.eu/project/id/101059511

[13] "Joining-Understanding the Basics Introduction to Joining," 2011. [Online]. Available: www.asminternational.orgCHAPTER1

[14] R. W. Messler, "Trends in key joining technologies for the twenty-first century Classical and changing reasons for joining." [Online]. Available: http://www.mcbup.com/research_registers/aa.asp

[15] M. Gerendás *et al.*, "IMPROVEMENT OF OXIDE/OXIDE CMC AND DEVELOPMENT OF COMBUSTOR AND TURBINE COMPONENTS IN THE HIPOC PROGRAM," 2011. [Online]. Available: http://www.asme.org/about-asme/terms-of-use

[16] G. Barroso, Q. Li, R. K. Bordia, and G. Motz, "Polymeric and ceramic silicon-based coatings-a review," *Journal of Materials Chemistry A*, vol. 7, no. 5. Royal Society of Chemistry, pp. 1936–1963, 2019. doi: 10.1039/c8ta09054h.

[17] E. H. Penilla *et al.*, “Ultrafast laser welding of ceramics.”

[18] C. Gadelmeier, “Joining of Ceramic and Metal Parts.” [Online]. Available: www.ceramic-applications.com

[19] A. G. Razzell, “4.23 Joining and Machining of Ceramic Matrix Composites.”

[20] S.-I. Matsuoka, “Ultrasonic welding of ceramics/metals using inserts,” 1998.

[21] P. Dong, Z. Wang, W. Wang, S. Chen, and J. Zhou, “Understanding the spark plasma sintering from the view of materials joining,” *Scr Mater*, vol. 123, pp. 118–121, Oct. 2016, doi: 10.1016/j.scriptamat.2016.06.014.

[22] M. Tokita, “Progress of spark plasma sintering (Sps) method, systems, ceramics applications and industrialization,” *Ceramics*, vol. 4, no. 2, pp. 160–198, Jun. 2021, doi: 10.3390/ceramics4020014.

[23] S. X. Song, Z. Wang, and G. P. Shi, “Heating mechanism of spark plasma sintering,” *Ceram Int*, vol. 39, no. 2, pp. 1393–1396, Mar. 2013, doi: 10.1016/j.ceramint.2012.07.080.

[24] S. Rizzo, S. Grasso, M. Salvo, V. Casalegno, M. J. Reece, and M. Ferraris, “Joining of C/SiC composites by spark plasma sintering technique,” *J Eur Ceram Soc*, vol. 34, no. 4, pp. 903–913, Apr. 2014, doi: 10.1016/j.jeurceramsoc.2013.10.028.

[25] Y. Sechi, T. Tsumura, and K. Nakata, “Dissimilar laser brazing of boron nitride and tungsten carbide,” *Mater Des*, vol. 31, no. 4, pp. 2071–2077, Apr. 2010, doi: 10.1016/j.matdes.2009.10.009.

[26] S. Hausner and B. Wielage, “Brazing of metal and ceramic joints,” in *Advances in Brazing: Science, Technology and Applications*, Elsevier Ltd., 2013, pp. 361–393. doi: 10.1533/9780857096500.2.361.

[27] F. A. Mir, N. Z. Khan, and S. Parvez, “Recent advances and development in joining ceramics to metals,” in *Materials Today: Proceedings*, 2020, vol. 46, pp. 6570–6575. doi: 10.1016/j.matpr.2021.04.047.

[28] M. Way, J. Willingham, and R. Goodall, “Brazing filler metals,” *International Materials Reviews*, vol. 65, no. 5, pp. 257–285, Jul. 2020, doi: 10.1080/09506608.2019.1613311.

[29] H. Ezzat Khalifa and L. Jolla, “2) United States Patent (45) Date of Patent: (54) (71) (72) (73) (*) (21) (22) (65) (60) (51) (52) (58) HIGH DURABILITY JOINTS BETWEEN CERAMICARTICLES, AND METHODS OF MAKING AND USING SAME Applicant: General Atomics, San Diego, CA (US,” 2015.

[30] P. Colombo, G. Mera, R. Riedel, and G. D. Sorarù, “Polymer-derived ceramics: 40 Years of research and innovation in advanced ceramics,” *Journal of the American Ceramic Society*, vol. 93, no. 7, pp. 1805–1837, Jul. 2010, doi: 10.1111/j.1551-2916.2010.03876.x.

[31] J. He, M. Song, K. Chen, D. Kan, and M. Zhu, “Polymer-Derived Ceramics Technology: Characteristics, Procedure, Product Structures, and Properties, and Development of the Technology in High-Entropy Ceramics,” *Crystals*, vol. 12, no. 9. MDPI, Sep. 01, 2022. doi: 10.3390/cryst12091292.

[32] Z. Ren, S. bin Mujib, and G. Singh, “High-temperature properties and applications of Si-based polymer-derived ceramics: A review,” *Materials*, vol. 14, no. 3. MDPI AG, pp. 1–18, Feb. 01, 2021. doi: 10.3390/ma14030614.

[33] S. Fu, M. Zhu, and Y. Zhu, “Organosilicon polymer-derived ceramics: An overview,” *Journal of Advanced Ceramics*, vol. 8, no. 4. Tsinghua University, pp. 457–478, Dec. 01, 2019. doi: 10.1007/s40145-019-0335-3.

[34] P. Greil, “Polymer Derived Engineering Ceramics.”

[35] R. P. Chaudhary *et al.*, “Additive manufacturing of polymer-derived ceramics: Materials, technologies, properties and potential applications,” *Progress in Materials Science*, vol. 128. Elsevier Ltd, Jul. 01, 2022. doi: 10.1016/j.pmatsci.2022.100969.

[36] D. Galusek, J. Sedláček, and R. Riedel, “Al2O3-SiC composites prepared by warm pressing and sintering of an organosilicon polymer-coated alumina powder,” *J Eur Ceram Soc*, vol. 27, no. 6, pp. 2385–2392, 2007, doi: 10.1016/j.jeurceramsoc.2006.09.007.

[37] R. Haug, M. Weinmann, J. Bill, and F. Aldinger, “Plastic Forming of Preceramic Polymers.”

[38] A. Xia, J. Yin, X. Chen, X. Liu, and Z. Huang, “Polymer-derived Si-based ceramics: Recent developments and perspectives,” *Crystals*, vol. 10, no. 9. MDPI AG, pp. 1–19, Sep. 01, 2020. doi: 10.3390/cryst10090824.

[39] Q. Wen, F. Qu, Z. Yu, M. Graczyk-Zajac, X. Xiong, and R. Riedel, “Si-based polymer-derived ceramics for energy conversion and storage,” *Journal of Advanced Ceramics*, vol. 11, no. 2. Tsinghua University, pp. 197–246, Feb. 01, 2022. doi: 10.1007/s40145-021-0562-2.

[40] G. D. Sorarù, S. Modena, P. Colombo, J. Egan, and C. Pantano, “Chemical Durability of Silicon Oxycarbide Glasses.”

[41] Y. Jia *et al.*, “Thermal properties of polymer-derived ceramic reinforced with boron nitride nanotubes,” *Journal of the American Ceramic Society*, vol. 102, no. 12, pp. 7584–7593, Dec. 2019, doi: 10.1111/jace.16670.

[42] G. D. Sorarù *et al.*, “The effect of B-doping on the electrical conductivity of polymer-derived Si(B)OC ceramics,” *Journal of the American Ceramic Society*, vol. 100, no. 10, pp. 4611–4621, Oct. 2017, doi: 10.1111/jace.14986.

[43] M. A. R. Chowdhury, K. Wang, Y. Jia, and C. Xu, “Semiconductor-conductor transition of pristine polymer-derived ceramics SiC pyrolyzed at temperature range from 1200°C to 1800°C,” *Journal of the American Ceramic Society*, vol. 103, no. 4, pp. 2630–2642, Apr. 2020, doi: 10.1111/jace.16961.

[44] G. D. Sorad, G. D’andrea, R. Campostrini, F. Babonneau, and G. Mariotto, “Structural Characterization and High-Temperature Behavior of Silicon Oxycarbide Glasses Prepared from Sol-Gel Precursors Containing Si-H Bonds,” 1995.

[45] S. S6miya and P. Greil, “Handbook of Advanced Ceramics 5.2 Pyrolysis of Active and Passive Filler-loaded Preceramic Polymers,” 2003.

[46] P. Greil, “Near Net Shape Manufacturing of Polymer Derived Ceramics.”

[47] M. Kgaa, “technical datasheet 214049 Durazane ® 1800.”

[48] A. Qazzazie-Hauser, K. Honnef, and T. Hanemann, “Crosslinking behavior of UV-cured polyorganosilazane as polymer-derived ceramic precursor in ambient and nitrogen atmosphere,” *Polymers (Basel)*, vol. 13, no. 15, Aug. 2021, doi: 10.3390/polym13152424.

[49] G. Barroso, M. Döring, A. Horcher, A. Kienzle, and G. Motz, “Polysilazane-Based Coatings with Anti-Adherent Properties for Easy Release of Plastics and Composites from Metal Molds,” *Adv Mater Interfaces*, vol. 7, no. 10, May 2020, doi: 10.1002/admi.201901952.

[50] Y. Zhan, R. Grottenmüller, W. Li, F. Javaid, and R. Riedel, “Evaluation of mechanical properties and hydrophobicity of room-temperature, moisture-curable polysilazane coatings,” *J Appl Polym Sci*, vol. 138, no. 21, Jun. 2021, doi: 10.1002/app.50469.

[51] M. Lenz Leite, A. Viard, D. Galusek, and G. Motz, “In Situ Generated β-Yb2Si2O7 Containing Coatings for Steel Protection in Extreme Combustion Environments,” *Adv Mater Interfaces*, vol. 8, no. 13, Jul. 2021, doi: 10.1002/admi.202100384.

[52] “NN 120-20 (A).” [Online]. Available: www.az-em.com

[53] F. Bauer *et al.*, “Preparation of moisture curable polysilazane coatings: Part I. Elucidation of low temperature curing kinetics by FT-IR spectroscopy,” *Prog Org Coat*, vol. 53, no. 3, pp. 183–190, Jul. 2005, doi: 10.1016/j.porgcoat.2005.02.006.

[54] “SiC substrate (plate).” [Online]. Available: https://www.mersen.it/sites/italy/files/publications-media/gs-boostec-sic-silicon-carbide-mersen_0.pdf

[55] “Cutting machine.” https://www.qatm.com/products/cut-off-machines/benchtop/brillant-220/?gclid=Cj0KCQiAxbefBhDfARIsAL4XLRqfI-Tp4zuqOFGmeh8-0IBIbVquhECEBh3XvCHTXyr2SRNCf1Wsus8aAte4EALw_wcB

[56] “Rotavapor.” [Online]. Available: https://www.keison.co.uk/products/bibbyscientific/re300.pdf

[57] “Silica powder.” https://www.alfa.com/it/catalog/044781/

[58] “PlasmaTEC-X-Atmospheric Plasma New Atmospheric PlasmaTEC-X System with highly improved features.” [Online]. Available: www.tantec.com

[59] “Red oven.” https://www.binder-world.com/int-en/product/ed-23

[60] “Carbolite CWF 1300.” https://www.carbolite-gero.com/products/chamber-furnaces/laboratory-furnaces/cwf-standard-chamber-furnaces/

[61] “Carbolite Gero STF 16/180.” https://norrscope.com/product/carbolite-stf-16-180-tube-furnace/

[62] “STA 2500 Regulus Simultaneous Thermal Analysis Technique, Instrument, Applications.” [Online]. Available: https://analyzing-testing.netzsch.com/